NAVWEPS REPORT 8140

15 MARCH 1963

NAVWEPS REPORT 8140

SOME CALCULATIONS OF TARGET TEMPERATURES IN MICROWAVE RADIOMETRY

JOHN O. HOOPER

JAMES W. BATTLES

RESEARCH DEPARTMENT

NAVAL ORDNANCE LABORATORY CORONA

CORONA, CALIFORNIA

NAVAL ORDNANCE LABORATORY CORONA

W. R. KURTZ, CAPT., USN
Commanding Officer

F. S. ATCHISON, Ph.D.
Technical Director

FOREWORD

As authorized by WepTask RMWC-42-016/211-1/F008-22-07, the Microwave Systems Branch of the Naval Ordnance Laboratory Corona is conducting studies of microwave radiometry techniques. As part of these studies, target temperature calculations have been made and are set forth in this report. The effect of varying the parameters of target, system, and weather has been analyzed and is also reported herein. This phase of the work began in August 1962. The task is a continuing one.

C. J. HUMPHREYS
Head, Research Department

ABSTRACT

Calculations of the radiometric temperature differences between various targets and backgrounds have been performed, and the results are presented in graphical form. In addition, an analysis is made of the effects of the varying target, radiometer system, and weather parameters on the detectability of targets.

The data indicate that variable-area targets, such as roads and rivers (especially rivers), will be detectable from very high altitudes during all weather conditions considered. Constant-area targets, such as military tanks and aircraft, will be detectable at much lower altitudes or ranges, unless the area of the target is very large.

CONTENTS

Table

INTRODUCTION

The attractive military features of the microwave radiometer—such as passive detection, immunity to countermeasures,[1] and all-weather capability—have generated interest in the possible military uses of the microwave radiometer. To date, very little has been done to define the boundary conditions on the military uses of microwave radiometric techniques and systems. This report presents the results of calculations made at NOLC to investigate the boundary conditions for applying microwave radiometry to the problems of detection, guidance, and navigation.

The data obtained from these calculations are presented in the form of graphs that show the radiometric temperature difference of specific targets against specific backgrounds as a function of distance when other variables (such as weather conditions, target area, and target material) are held constant. Available experimental and theoretical data were used in making the calculations. Many of the data found in the literature are preliminary in nature, are incomplete, and contain some contradictions. Consequently, the data presented in this report should be viewed with commensurate caution. Nevertheless, the data should help to indicate the limitations, as well as the areas of possible application of the microwave radiometer for present and near-future state-of-the-art systems. The assumptions and conditions upon which these calculations are based appear in the Appendix, and the nomenclature is defined at the end of the report.

RADIOMETRIC TARGET TEMPERATURE

All matter emits radiation as a function of temperature and frequency in accordance with Planck's law; but, in the microwave region of the

[1]For a military system (e.g., missile guidance) that utilizes gross terrain features (e.g., map-matching) in the radiometric map of the target or combat area, the radiometer system may be considered essentially immune to countermeasures. Jamming transmitters operating in the band of frequencies utilized by the radiometer will only result in relatively small hot targets in the radiometric map, but will not destroy the overall features of the map.

electromagnetic spectrum, the Rayleigh-Jeans approximation holds. The Rayleigh-Jeans equation is

$$J = \epsilon \frac{2kf^2 T \Delta f}{c^2} \frac{\text{watts}}{\text{steradian (meters)}^2}$$

where

J = radiation power density

ϵ = emissivity

k = Boltzmann's constant

f = frequency of radiation

T = thermometric temperature

c = velocity of light

Dicke (Ref. 1) has shown that, if an antenna is completely surrounded by a perfect absorber (or black body) at temperature T and is matched to a transmission line terminating in a resistor also at temperature T, then the second law of thermodynamics prohibits the transfer of any energy in the system. This implies that the available noise power at the line termination is given by

$$P = kBT \qquad (1)$$

where

P = received radiation power available from the radiation resistance of the antenna

k = Boltzmann's constant

B = bandwidth of the system

Stated in another way, the antenna radiation resistance may be thought of as having a noise temperature T equal to the temperature of the absorber. This temperature is called the antenna temperature.

Consider the case when the absorbing material surrounding the antenna is not all at the same temperature. The antenna temperature will then be a weighted average that will maintain equilibrium in the system. This weighting function is the antenna power gain function. To obtain the antenna temperature T, the antenna gain function G must be convolved with the function T_f, which describes the radiometric temperature distribution of the material surrounding the antenna. Hence,

$T = G * T_f$, where * means "convolved with." This is generally a very complicated integral; consequently, to simplify calculations, an idealized antenna gain function is assumed such that G is constant over the beam width β and zero elsewhere. This is a good approximation to a narrow pencil-beam antenna with low side lobes.

The target has, to this point, been assumed to be a perfect absorber, intercepting the whole of the antenna beam, although in practical situations, the radiometer will not observe a perfect absorber and the target will not fill the antenna beam. In general, however, targets will absorb, reflect, radiate, and transmit radiation. Therefore, a real target may usually be defined as a gray body—a material that absorbs part, reflects part, and transmits part of the incident radiation upon it. This implies that a gray body will emit energy at a rate somewhat less than would a black body; therefore Equation (1) must be modified by a factor ϵ (where $0 \leq \epsilon \leq 1$). In addition, the terms due to reflected and transmitted incident radiation must be accounted for in Equation (1). The equation for the total energy in the microwave region emanating from a real target in a given bandwidth may now be written:

$$P = kBT_T = \epsilon_t kBT_t + \rho kBT_r + \gamma kBT_\gamma \qquad (2)$$

where

T_T = radiometric temperature of the target

T_t = thermometric temperature of the target

T_r = radiometric temperature of a source that is reflected by the target. (In most cases, $T_r = T_s$ = sky temperature.)

T_γ = radiometric temperature of a source that is transmitted through the target

ϵ_t = emissivity or absorptivity of the target

γ = transmissibility of the target

ρ = reflectivity of the target

Most targets of interest are opaque; hence $\gamma = 0$, and under equilibrium conditions $\rho = (1 - \epsilon_t)$. Substituting this into Equation (2) and dividing by kB, we have

$$T_T = \epsilon_t T_t + (1 - \epsilon_t) T_r \qquad (3)$$

where T_T is the antenna noise temperature looking at a specified target, and hence is the apparent radiometric temperature of a target that fills the beam.

Considering the background material surrounding the target as another target, we may write

$$T_B = \epsilon_b T_b + (1 - \epsilon_b) T_r \tag{4}$$

where

T_B = radiometric temperature of the background

T_b = thermometric temperature of the background

ϵ_b = emissivity of the background

Subtracting Equations (3) and (4), we obtain an expression for the radiometric temperature difference $\Delta T'$ between the target and its background.

$$\Delta T' = \epsilon_t T_t + \epsilon_b T_b + (\epsilon_b - \epsilon_t) T_r \tag{5}$$

To determine the temperature difference ΔT (available at the radiometer), atmospheric attenuation and antenna gain (or the target beam-filling effects) must be considered. The atmospheric attenuation is expressed as atmospheric transmissibility γ, where $\gamma \leq 1$. The atmospheric gain for the weather models used was calculated, utilizing the data given in Figure 1 and Reference 2. It is clear that

$$\gamma = e^{-0.23\, \alpha h \sec \theta} \tag{6}$$

where

α = atmospheric attenuation in db/km

h = height in k/m above earth

θ = incident look angle

To provide for the fact that the target generally does not fill the antenna beam, $\Delta T'$ is reduced by a factor Ω, equal to the ratio of the target area to the antenna beam area. That is,

$$\Omega = \frac{A_t}{A_a} = \frac{\Omega_t}{\Omega_a} \qquad (\Omega \leq 1) \tag{7}$$

where

A_t = target area (as viewed from the radiometer)

A_a = antenna beam area at the target

Ω_t = solid angle subtended by the target

Ω_a = solid angle subtended by the antenna beam

Furthermore,

$$\Omega_t = \frac{A_t}{r^2} \cos\theta = \frac{A_t}{h^2} \cos^3\theta$$

$$\Omega_a = \frac{4\pi}{G} = \frac{\pi}{4}\beta^2 \text{ (for a lossless antenna)}$$

where

r = radiometer-to-target range

β = beam width of radiometer antenna in radians

Hence,

$$\Omega = \frac{A_t G}{4h^2} \cos^3\theta = \frac{4A_t}{\pi\beta^2 h^2} \cos^3\theta \qquad (8)$$

We are now in a position to write a general expression for ΔT. Using Equations (5), (6), and (8), we have

$$\Delta T = \Omega\gamma\Delta T' = \frac{4A_t e^{-0.23\alpha h \sec\theta}}{\pi\beta^2 h^2} \cos^3\theta\left[\epsilon_t T_t - \epsilon_b T_b + (\epsilon_b - \epsilon_t)T_r\right] \qquad (9)$$

This is the basic equation used in calculating the data presented in this report. Calculations were made by assuming h or r to be the independent variable.

It is easily seen from Equation (9) that if ΔT is a function of β only, it obeys the inverse square law. However, as a function of h only, ΔT is the product of an inverse square function and a decaying exponential. The latter is due to the fact that, as observations are made with the radiometer at increasingly higher altitudes, the target fills less and less of the antenna beam. The decaying exponential is, of course, due to the increase in atmospheric attenuation as observation height is increased. In general, α is also a function of h, thus making γ more complicated than it appears.

It should be noted that ΔT can be either positive or negative, depending on whether the target is hotter or colder than the background. The possible change in sign of ΔT has no effect on the detectability of target signal; consequently, the absolute value of ΔT (i.e., $|\Delta T|$) is shown in all the data presented in this report.

RADIOMETER SYSTEM AND SCANNING EFFECTS

The data presented in this report have been obtained from calculations that disregarded the effects of the radiometer system, except the antenna beam width as it affects the target beam-filling factor. It is the purpose of this section to consider these effects without going into detailed analysis, but rather by presenting the results of such analysis. For a detailed analysis of the derivation of the results presented here, see References 3 and 4.

The sensitivity or minimum detectable temperature change δT of a radiometer system (Ref. 3) is given by

$$\delta T = QFT_0\sqrt{\frac{b}{B}} \tag{10}$$

where

- Q = constant that depends upon the type of radiometer; e.g., for a dc radiometer, $Q = 2$; for a Dicke radiometer with square wave switching, $Q = 2\sqrt{2}$
- F = noise figure
- T_0 = reference temperature (usually 290°K)
- b = postdetection filter bandwidth
- B = predetection bandwidth

To obtain information, such as for a map or picture, with a radiometer, it is necessary to scan the area of interest in two dimensions. Many types of scanning methods can be employed; one of the most common is diagrammed in Figure 2. The picture obtained in this manner is a mosaic of picture elements. Each picture element is the area of the antenna beam intersected by the target plane. The spatial resolution depends on this area, and the temperature resolution or sensitivity depends on the time devoted to the measurement of each element. The minimum postdetection filter bandwidth required to avoid degeneration

of the spatial resolution must be about $\frac{1}{2}$ p, where p is the number of picture elements scanned per second.

If the postdetection filter bandwidth b is assumed to be determined by an RC filter, it is the bandwidth between the 5.4-db points on the amplitude response curve given by

$$b = (4RC)^{-1}$$

The bandwidth b' used in resolution analysis is the 3-db bandwidth given by

$$b' = (2\pi RC)^{-1}$$

Then the number of picture elements scanned per second will be

$$p = 2b' = (\pi RC)^{-1}$$

and

$$b = \frac{\pi}{4} p \tag{11}$$

Substituting Equation (11) into Equation (10), the minimum detectable temperature difference δT, as a function of p, will be given by

$$\delta T = Q_p F T_0 \sqrt{\frac{p}{B}} \tag{12}$$

where

$$Q_p = \frac{\sqrt{\pi}}{2} Q$$

If a solid map or picture of the area of interest is desired, the number of picture elements scanned per second will be

$$p = \frac{2\phi_m v}{\beta^2 h} \cos^2 \theta \tag{13}$$

where

ϕ_m = maximum scan angle ($\frac{1}{2}$ of peak-to-peak) in radians

v = velocity of the aircraft containing the radiometer

β = beam width of radiometer antenna in any direction in radians

h = altitude of aircraft

Substituting this expression for p into Equation (12), we obtain

$$\delta T = \frac{Q_p F T_0}{\beta} \cos\theta \sqrt{\frac{2\phi_m v}{Bh}} \tag{14}$$

Rewriting Equation (9) for comparison

$$\Delta T = \frac{4A_t e^{-0.23\alpha h \sec\theta}}{\pi\beta^2 h^2} \cos^3\theta \left[\epsilon_t T_t - \epsilon_b T_b + (\epsilon_b - \epsilon_t) T_r\right] \tag{9}$$

We are now in a position to make an analysis of the effect that various parameters have on δT and ΔT and that will accordingly influence target detectability. A target is detectable if $\delta T \leq \Delta T$.[2] Obviously, to increase the detectability of targets, the parameters must be chosen so as to minimize δT and at the same time maximize ΔT. As each parameter is considered, it is assumed that all other parameters are held constant.

EFFECTS OF SYSTEM AND WEATHER PARAMETERS ON DETECTABILITY

The parameters Q_p, F, and B in Equation (14) are built into the radiometer system and have no effect on ΔT, but they will reduce δT if Q_p and F are small and B is large.

The parameter β is built into the system, but it also occurs in Equation (9), thus affecting ΔT at the same time that it affects δT. The beam width appears in Equation (14) to the -1 power and in Equation (9) to the -2 power; consequently, as β increases, both δT and ΔT decrease. However, ΔT decreases at a much faster rate than δT, and this results in a net degradation of the system detection capabilities. As β decreases, the reverse is true; ΔT increases at a faster rate than δT, thus resulting in an overall increase in the system detection capabilities. Moreover, the spatial resolution of the system is affected inversely by the antenna beam width.

[2] That is, where $\delta T = \Delta T$, the system signal-to-noise ratio is one and the probability of detection on a single scan is 0.5. For a probability of detection of 0.9995, eleven scans of the target are required.

The parameters v and ϕ_m, which appear only in Equation (14), have no effect on ΔT but have equal effect on δT. As the craft carrying the radiometer increases or decreases its speed, it correspondingly increases or decreases the system sensitivity by an amount proportional to the square root of the speed. The same relation is noted for the maximum scan angle.

The exact net effect of h on the system detection capabilities is not clear because α in Equation (9) may also be a function of h. Nevertheless, in all practical situations, h will have a greater inverse effect on ΔT than on δT because h is only to the $-\frac{1}{2}$ power in Equation (14) and is to the -2 power and in the decreasing exponential in Equation (9). In other words, as the radiometer increases in altitude, the system sensitivity increases (i.e., δT decreases); at the same time, however, the available target temperature difference ΔT decreases at a much faster rate, resulting in an overall decrease in the target detectability of the system.

As the look angle θ varies from 0 to 90 deg, the radiometer moves from a vertical look at the earth to a look at the horizon. At the same time, the cosine factors in Equations (14) and (9) take on values ranging from one to zero, and the value of the exponential factor in Equation (9) moves very rapidly from -0.23h to zero. The net result is that detectability is maximum at $\theta = 0$ and decreases as θ increases. This neglects possible polarization effects of target radiation and reflection.

The atmospheric and weather effects on ΔT range from negligible to very severe because of the position of α in the decaying exponential in Equation (9) and because α is very dependent on the frequency chosen. For example, the values of α for moderate rain is 0.055 db/km at 10 kMc, 0.95 db/km at 35 kMc, and 2.8 db/km at 100 kMc.

On the basis of operational considerations, it is clear that only two parameters, v and h, are likely to vary greatly. Missiles and aircraft will fly at many different altitudes and speeds. To illustrate the relationship between the speed and height of an operational radiometer and the minimum detectable temperature of the system, a graph of δT as a function of the ratio v/h is shown in Figure 3. The remaining parameters listed in the figure were chosen to represent a typical microwave radiometer system.

An airborne radiometer system (as described above) flying at 2000 mph and at 100,000 ft altitude results in a speed-to-height ratio of 0.0293 sec^{-1}. From the expanded portion of Figure 3, it is easily seen that $v/h = 0.0293\ sec^{-1}$ and gives about 0.81°K for δT. For a speed of 2000 mph at 2000 ft altitude, v/h would equal 1.466 sec^{-1} and would give about 5.8°K for δT. It is interesting to note that both these values for δT would

be reduced by a factor of $\frac{1}{2}$ if the beam width were increased to 2 deg. However, one must not forget about the greater effect that β would have on ΔT.

EFFECTS OF TARGET PARAMETERS ON DETECTABILITY

The target and background parameters play an important role in determining the value of ΔT. The purpose of this analysis is to consider and determine the combinations of and relationships between the target parameters which (1) render targets undetectable from their backgrounds, or (2) enhance target detectability.

The effect of target area on ΔT is direct; as targets decrease in size, they eventually become undetectable. There exists, for a given system in a specified environment, a minimum target size that can be detected. The relations of the other target and background parameters are not so obvious.

For an analysis of the remaining target and background parameters, consider Equation (5) with $T_r = T_s$ and ϵ_t factored out of the expression. This gives

$$\Delta T' = \epsilon_t \left| T_t - T_s - \frac{\epsilon_b}{\epsilon_t}\left(T_b - T_s\right) \right| \tag{15}$$

Let

$$T_1 = T_s + \frac{\epsilon_b}{\epsilon_t}\left(T_b - T_s\right)$$

then $\Delta T'$ becomes

$$\Delta T' = \epsilon_t \left| T_t - T_1 \right| \tag{16}$$

The graph of Equation (16) (see Figure 4) shows that, if we start out at some target temperature less than T_1 and gradually heat the target, the radiometric temperature $\Delta T'$ will decrease at first and then increase again when $T_t > T_1$. The region around $T_t = T_1$ is most important because this is where the probability of target detection becomes small. It is important to consider how T_t must behave to stay in this region as ϵ_b/ϵ_t, T_b, and T_s are changed.

The ratio ϵ_b/ϵ_t is fixed for a given target in a given background. Thus, for different ratios, we are changing the target, the background, or both. If we hold T_b and T_s constant, we see that $\Delta T'$ is small: (1) for some value of $T_t < T_b$ when $\epsilon_b/\epsilon_t < 1$; (2) for $T_t \approx T_b$ when $\epsilon_b/\epsilon_t = 1$; and (3) for some value of $T_t > T_b$ when $\epsilon_b/\epsilon_t > 1$.

Figure 5 is a graph of Equation (15). T_t has been placed on the right so that, if T_t and ϵ_b/ϵ_t are known, then $T_t - T_1$ can be found from the graph in terms of T_b and T_s. To show how this works, suppose $T_t = T_a$ (where T_a is some arbitrary temperature) and $\epsilon_b/\epsilon_t = 1.5$; then $T_1 = T_c$ and $T_t - T_1 = T_a - T_c$, where T_c and T_a can be given in terms of T_s and T_b because T_s and T_b define the scale of the graph. This gives

$$\Delta T' = \epsilon_t \left| T_c - T_a \right|$$

If $|T_c - T_a|$ is small, then the target has a low probability of detection. Points that are equidistant from the line that gives T_1 in Figure 5 give the same $\Delta T'$ for a given target. The farther these points are from the T_1 line, the larger $\Delta T'$ becomes. We see that when the point $(T_t, \epsilon_b/\epsilon_t)$ lies near the T_1 line, the probability of target detection is small.

Figure 6 is a graph of ΔT for several different targets with a given background and two different target temperatures. All the targets have the same surface area, and a change in target means a change in target emissivity. When $T_t = T_b = 300°K$, we see that, as ϵ_t increases, the altitude at which $\Delta T = 1°K$ decreases. ΔT would be zero for all altitudes at $\epsilon_t = \epsilon_b$. The other case is $T_t = 325°K$ and $T_b = 300°K$; here, we see that for some value of ϵ_t between 0.88 and 0.90, ΔT would be zero for all altitudes.

The only parameters that have been changed are the target emissivity and the target temperature; therefore, ΔT has changed only because $\Delta T'$ has changed. A change in target temperature of only 25°K for a given target has caused a change of over 2000 ft in the altitude at which $\Delta T = 1°K$. Thus, a change in target thermometric temperature can have a large effect on ΔT.

CALCULATION OF RADIOMETRIC TARGET TEMPERATURES AS A FUNCTION OF RANGE FOR VARIOUS TARGETS AND WEATHER CONDITIONS

The data are presented in graphical form for (1) variable-area targets and (2) constant-area targets. The variable-area targets are roads and rivers. The constant-area targets are tanks and aircraft. In all cases, the targets were assumed to be at rest with respect to the radiometer and the background. The only assumed property of the radiometer was the antenna beam width. It was, however, assumed that interest lies in the parameters at the threshold of detectability by state-of-the-art radiometer systems. The discrimination threshold region was defined to be between 1 and 6°K. Consequently, all the data were plotted as a function of range (or height) within the given threshold region. Tables were also constructed, listing the height H at which a difference of 1°K exists between a target and background for each group of data.

The Appendix contains a list of the assumptions and conditions used in the calculations.

ROADS AND RIVERS

In this section, a general expression will be determined for ΔT when the target is a strip, such as a road or river, viewed from a radiometer in an aircraft, and the data obtained from this expression will be presented for particular cases. The specific cases considered are (1) a right-angle intersection of two 20-ft-wide concrete roads, (2) a 20-ft-wide concrete road, and (3) a 200-ft-wide river. The roads and rivers are assumed to be straight and to extend in length so that they do not end within intercept of the antenna beam and the earth. In addition, these targets are against a grassy background.

A major difference between the strip target and the fixed-area targets is that the target area increases as the position of observation moves away from the target. The problem of deriving a function for ΔT is then primarily one of determining a function for the beam-filling factor Ω. To derive a general equation for what will be called the strip-target case, let us consider the antenna beam intercept with the road intersection as shown in Figure 7.

In general, the shape of the antenna beam intercept with the ground will be an ellipse; consequently, the area of the beam intercept is πab. The area of the target within the beam intercept is $2aw + 2by - wy$, if we assume that the arc portion of the beam intercept across the target

is a straight line. This will be a good approximation when $w << 2b$ and $y << 2a$, which will be the case for the calculations made. Therefore, we may write

$$\Omega = \frac{A_t}{A_a} = \frac{2aw + 2by - wy}{\pi ab} \tag{17}$$

where

a = semimajor axis of elliptical intersection of antenna beam with the earth

b = semiminor axis of elliptical intersection of the antenna beam with the earth

w = width of road normal to b

y = width of road normal to a

It is easily seen from Figure 7 that $2b = r\beta$, $2a = r\xi \sec\theta$, and $r = h \sec\theta$. Substituting the above relationships into Equation (17), we obtain

$$\Omega = \frac{4(\beta hy \sec\theta + \xi hw \sec^2\theta - wy)}{\pi\xi\beta h^2 \sec^3\theta} \tag{18}$$

If the term wy is a small portion of the total area of the target, which is the case when h is large, it may be disregarded without resulting in significant error. Dropping wy in Equation (18), we have

$$\Omega = \frac{4(\beta y + \xi w \sec\theta)}{\pi\beta\xi h \sec^2\theta} \tag{19}$$

The percentage of error in Ω, caused by disregarding the wy term in Equation (18), will be given by

$$\frac{100\ wy}{\beta hy \sec\theta + \xi hw \sec^2\theta - wy}$$

For the specific example considered, the error in the data as a result of the above factor was always less than 2 percent.

For the case of a single straight road or river along the flight path, $y = 0$, and Equation (18) becomes

$$\Omega = \frac{4w \cos \theta}{\pi \beta h} \tag{20}$$

It is significant that the antenna beam dimension in the direction of the strip target has no effect on Ω. Moreover, for strip targets, Ω varies with respect to h only to the -1 power, instead of to the -2 power as in the case of fixed-area targets. Consequently, when the height of observation is doubled, the signal obtained from a strip target is reduced by a factor of $\frac{1}{2}$, but the signal obtained from fixed area targets is reduced by a factor of $\frac{1}{4}$. An equation for Ω, similar to Equation (20), may be obtained from a straight strip target running transverse to the flight path by allowing w = 0, but that will not be considered here.

Substituting Equations (19) and (20) for Ω into Equation (9) we obtain the desired equations for ΔT in terms of the strip target geometry.

$$\Delta T = \frac{4\gamma(\beta y + \xi w \sec \theta)\Delta T'}{\pi \beta \xi h \sec^2 \theta} \quad \text{for intersection of roads} \tag{21}$$

$$\Delta T = \frac{4\gamma w \cos \theta \Delta T'}{\pi \beta h} \quad \text{for single road or river} \tag{22}$$

Equations (21) and (22) have been evaluated for the three cases described earlier, and the data are shown in Figures 8 through 25. In addition, Table 1 lists the altitude H at which $\Delta T = 1°K$ for all situations considered. The data for the road intersection at X-band frequencies were obtained by assuming a 2-deg antenna beam width; however, the values listed in Table 1 are for a 1-deg beam width for ease of comparison. The most obvious feature of these data is the great heights

TABLE 1. Altitudes at Which $\Delta T = 1°K$ for Roads and a River (Grassy Background)

All values expressed in ft x 1000; β = 1 deg

Weather Conditions	20-ft Concrete Road Intersection		20-ft Concrete Road		200-ft River	
	X-Band	K_a-Band	X-Band	K_a-Band	X-Band	K_a-Band
Clear	53.0	44.0	31.0	25.8	1950	1687
Moderate clouds	87.4	68.6	51.2	40.2	1920	1535
Moderate rain	82.0	43.0	47.7	23.9	1765	875

at which the strip-type target may be detected in all weather conditions considered. This is especially true in the case of the river, which develops a temperature difference of 1°K at an altitude of 334 miles during moderate rain at X-band frequencies. The river develops a much stronger signal than the roads because the river is 10 times wider than the roads and the water generates a greater $\Delta T'$ than concrete against a grass background.

It is interesting to note that the heights given in Table 1 for the road intersection and the straight road are considerably greater for cloud and rain conditions at X-band frequencies than for the clear-weather case. This phenomenon is, of course, due to the assumptions made concerning the thermometric temperatures of the roads and the background, especially during clear weather, and to the fact that the emissivity of the concrete road is slightly less than the emissivity of the grassy background. That is, if the concrete is assumed to possess a higher thermometric temperature than the grass (which is a realistic situation during a clear sunny day), the higher temperature of the concrete tends to bring the radiometric temperature of the concrete closer to that of the grass, thus reducing the difference between the two. This phenomenon may result in the target becoming undetectable at times under certain conditions of target-background emissivity and thermometric temperature. (A more detailed analysis of this phenomenon is given in the section on "Radiometer System and Scanning Effects" of this report.) The same phenomenon is present in the K_a-band data; however, the increased atmospheric attenuation at these frequencies, especially during rain, reduces the difference that would otherwise be obtained.

The difference between the data for the road intersection and for the single road at a given frequency results from the greater target area of the intersection. It can be shown that the altitude for the intersection should be greater than it is for the straight road by the factor $1 + \cos\theta$ for an equal ΔT. Also, the temperature at a fixed altitude for the intersection is $1 + \cos\theta$ times the temperature for the single road at that altitude.

The data in Table 1 for the 200-ft river do not experience the fluctuation in height as do similar data for the roads, because the river does not possess a higher thermometric temperature during clear weather. In fact, the thermometric temperature of the river is assumed to be the same for all three weather conditions considered. Furthermore, the emissivity of water is much less than that of grass. These data also point out the effects of atmospheric attenuation on range of detectability. There is a small effect noticeable in the ranges for all targets during clear weather; however, the range for all targets at X-band is approximately twice that for the same target at K_a-band. Nevertheless, there is an advantage obtained at K_a-band over X-band, under the conditions

considered, if equal antenna aperture is assumed, instead of equal beam width. However, this advantage is quickly lost as the operating frequency becomes higher, where the atmospheric attenuation becomes extremely severe during foul weather.

TANKS

Calculations of ΔT for T-34 tanks in a grassy field, made by utilizing Equation (9), are shown in Figures 26 through 37. Two target situations have been considered: (1) a single tank against the grassy background, and (2) three tanks against a grassy background. The plane-view area of each tank is 180 sq ft.

The most noticeable feature of the data is that, for all conditions, ΔT is greater at a given altitude at K_a-band than it is at X-band. This is, of course, due to the fact that the beam widths assumed are 1 deg at K_a-band and 2 deg at X-band. If equal beam widths are assumed for both frequencies, then the values of ΔT will be somewhat greater for the X-band data than for the K_a-band data. This is because of the greater attenuation at K_a-band than at X-band frequencies, especially during bad weather conditions. It must not be forgotten, however, that the antenna size for a given beam width is considerably smaller at K_a-band than at X-band. For the parameters used, the antenna diameter is approximately 4 ft for a 2-deg beam width at X-band and 2 ft for a 1-deg beam width at K_a-band.

The altitudes H at which $\Delta T = 1°K$ have been listed in Table 2 for convenience. From the data in the table it is evident that the weather

TABLE 2. Altitudes at Which $\Delta T = 1°K$ for T-34 Tanks (Grassy Background)

All values expressed in ft x 1000

Weather Conditions	One Tank		Three Tanks	
	β = 2 deg X-Band	β = 1 deg K_a-Band	β = 2 deg X-Band	β = 1 deg K_a-Band
Clear	2.7	5.2	4.7	9.3
Moderate clouds	2.7	5.0	4.7	8.7
Moderate rain	2.6	4.9	4.5	6.7

conditions considered have practically no effect on the X-band data; however, it is equally evident that the weather significantly affects the K_a-band data, especially during rain and for three tanks. For one tank in rain, H is about 0.95 times the H for one tank in clear weather; but, for three tanks during rain, H is approximately 0.7 of the H during clear weather. The difference between the one-tank and three-tank data results from the greater path-length through the atmosphere and hence the greater attenuation for the three-tank data. The altitudes listed in Table 2 show that the heights given for clear weather are greater than those for foul weather, in spite of the fact that the thermometric temperature of the target for clear weather was assumed to be 25°C hotter than the background. It may be recalled that the effect of a greater thermometric temperature of the concrete roads resulted in ΔT for clear weather being less than ΔT for foul weather. The reason that this effect is not evident for the tank targets is that the metal tanks have a much smaller emissivity than the concrete roads.

It is also interesting to note that the altitude given in Table 2 for three tanks is approximately $\sqrt{3}$ times the altitude given for one tank for the same weather conditions and frequencies, but the area of the target has in effect increased by a factor of three. This is because ΔT is a function of the inverse square of the altitude for constant-area targets. In general, if the area A_t of a constant-area target is increased by a constant factor c and all other parameters except h remain constant, then H is increased by the factor $\sqrt{c}$.

AIRCRAFT

Calculations have been made of the radiometric temperature difference between a USSR supersonic bomber (Ref. 5), code-named "Bounder," and its surroundings. The calculations are based on three distinct types of observations:

1. Air to ground. Bounder is on a concrete airfield and the radiometer is in flight.

2. Air to air. Bounder and the radiometer are assumed to be above all atmospheric effects (35,000 ft). Two variations of conditions in this case have been considered: (a) Bounder is above the observing radiometer; (b) Bounder is below the observing radiometer.

3. Ground to air. Bounder is in flight, and the radiometer is on the ground.

In all calculations, the plane-view area of the Bounder was used (Figure 38). Although the calculations were made for an area of 5200 sq ft, the graphs (Figures 39 to 74) can be used for similar targets of other sizes in the same environment. Because ΔT is directly proportional to the target area, ΔT may be changed by an appropriate factor (area of new target/5200 sq ft) to give ΔT for the new target.

Air to Ground

Figures 39 through 54 show plots of the apparent radiometric temperature difference ΔT versus height above a Bounder parked on a concrete airfield. The data at K_a-band are shown in Figures 39 through 46, and at X-band in Figures 47 through 54.

The graphs show how ΔT varies as a function of altitude, with weather conditions and antenna beam width as parameters. Data are shown for 1- and 2-deg beam widths under four weather conditions. Table 3 summarizes the significant data of these calculations by listing the altitude at which $\Delta T = 1°K$ for all the parameter variations.

TABLE 3. Altitudes at Which $\Delta T = 1°K$ for Bounder in Air-to-Ground Case (Concrete Background)

All values expressed in ft x 1000; $\theta = 45$ deg

Weather Conditions	X-Band		K_a-Band	
	$\beta = 1$ deg	$\beta = 2$ deg	$\beta = 1$ deg	$\beta = 2$ deg
Clear	26.5	13.1	24.80	12.40
Moderate clouds	25.5	12.5	22.80	11.70
Moderate rain	24.4	12.0	17.45	9.00
Cumulus clouds	23.4	12.0	14.55	9.55

The table shows that under the weather conditions of moderate rain and cumulus clouds the altitude H for $\Delta T = 1°K$ at X-band decreases from 24,400 to 23,400 ft, respectively, at 1-deg beam width; but does not change under the given conditions for a beam width of 2 deg. Although a somewhat similar situation exists at K_a-band, there is a greater decrease in H from moderate rain to cumulus conditions at a 1-deg beam width, but at a 2-deg beam width, there is an increase in H from moderate rain to cumulus conditions. These somewhat unexpected data are the result of (1) the difference between X-band and K_a-band radiation attenuation characteristics under the given weather condition, and (2)

the structure of the weather model used. The moderate-rain model consists of rain from 0 to 3000 ft; the cumulus-cloud model assumes clear atmospheric conditions from 0 to 5000 ft and a cloud of varying composition from 5000 to 20,000 ft. (For a detailed description of the weather models used, see the Appendix.)

Air to Air

This section deals with the calculations of the apparent radiometric temperature difference between the Bounder and its background when the aircraft and the observing radiometer are both at an altitude of approximately 35,000 ft, where atmospheric effects are negligible. Two geometric situations are considered in the calculations:

1. Looking up at the aircraft with sky background and, alternatively, a hot land reflection source or a cold, watery earth reflection source.

2. Looking down at the aircraft with a cold, watery earth background and sky reflection source.

To obtain general equations for ΔT in these two geometric situations, it is necessary to determine the background temperature and the temperature of the reflection source at the target. The background and the reflection source are the sky temperature or the earth temperature, depending upon whether geometric situation 1 or 2 is assumed. Sky temperature is defined as the sky temperature as it appears at the aircraft looking away from the earth. The sky temperature as it appears from the earth's surface is included in the apparent earth temperature as it appears at the aircraft. Consequently, there are two sky temperatures to consider in these calculations. We may simplify matters by assuming the sky temperature as it appears from the aircraft to be zero. This is a fair approximation if celestial radio sources are disregarded. Therefore, we need only to derive an expression for the apparent earth temperature to obtain the desired equations for ΔT.

By referring to Figure 55, the expression for the apparent radiometric temperature of the earth is easily derived. The apparent earth temperature is composed of two parts: a portion that is due to thermometric temperature and emissivity, $\epsilon_e T_e$, and a portion that is due to atmospheric radiation and absorption. The contribution of the sky temperature T_s to the apparent earth temperature is twofold. The earth reflects a portion of the sky temperature, $(1 - \epsilon_e)T_s$, and the atmosphere absorbs a portion of the radiation leaving the surface of the earth, which is at the temperature $\epsilon_e T_e + (1 - \epsilon_e)T_s$. The radiation leaving the surface of the earth is reduced by the atmospheric transmissivity factor. The atmosphere also radiates directly into the radiometer at

temperature T_s. Combining these terms gives $\gamma[\epsilon_e T_e + (1 - \epsilon_e)T_s] + T_s$, which is the desired expression for the apparent radiometric temperature of the earth. Utilizing this expression alternately as a reflection source from the target and as a background in Equation (9), the apparent radiometric temperature difference between the aircraft and its background was calculated for the two geometric situations considered.

The sky temperature T_s may be expressed in terms of the atmospheric transmissivity and the radiometric temperature $\epsilon_e T_e$ of the earth at the surface of the earth, if it is assumed that the earth and the atmosphere are in thermal equilibrium, as was done in the ground-to-air case. It was determined that the difference resulting from using a hot sky temperature in the cold earth situation was negligible; consequently, in the air-to-air case we have assumed that T_s for a water-earth model is equal to T_s for a land-earth model.

The data obtained from these calculations are presented in graphical form in Figures 56 through 67. The apparent radiometric temperature ΔT is plotted as a function of range. A summary of these data is given in Table 4 by listing the range H at which ΔT is 1°K. It is interesting

TABLE 4. Ranges at Which ΔT = 1°K for the Bounder in Air-to-Air Case

All values expressed in ft x 1000

Background	Reflected Source	X-Band θ = 45 deg		K_a-Band θ = 45 deg		K_a-Band θ = 0 deg	
		β = 1 deg	β = 2 deg	β = 1 deg	β = 2 deg	β = 1 deg	β = 2 deg
Sky	Cold watery earth	32.2	16.1	33.2	16.6	42.1	21.0
Cold watery earth	Sky	20.0	10.0	22.3	11.2	32.4	16.2
Sky	Hot earth	46.0	22.8	45.7	22.6	--	--

to note that H is essentially the same for X- and K_a-bands, given the same antenna beam width and situation. This would imply that detection range is not a function of frequency but of beam width. We might recall that for a 1-deg beam width the diameter of a parabolic antenna is 6.8 ft at X-band and 1.9 ft at K_a-band. One would expect to obtain very great

detection ranges with a small antenna operating at the higher microwave frequencies. Such is the case in the infrared region of the spectrum, where detection ranges are very great above the atmospheric effects (35,000 ft).

For the second geometric situation mentioned above—looking down at the aircraft with a cold, watery earth background—there is a definite increase in the detection range at K_a-band over X-band, whereas in both cases of the first geometric situation there is little difference. This effect is undoubtedly due to the greater effect that the sky temperature at the earth has on the apparent earth temperature at the aircraft, when a cold earth is assumed. Moreover, T_s increases as the frequency of operation is increased. This effect is also noted to a lesser degree when the cold earth is the reflection source.

When a hot earth is assumed to be the reflection source, we note the reverse effect. The detection range at K_a-band is less than that at X-band, which indicates that the sky temperature is a lesser part of the apparent earth temperature, because of the greater earth temperature.

The calculations made at normal incident angles at K_a-band show the effect of the increased solid angle subtended by the aircraft on the range of detection. These ranges are the maximum possible for the given conditions. The range at other values of θ is approximately equal to the maximum value at $\theta = 0$ deg times the cosine of θ. This would actually be equal if it were not for the change in the apparent earth temperature with look angle, which in turn is caused by the change in apparent sky temperature with look angle.

Ground to Air

This section is concerned with the calculation of the apparent radiometric temperature difference of an airborne target as viewed from the ground. Two cases are considered: (1) the aircraft over a watery earth (e.g., the ocean), and (2) the aircraft over a grassy-land earth. These two conditions were chosen because they represent the extremes of the earth's reflectivity in the microwave region. To derive a general expression for ΔT in this situation, see Figure 68.

The "temperature" of the energy emanating from the target consists of two parts: a portion that is due to the thermal emission, $\epsilon_t T_t$, and a portion reflected from the target, $(1 - \epsilon_t)T_r$. The temperature T_r is due to the earth temperature $\epsilon_e T_e$, sky temperature T_s, and the atmospheric transmissibility γ. If we assume that the target is at an altitude where there is negligible difference between the atmospheric transmissibility to the target and the total transmissibility of the atmosphere, it can be stated that

$$T_r = \gamma\left[\epsilon_e T_e + \left(1 - \epsilon_e\right)T_s\right] + T_s \tag{23}$$

The radiometric temperature leaving the target will be

$$\epsilon_t T_t + (1 - \epsilon)T_r$$

The temperature available at the radiometer will be (1) that at the target reduced by the atmospheric absorption and the portion of the antenna beam filled by the target, and (2) the sky temperature. The background temperature is the sky temperature. Subtracting the temperature observed while looking at the background from that obtained while looking at the target, ΔT becomes

$$\Delta T = \gamma\Omega\left[\epsilon_t T_t + \left(1 - \epsilon_t\right)T_r\right] \tag{24}$$

If it is assumed that the atmosphere and the earth are in thermal equilibrium, it may be said that

$$T_s = (1 - \gamma)\left[\epsilon_e T_e + \left(1 - \epsilon_e\right)T_s\right]$$

Solving this for T_s

$$T_s = \frac{(1 - \gamma)\epsilon_e T_e}{\epsilon_e + \gamma\left(1 - \epsilon_e\right)} \tag{25}$$

Replacing T_s in Equation (23) with Equation (25) and substituting Equation (23) for T_r in Equation (24), a function for ΔT is obtained in terms of the target, earth, and atmospheric parameters in place of T_r or T_s.

$$\Delta T = \gamma\Omega\left[\epsilon_t T_t + \frac{\left(1 - \epsilon_t\right)\epsilon_e T_e}{\epsilon_e + \gamma\left(1 - \epsilon_e\right)}\right] \tag{26}$$

Equation (26) has been plotted in Figures 70 through 74 for the Bounder over water. Three weather conditions, two frequency bands, one antenna beam width, and one look angle are considered. The outstanding feature of these graphs is that they are practically identical, except for the condition of moderate rain at K_a-band, which deviates very little from the other curves. This uniformity of results under various environmental conditions is due to two factors.

The first factor causing uniformity is the all-weather characteristic of the microwave radiometer at the frequencies considered. However,

as the operating frequency of the radiometer is increased, the atmosphere absorption becomes very severe. The effect of the increasing atmospheric absorption at high microwave frequencies can be noted in the decrease in ΔT at K_a-band during moderate rain conditions (Figure 72) as compared with the other curves. For example, at a look angle of 45 deg the total atmospheric transmissivity for moderate rain is 0.979 at X-band and it decreases to 0.73 at K_a-band.

The second factor that causes greater uniformity in the data obtained in the ground-to-air geometry than occurs in some of the other situations considered can be described in the following way. The sky temperature reflected from the earth is reflected from the target in addition to the sky temperature (looking back at the earth). The sky temperature is, among other factors, a function of the atmospheric absorption. As the weather worsens, the atmospheric absorption increases, which tends to decrease ΔT; but at the same time the sky temperature increases, which tends to increase ΔT. These effects offset each other to some extent, but the overall effect as the weather worsens, especially at the higher microwave frequencies, is to reduce ΔT.

Figure 69 shows how ΔT varies with γ for the over-water case at an altitude of 20,000 ft. It is to be noted that, as γ decreases from 1 (indicative of bad weather), the curve decreases very slowly until γ is approximately 0.75, at which point γ decreases at a faster rate. This compensating effect is, of course, significant only when the target and earth are good reflectors (i.e., when ϵ_t and ϵ_e are small), which is generally the case with aircraft over water.

Nevertheless, the increase in radiometric temperature of the earth over land results in an increase in ΔT for all conditions considered. This is illustrated by the values of H shown in Table 5, which are approximately 10,000 ft greater than those over water. The curves of ΔT for the over-land case are not included in the report because they are similar in shape to those presented for the over-water case, and the essential information is contained in Table 6.

TABLE 5. Altitudes at Which ΔT = 1°K for Bounder in Ground-to-Air Case (Over Grassy-Land Earth)

All values expressed in ft x 1000; β = 1 deg

Weather Conditions	K_a-Band	X-Band
Clear	31.5	32.3
Moderate clouds	31.0	32.0
Moderate rain	28.1	32.0

TABLE 6. Altitudes at Which ΔT = 1°K for Bounder in Ground-to-Air Case (Over Watery Earth)

All values expressed in ft x 1000; β = 1 deg

Weather Conditions	K_a-Band	X-Band
Clear	21.3	21.7
Moderate clouds	21.2	21.6
Moderate rain	20.2	21.6

CONCLUSIONS

Because of the limited and approximate nature of the available data on which the calculations are based, it is impossible to reach any definitive conclusions at the present time. Nevertheless, the microwave radiometer appears to be capable of detecting rivers at extremely high altitudes under all the weather donditions considered. In general, roads can be detected at fairly high altitudes and during all the weather conditions considered; but for certain conditions of background, road material, and thermometric temperatures they will be detectable at only very short ranges.

The maximum detectable range for such ground and air targets as tanks and aircraft is much shorter than the ranges attainable for road and river targets. This results primarily from the smaller area of the tanks and aircraft. If the microwave radiometer is to be used against these types of target, the range limitations of the system should be considered.

To optimize the detection range in all weather conditions, careful consideration must be given to the selection of the system frequency and the type of antenna. Although in most practical systems the antenna size is limited by space considerations, narrow beam widths require large antennas. Consequently, to accommodate the requirement of small antenna size and at the same time satisfy the need for large antenna size in order to increase spatial resolution and target temperature, higher operating frequencies are considered. However, atmospheric absorption increases with an increase in frequency, especially in foul weather, and thus degrades the all-weather characteristic of the system.

On the basis of this study, it is evident that additional experimental work should be performed. In this experimental work, it is important

that all parameters having significant effect on the radiometric temperature of materials under examination should be recorded accurately. More complete and more exact data are necessary to predict reliably the effects of parameters on the radiometric temperature of targets in specified environments.

Appendix

ASSUMPTIONS AND CONDITIONS

1. The projected areas of targets are used; that is, all targets are flat.

2. Hot areas on targets caused by engine heat and exhausts and by aerodynamic heating are disregarded.

3. Rain-water effects on targets are disregarded, except as a cooling effect.

4. Temperatures caused by celestial sources are disregarded.

5. The radiometer antenna is stationary; i.e., scanning effects are not included in the calculations. A discussion of scanning is given in the report under the heading, "Radiometer System and Scanning Effects."

6. The effect of antenna side lobes is disregarded. The $\frac{1}{2}$-power beam width is considered the effective antenna beam width. In all calculations, antenna efficiency is 55 percent.

7. Apparent sky temperatures (Ref. 4) are as follows:

Frequency	Look Angle (deg)	Clear (°K)	Moderate Clouds (°K)	Moderate Clouds & Moderate Rain (°K)
X-band	0	3	5	8
	45	5	7	12
K_a-band	0	18	28	75
	45	25	40	104

The sky temperature as viewed from above 35,000 ft, looking away from the earth, is zero for both X-band and K_a-band frequencies.

8. Emissivities of selected materials at K_a-band for $\theta = 45$ deg (Ref. 3) are as follows:

Material	Emissivity
Water	0.34
Grass	0.97
Concrete	0.8

The emissivity of metal is approximately 0.2. The emissivity of water for $\theta = 0$ deg is given as 0.467 in Reference 3. These data are assumed also to hold at X-band.

9. Thermometric temperatures of target and background materials on a clear sunny day are as follows:

Material	Temperature[3] °K	Temperature[3] °F
Concrete (roads and airfield apron)	325	125.6
Grass	300	80.0
Metal (tanks and aircraft on the ground)	325	125.6
Metal (aircraft in flight)	250	-9.4
Water	290	62.6

10. Thermometric temperatures of target and background materials during moderate cloud conditions are as follows: all targets and backgrounds, except water, have a temperature of 300°K; water temperature is 290°K.

11. Thermometric temperatures of target and background materials during moderate rain conditions are as follows: all targets and backgrounds have a temperature of 290°K.

12. Weather models (Ref. 4 and 6) are as follows:

Clear sky—1 percent absolute water vapor at sea level.

Moderate cloud—uniform condensed water content of 0.3 g/m^3 from 3000 to 6000 ft superimposed on the clear sky condition. (Visibility in cloud is about 400 ft.)

[3]The thermal temperatures assumed for the targets do not represent measured values. They were chosen to demonstrate the effect thermal temperatures have on radiometry.

Moderate rain—uniform precipitation rate of 4 mm/hr from 0 to 3000 ft superimposed on the moderate cloud model.

Cumulus cloud—

Height (ft x 1000)	Water Content (g/m^3)
5.0	0.0
7.0	1.0
9.0	1.6
13.0	2.8
17.0	3.0
19.0	2.8
21.0	0.5
22.5	0.0

REFERENCES

1. Dicke, R. H., "The Measurement of Thermal Radiation at Microwave Frequencies," Review of Scientific Instruments, pp. 268-75, July 1946.

2. Porter, R. A., and M. D. Parker, A Survey of Microwave Radiometers With Terrain-Mapping Applications, RAD-TR-9-60-20, ASTIA AD 243 229, AVCO Corp., 23 August 1960.

3. Bell Telephone, Microwave Research—Final Report, Report No. 24269-K, Bell Telephone Laboratories, 30 March 1956.

4. Booth, L. L., and E. Weger, Feasibility Study of Target Location and Charting by Passive Microwave Radiometry, Report No. RADC-TR-59-125, Westinghouse, Air Arm Division, Baltimore, Md., 26 June 1956. (Confidential)

5. Jane's All the World's Aircraft, 1961-1962, Ed., John W. R. Taylor. New York: McGraw-Hill Book Company, Inc.

6. Wilcox, C. H., Effects of Atmospheric Attenuation on Reconnaissance Antenna Design, Report No. 1 on Contract AF19(604)-1708, Hughes Aircraft Co., 20 February 1957.

NOMENCLATURE

A_a	Intercept area of antenna beam
A_t	Target area
B	Predetection bandwidth of a radiometer
C	Capacitance
F	Noise figure
G	Antenna gain
H	Height or range at which $\Delta T = 1°K$
J	Radiation power density in microwave region
P	Available noise power at the transmission line termination; equal to the received radiation power available from the radiation resistance of the antenna
Q	Constant determined by the type of radiometer system used
Q_p	Lumped constant that results when the equation for T is in terms of p instead of b
R	Resistance
T	Antenna temperature
T_B	Radiometric background temperature
T_b	Thermometric background temperature
T_f	Function describing the radiometric temperature of the material surrounding the antenna
T_r	The apparent radiometric temperature of a reflected source at the target
T_s	Radiometric sky temperature at the target

T_T	Radiometric target temperature
T_t	Thermometric target temperature
T_0	Reference temperature for calculating noise figure (usually 290°K)
T_1	$T_s + (\epsilon_b/\epsilon_t)(T_b - T_s)$, the value of T_t which causes $\Delta T' = \Delta T = 0$
T_γ	Radiometric temperature of a source that is transmitted through the target
a	Semimajor axis of elliptical intersection of the antenna beam with the earth
b	Semiminor axis of elliptical intersection of the antenna beam with the earth and (in one instance only) postdetection bandwidth of radiometer
f_s	Scan frequency
h	Height of aircraft
p	Number of picture elements scanned per second
r	Slant range from radiometer to target
v	Aircraft ground speed
w	Width of road or river along flight path
y	Width of road or river transverse to flight path
α	Atmospheric attenuation (db/km)
β	Antenna beam width
γ	Atmospheric transmissivity
ΔT	Apparent radiometric temperature difference between target and background available at a radiometer with an antenna beam width β having circular symmetry
$\Delta T'$	Apparent radiometric temperature difference between target and background materials without antenna and range effects

δT	Minimum detectable temperature difference of radiometer system
ϵ	Emissivity
ϵ_b	Background emissivity
ϵ_e	Earth emissivity
ϵ_t	Target emissivity
θ	Radiometer look angle measured from the vertical
ξ	Antenna beam width along flight path
ρ	Target reflectivity
ϕ, ϕ_m	Scan angle and maximum scan angle (one half of peak-to-peak)
Ω	Ω_t/Ω_a, which equals A_t/A_a
Ω_a	Solid angle subtended by the antenna beam (3-db beam width)
Ω_t	Solid angle subtended by the target

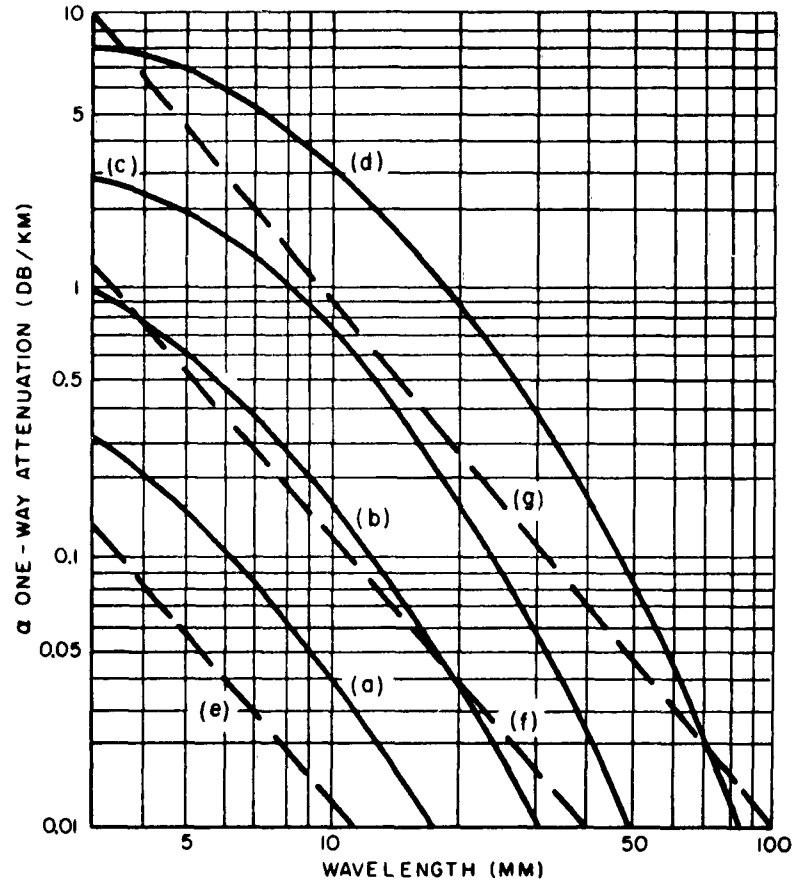

(a) 0.25 mm hr (Drizzle)
(b) 1 mm hr (Light Rain)
(c) 4 mm hr (Moderate Rain)
(d) 16 mm hr (Heavy Rain)
(e) 0.032 g/m^3 (Visibility about 2000 ft)
(f) 0.32 g/m^3 (Visibility about 400 ft)
(g) 2.3 g/m^3 (Visibility about 100 ft)

FIGURE 1. Theoretical Values of Attenuation by Rain and Fog. (Solid curves show attenuation in rain of intensity; dashed curves show attenuation in fog or cloud.)

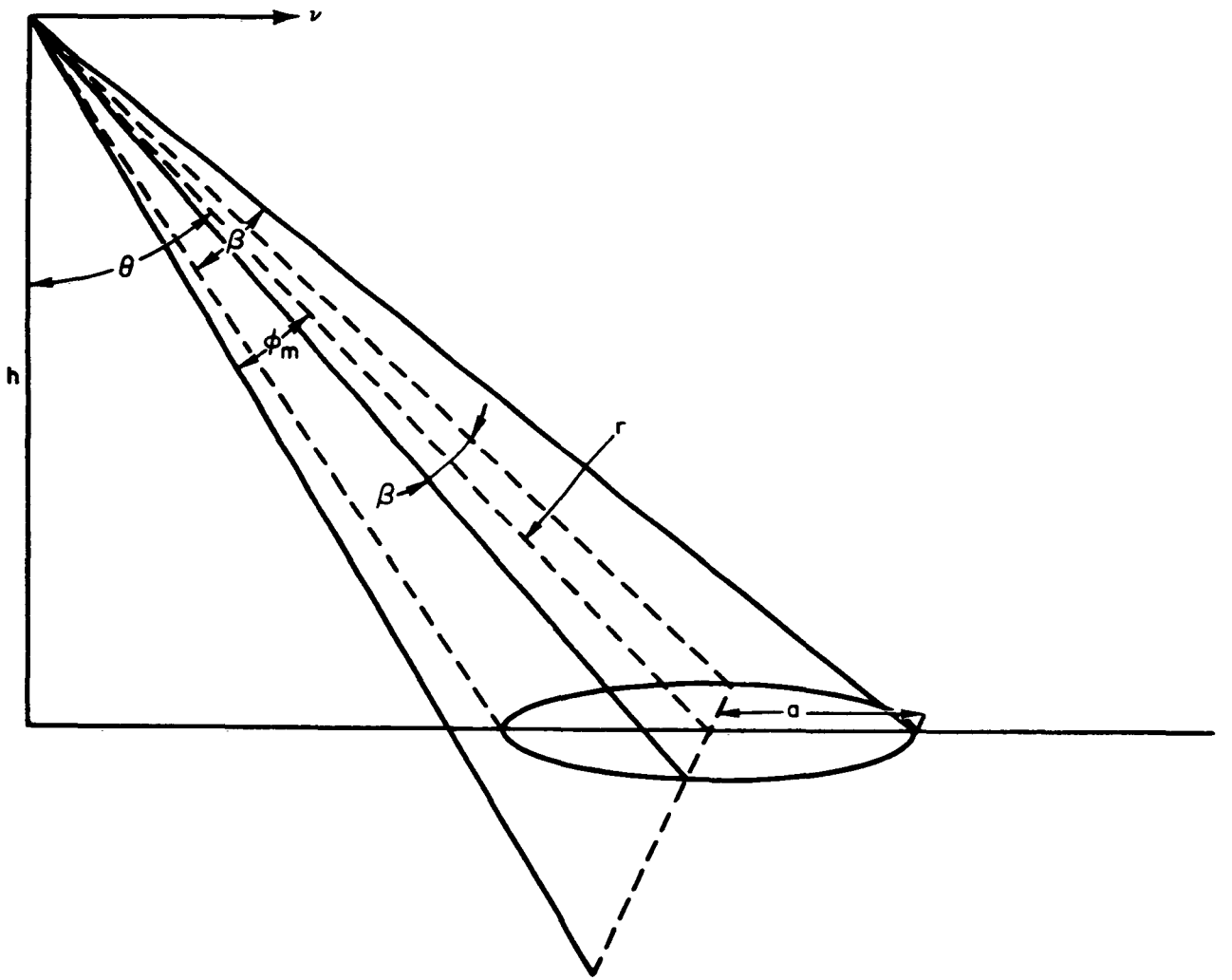

FIGURE 2. Scanning Geometry

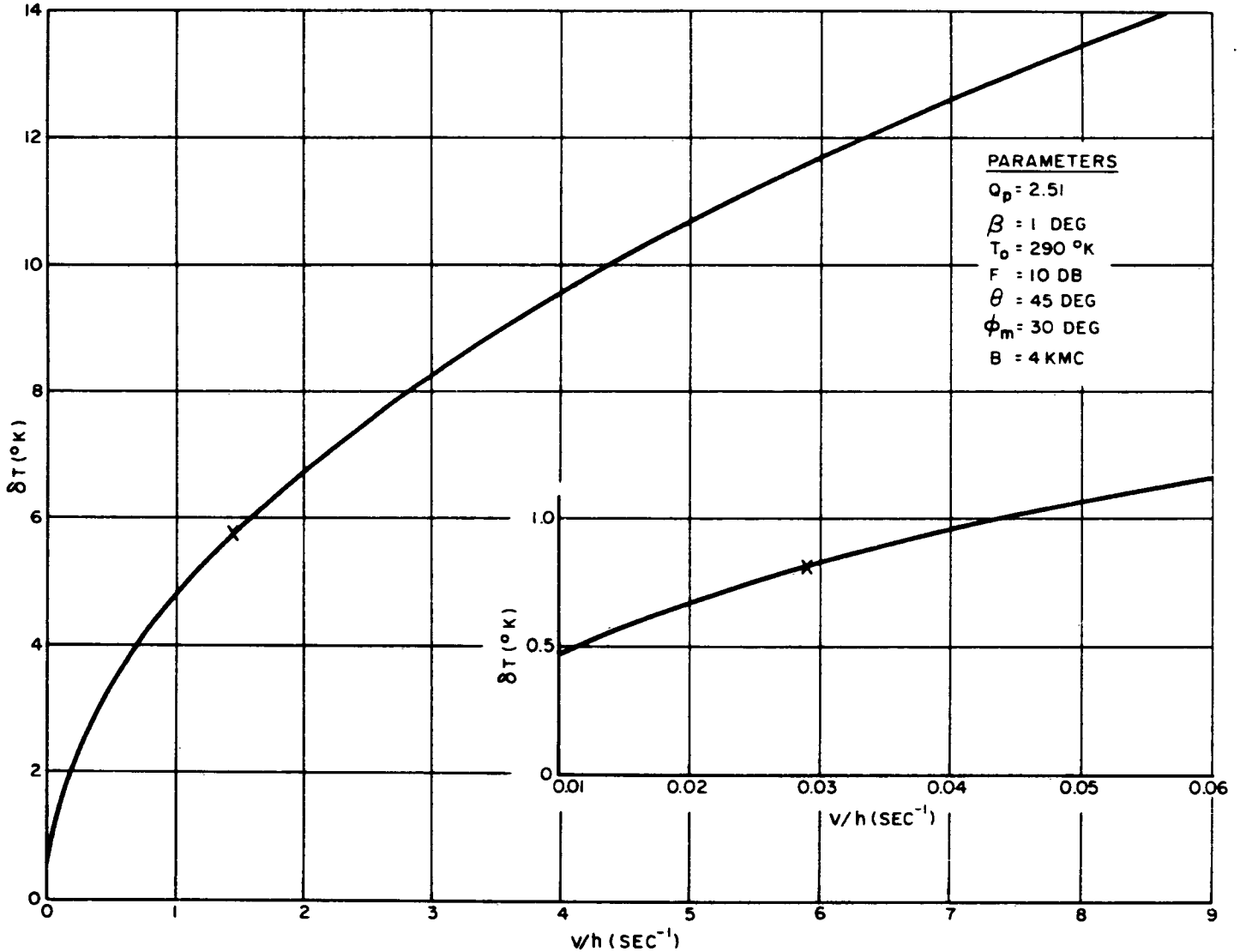

FIGURE 3. δT as a Function of (v/h)

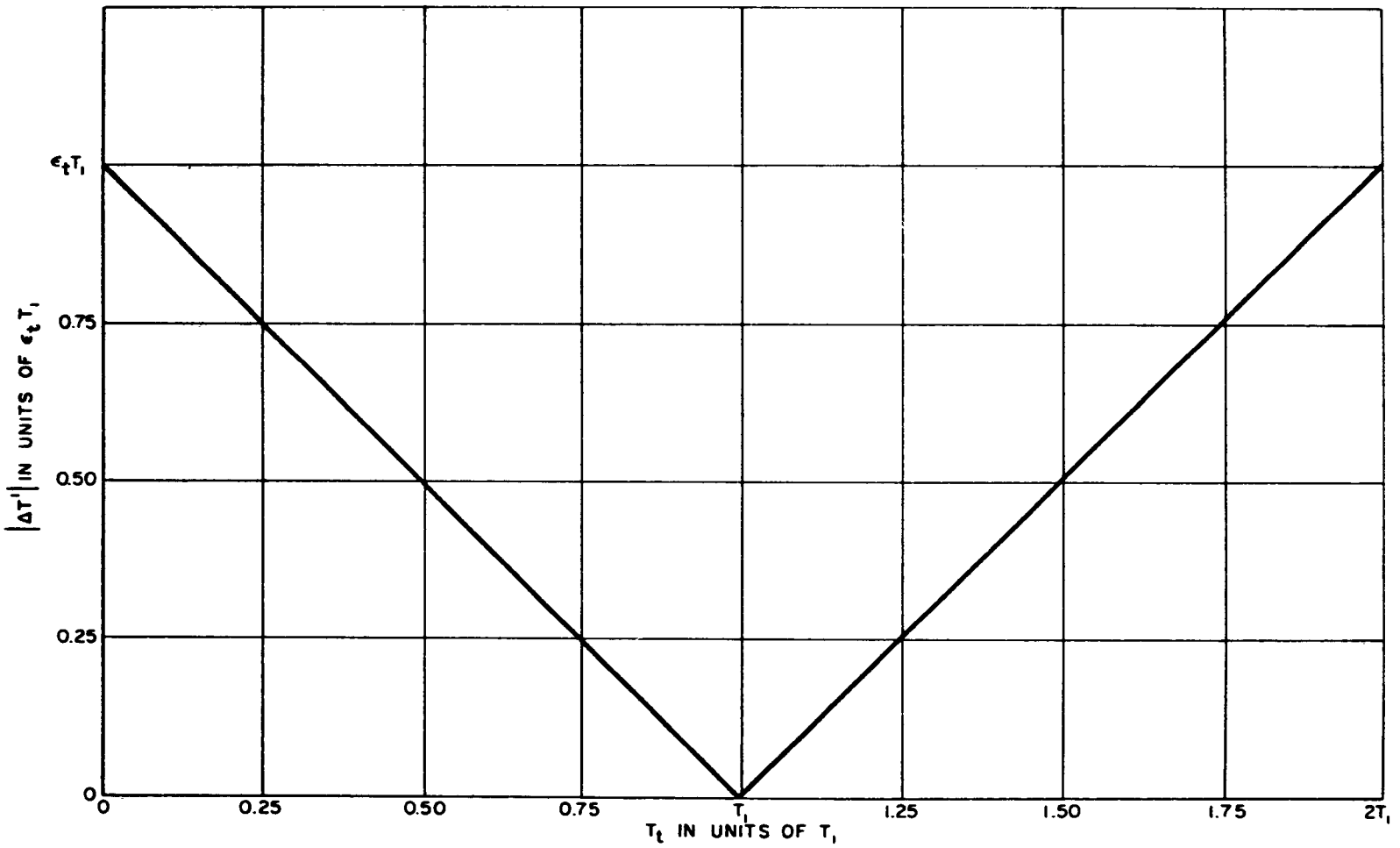

FIGURE 4. $\Delta T' = \epsilon_t | T_t - T_1 |$

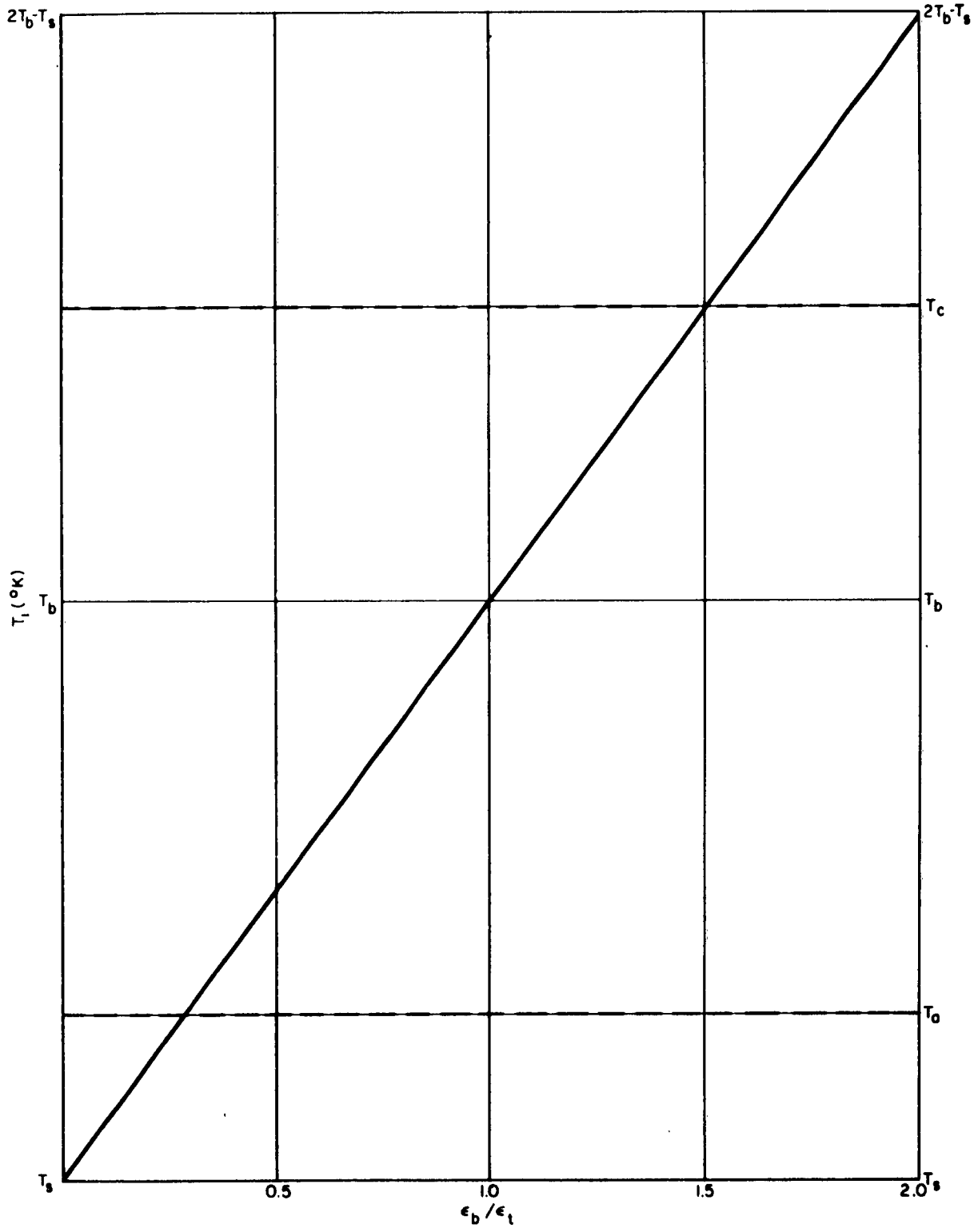

FIGURE 5. T_1 as a Function of (ϵ_b/ϵ_t)

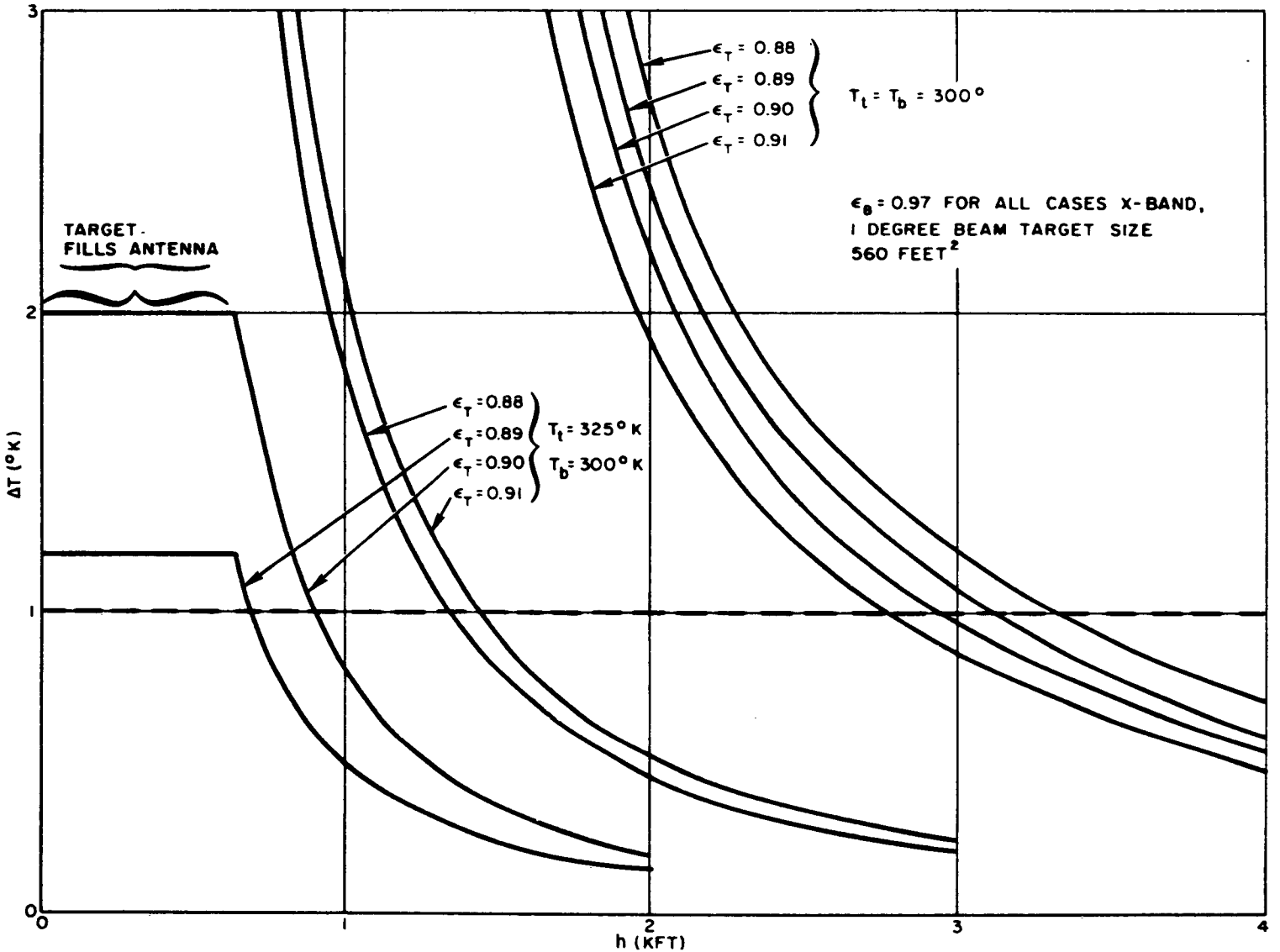

FIGURE 6. ΔT as a Function of Altitude for Various Targets in a Fixed Background

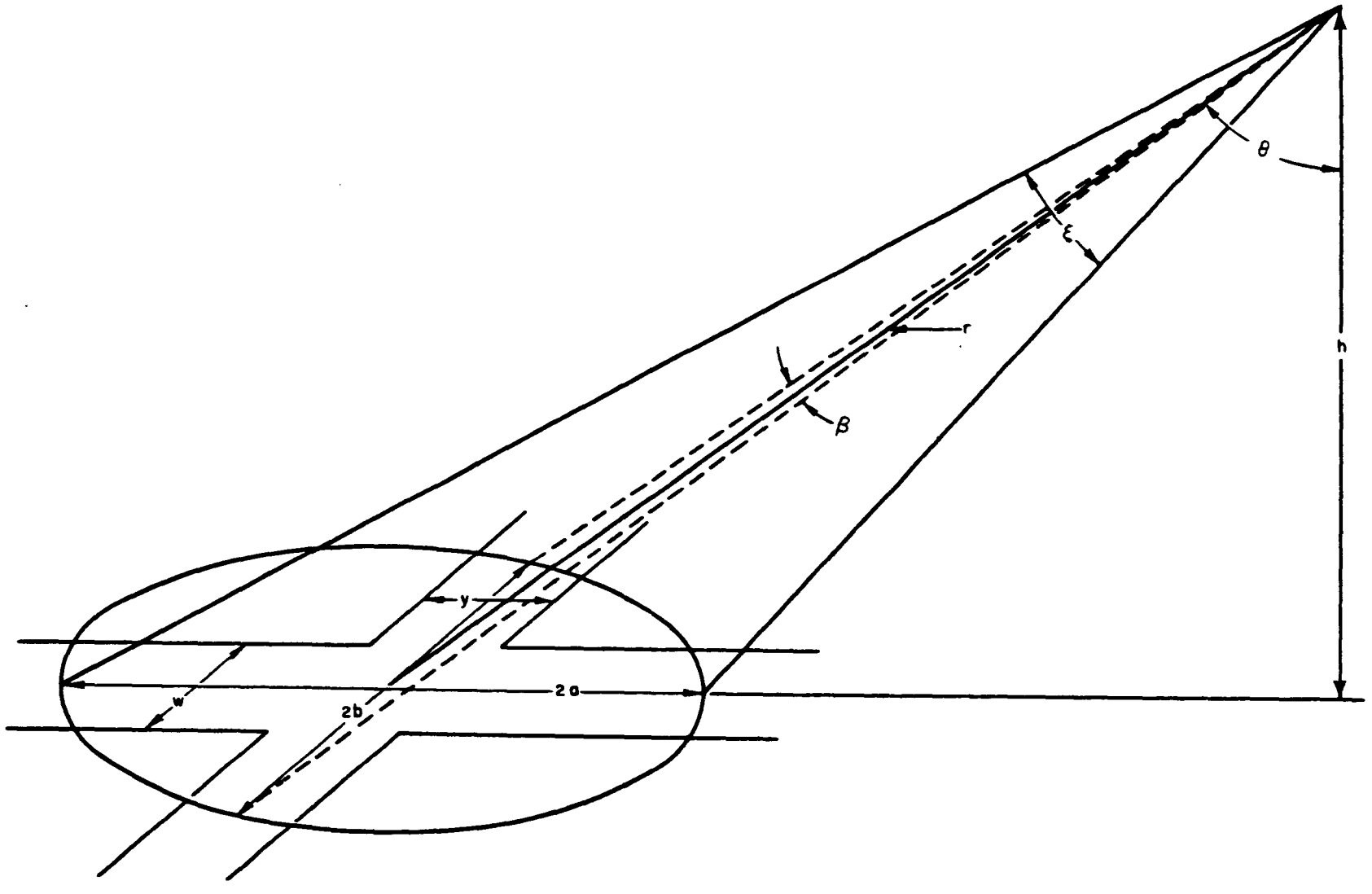

FIGURE 7. Road Intersection Geometry

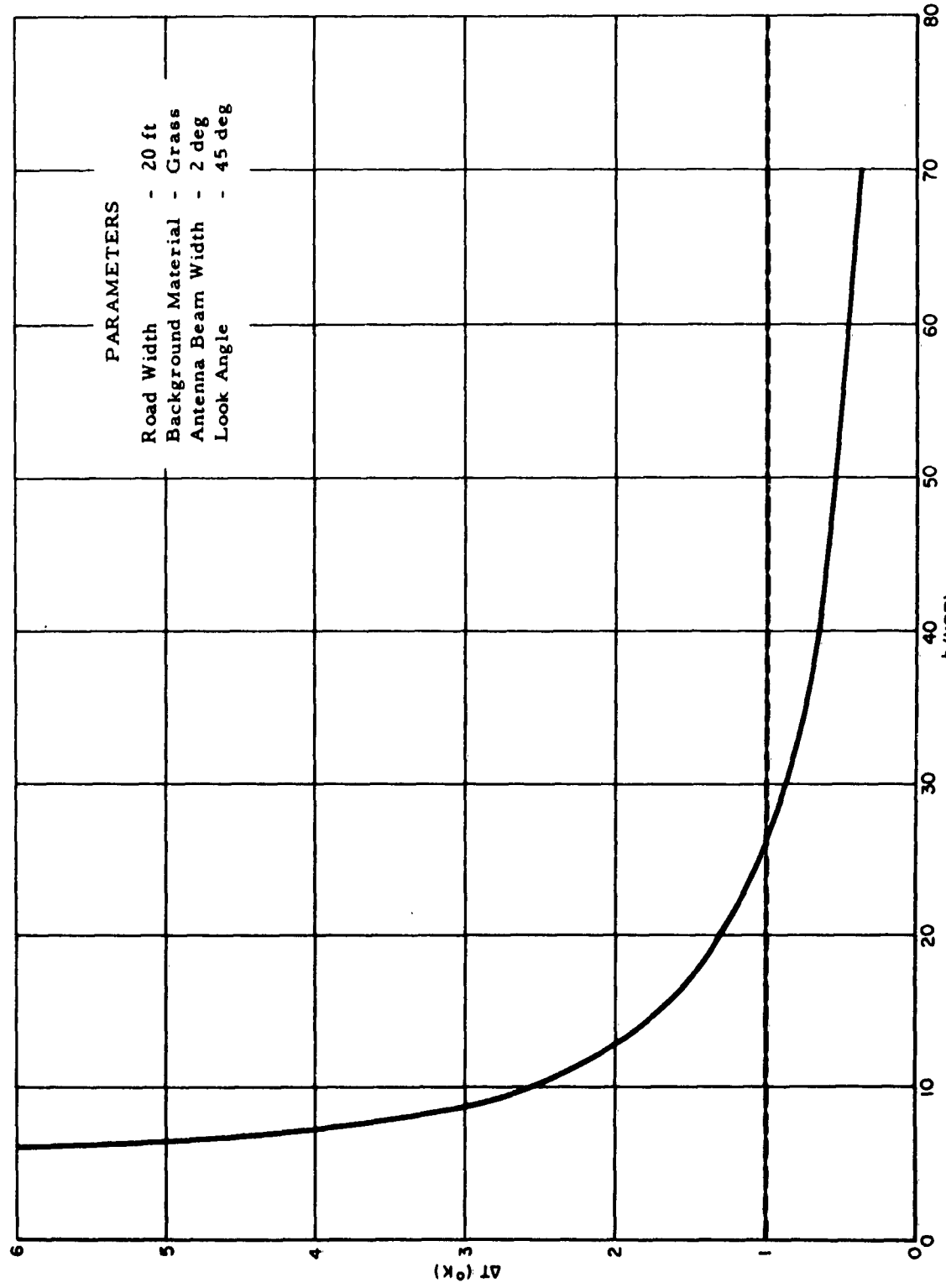

FIGURE 8. ΔT for a Concrete Road Intersection at X-Band in Clear Weather

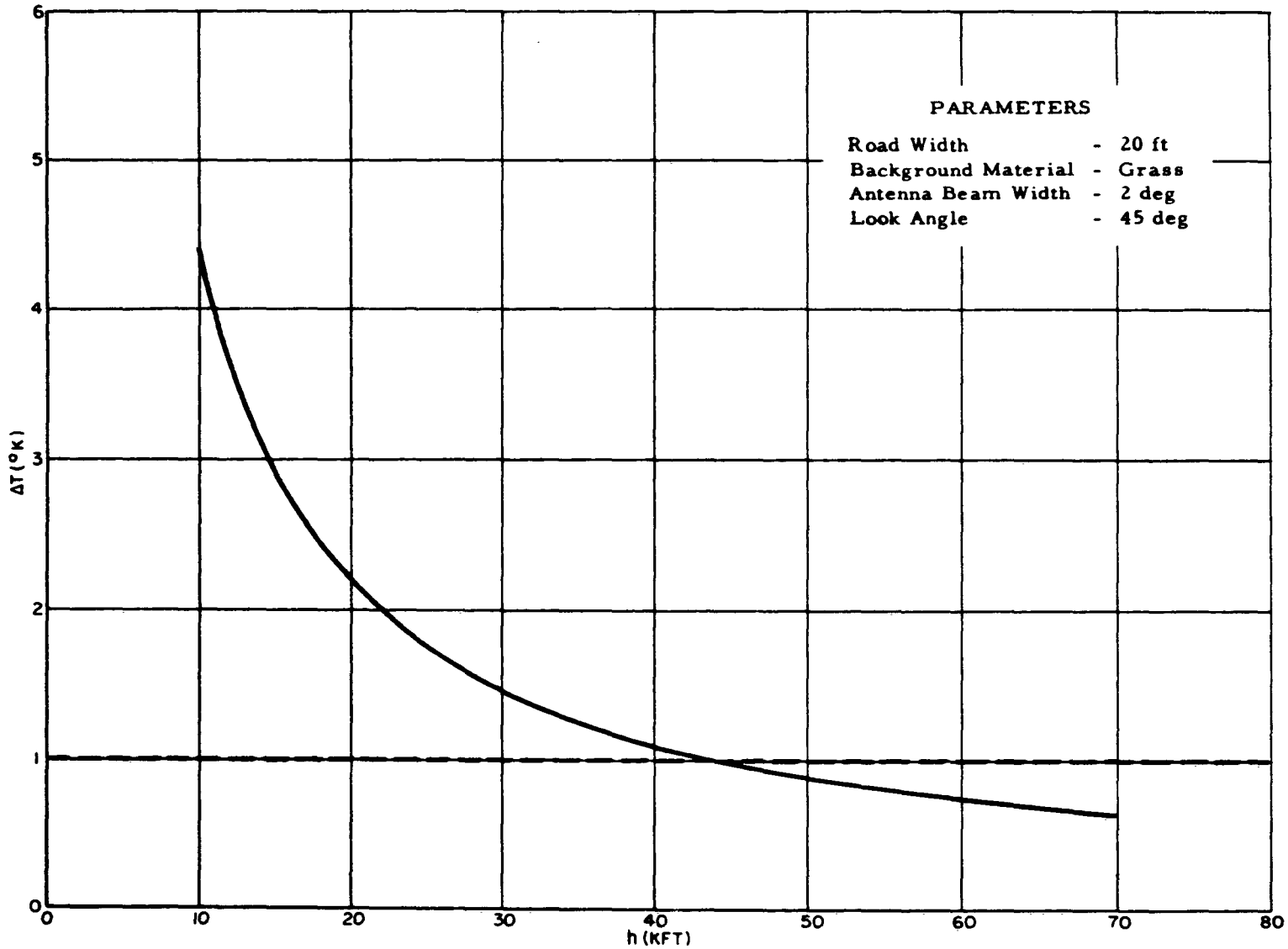

FIGURE 9. ΔT for a Concrete Road Intersection at X-Band in Moderate Clouds

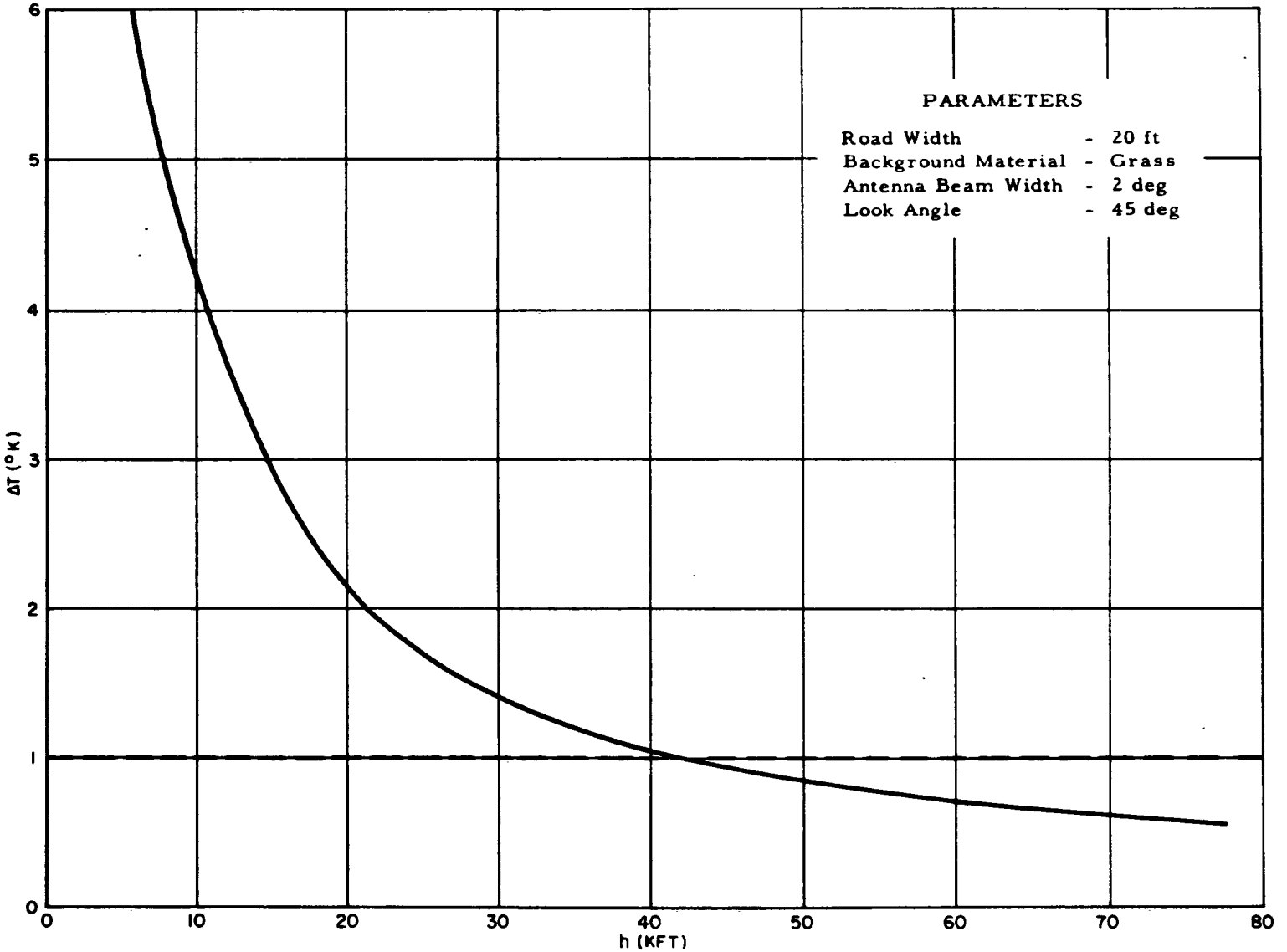

FIGURE 10. ΔT for a Concrete Road Intersection at X-Band in Moderate Rain

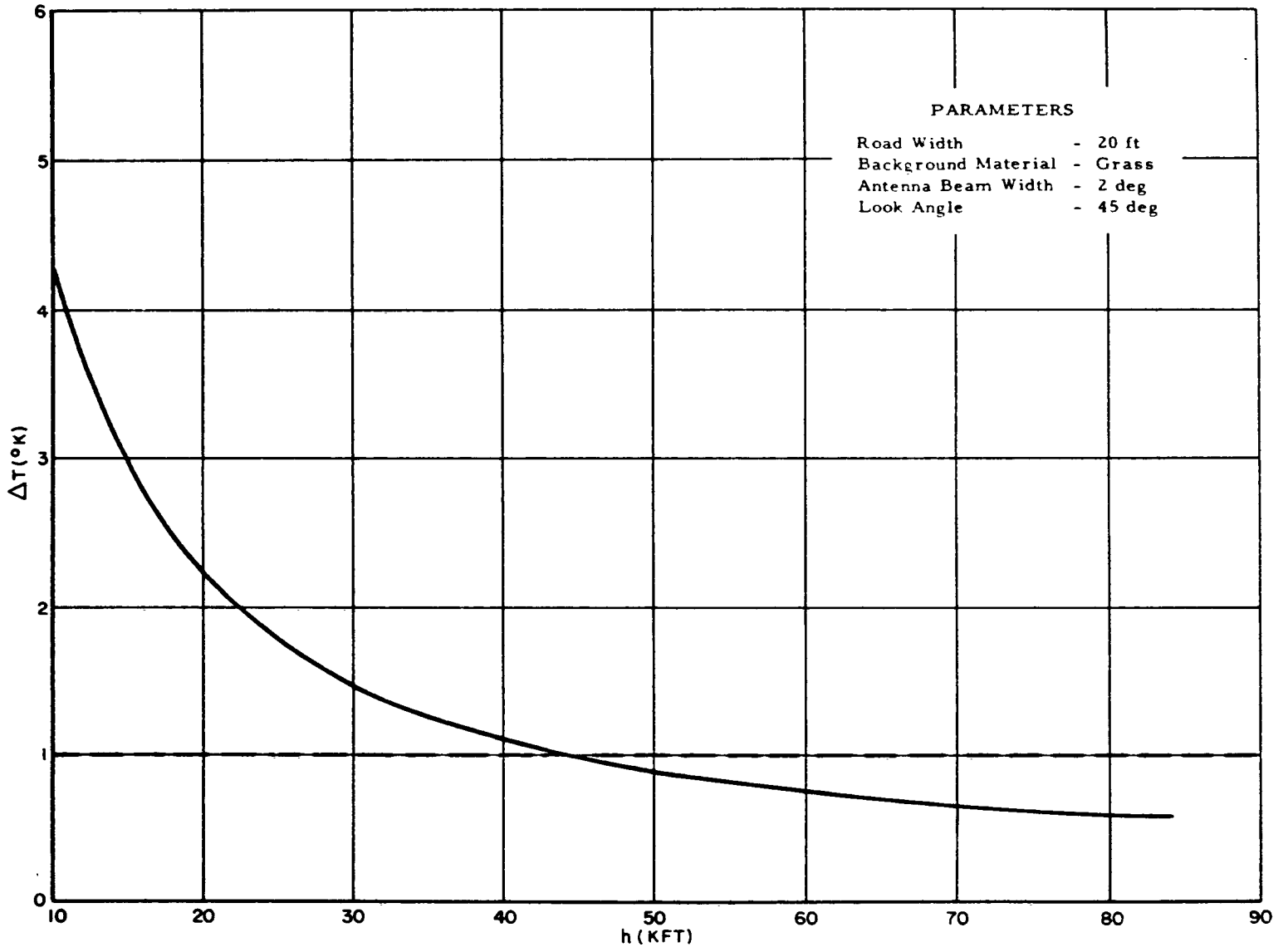

FIGURE 11. ΔT for a Concrete Road Intersection at K_a-Band in Clear Weather

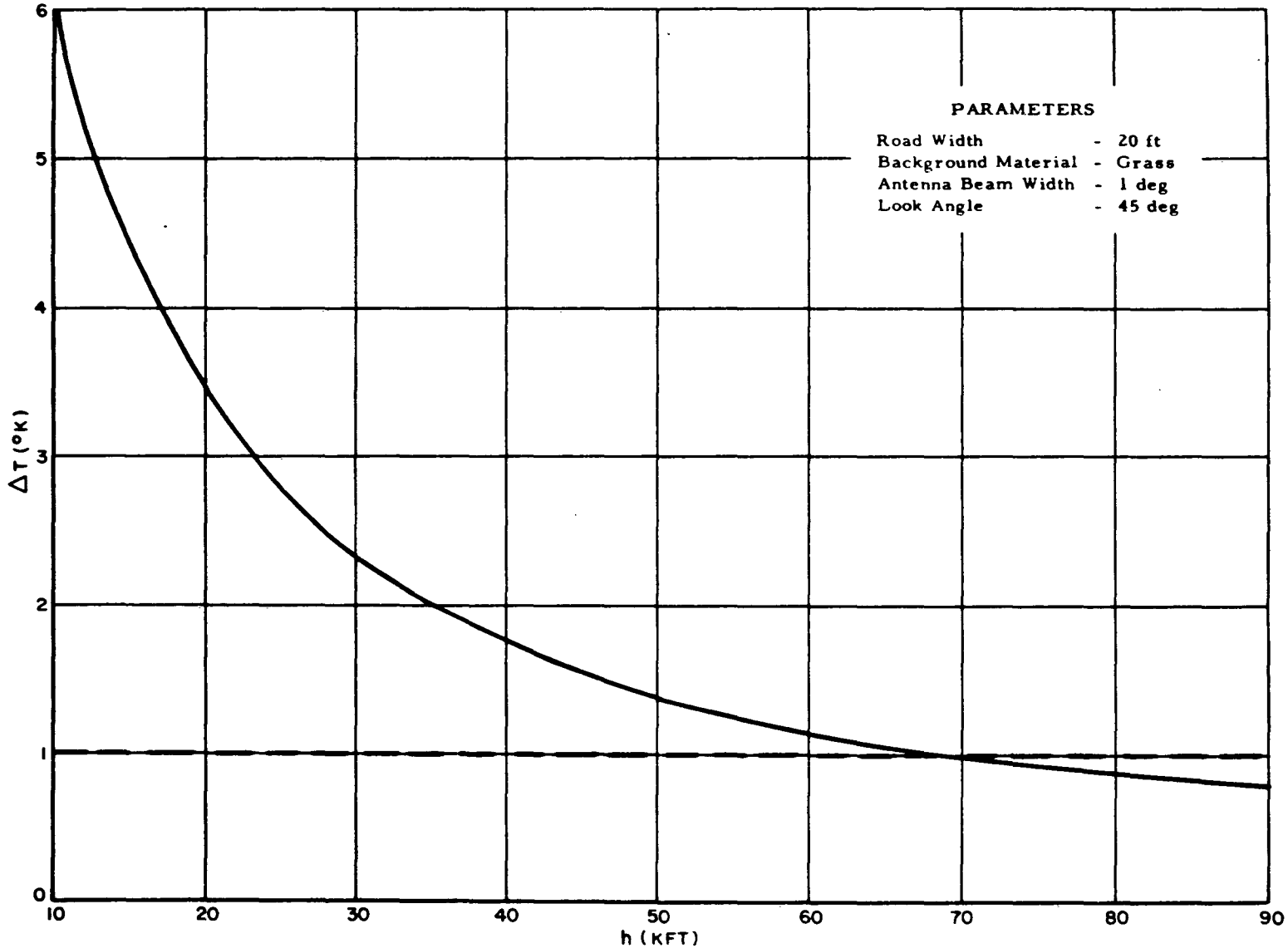

FIGURE 12. ΔT for a Concrete Road Intersection at K_a-Band in Moderate Clouds

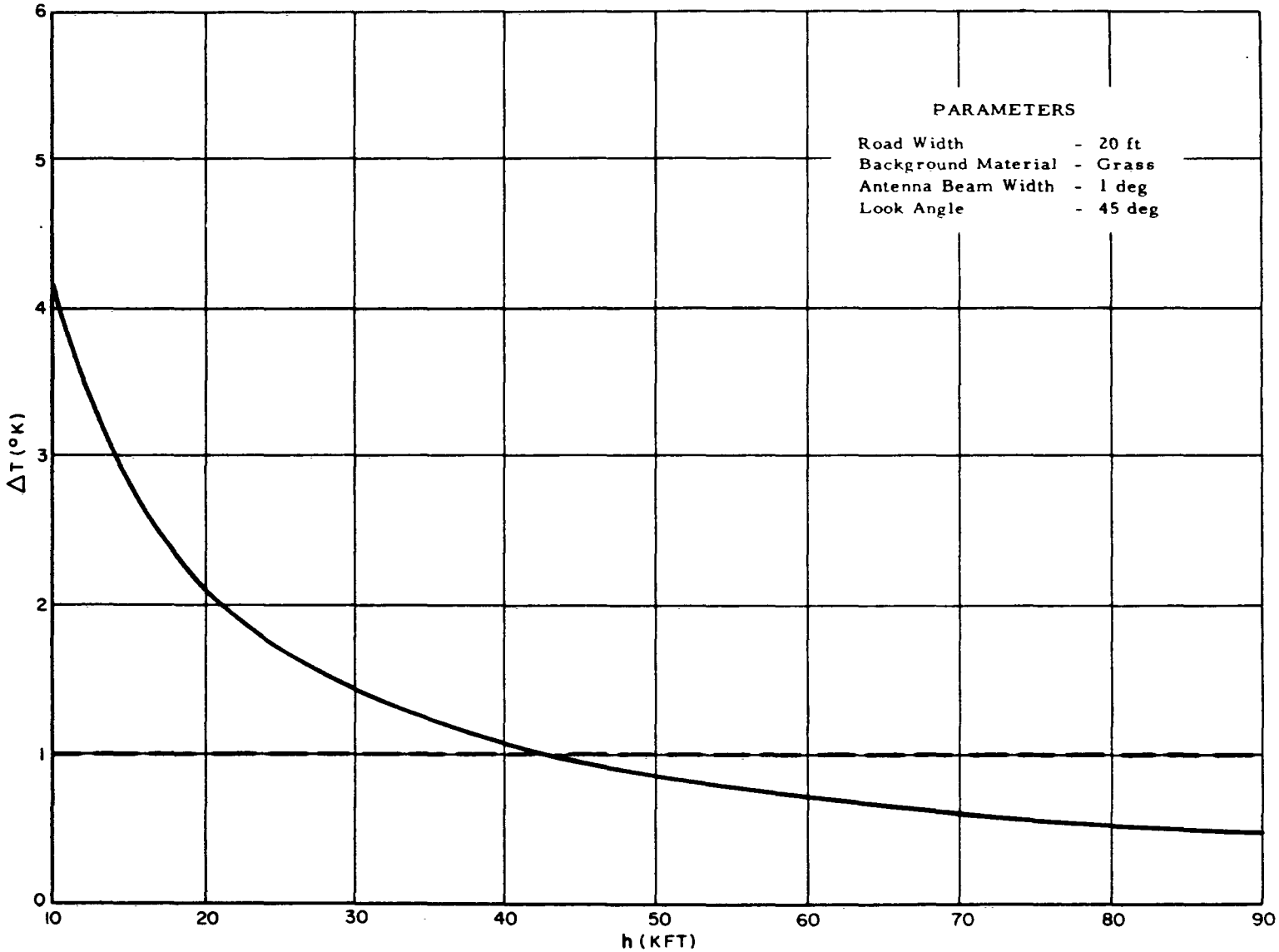

FIGURE 13. ΔT for a Concrete Road Intersection at K_a-Band in Moderate Rain

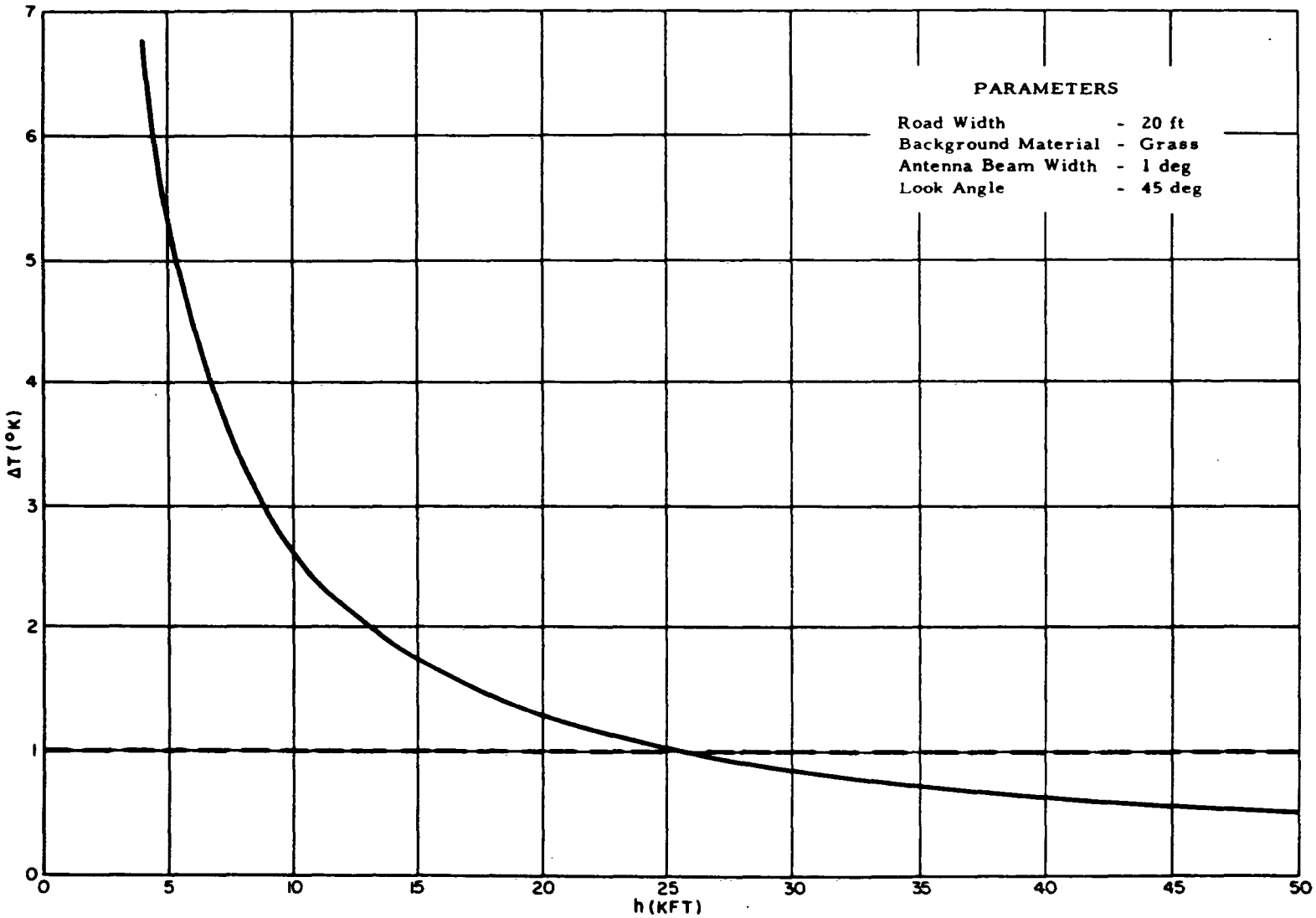

FIGURE 14. ΔT for a Concrete Road at K_a-Band in Clear Weather

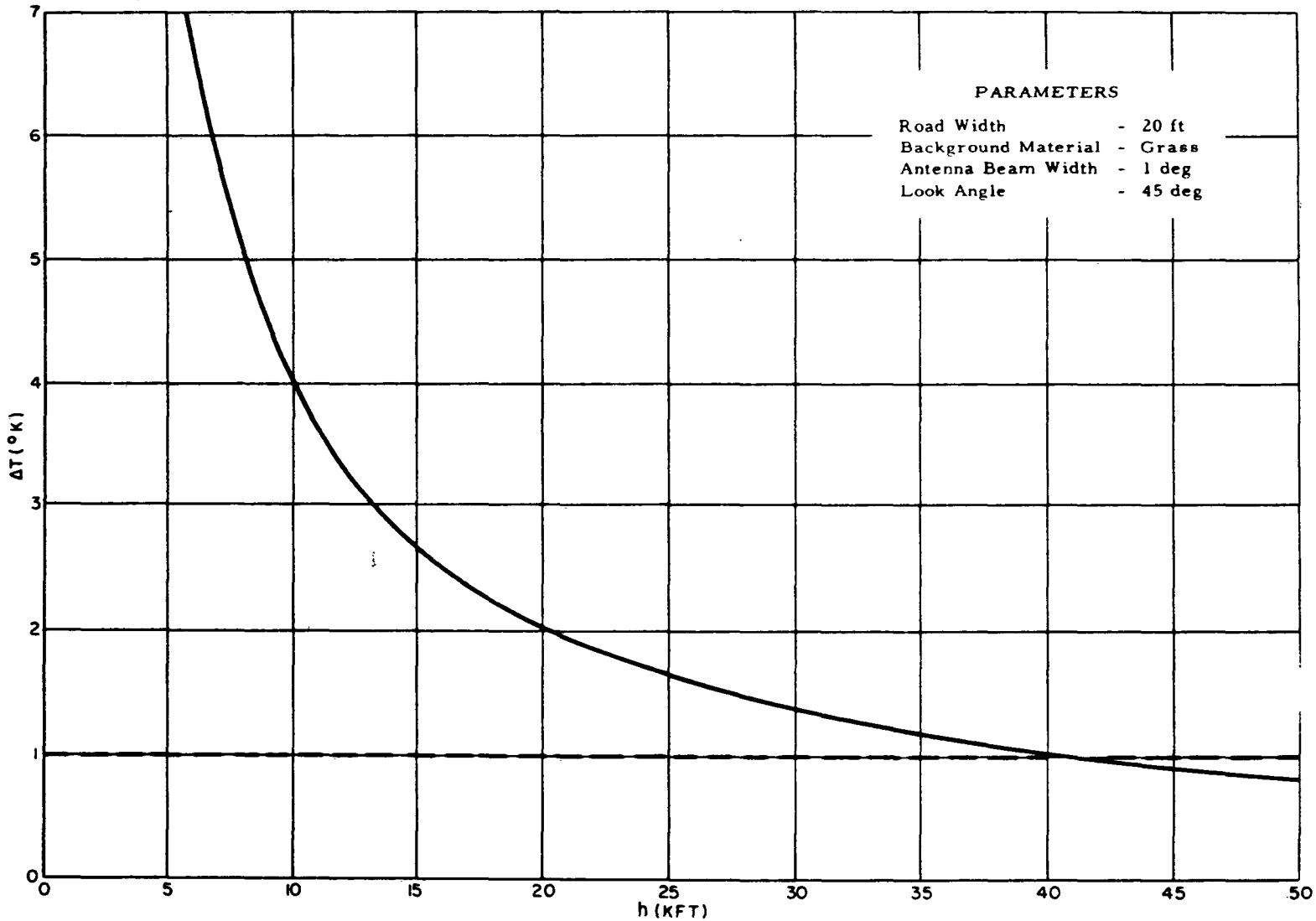

FIGURE 15. ΔT for a Concrete Road at K_a-Band in Moderate Clouds

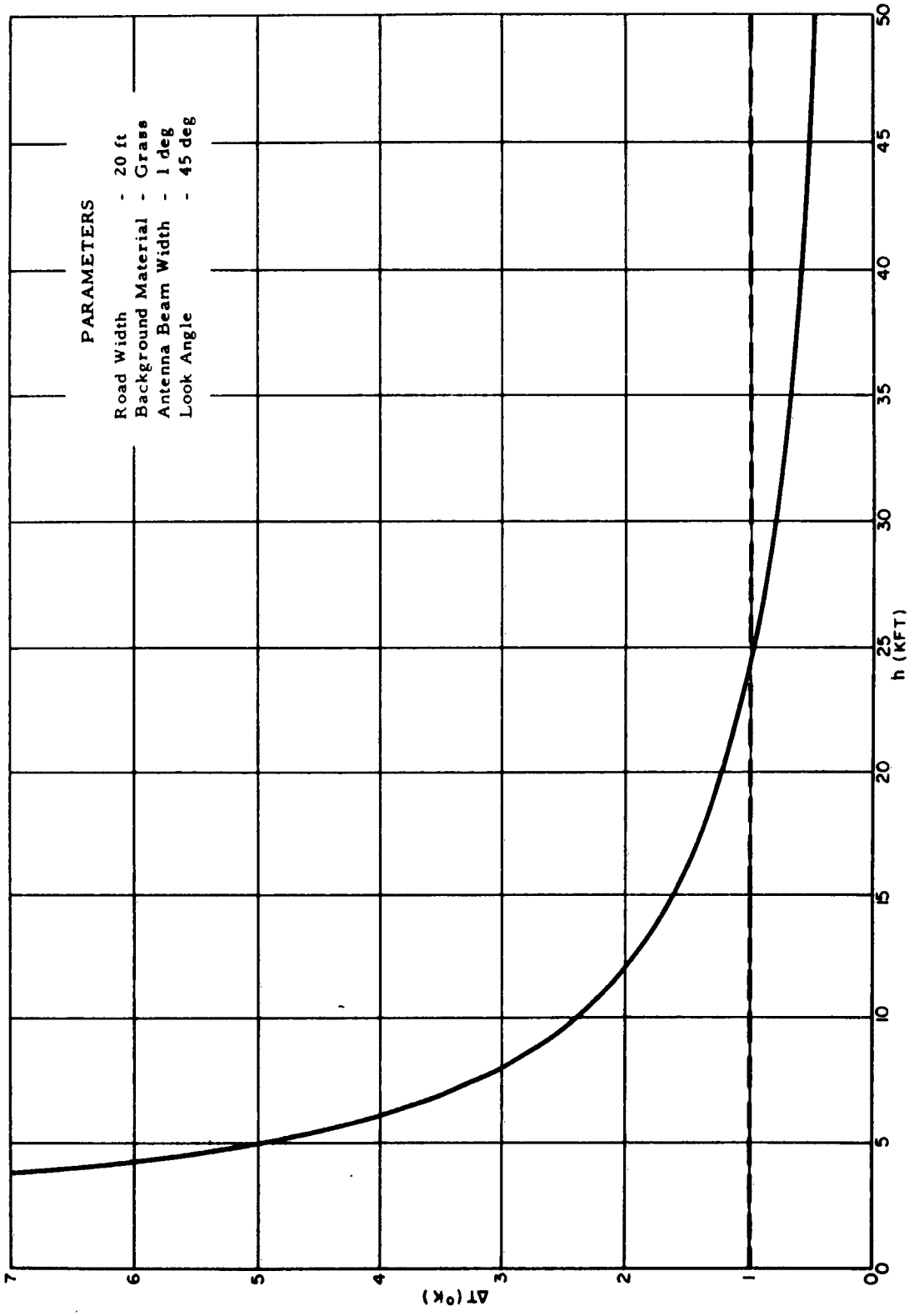

FIGURE 16. ΔT for a Concrete Road at K_a-Band in Moderate Rain

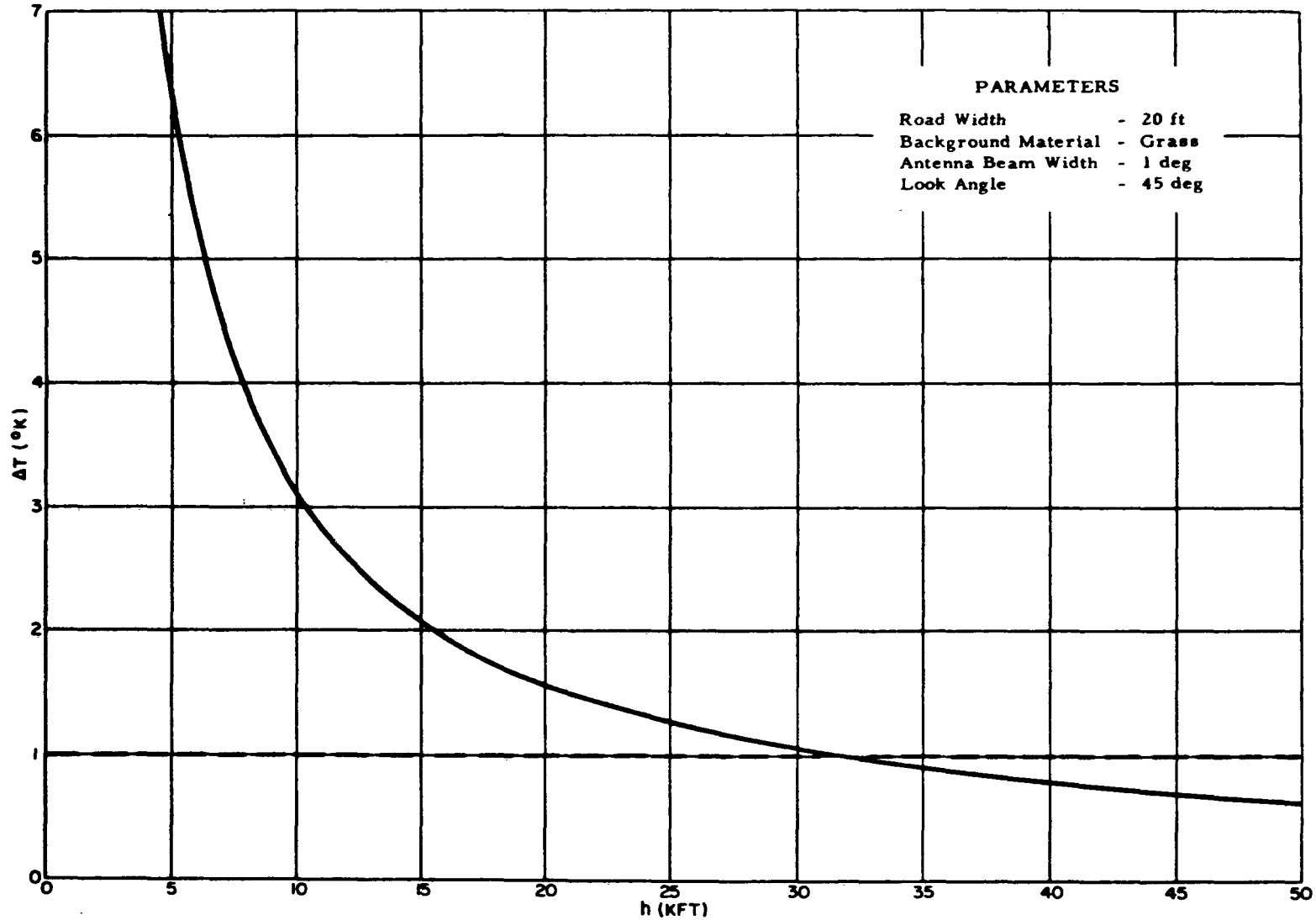

FIGURE 17. ΔT for a Concrete Road at X-Band in Clear Weather

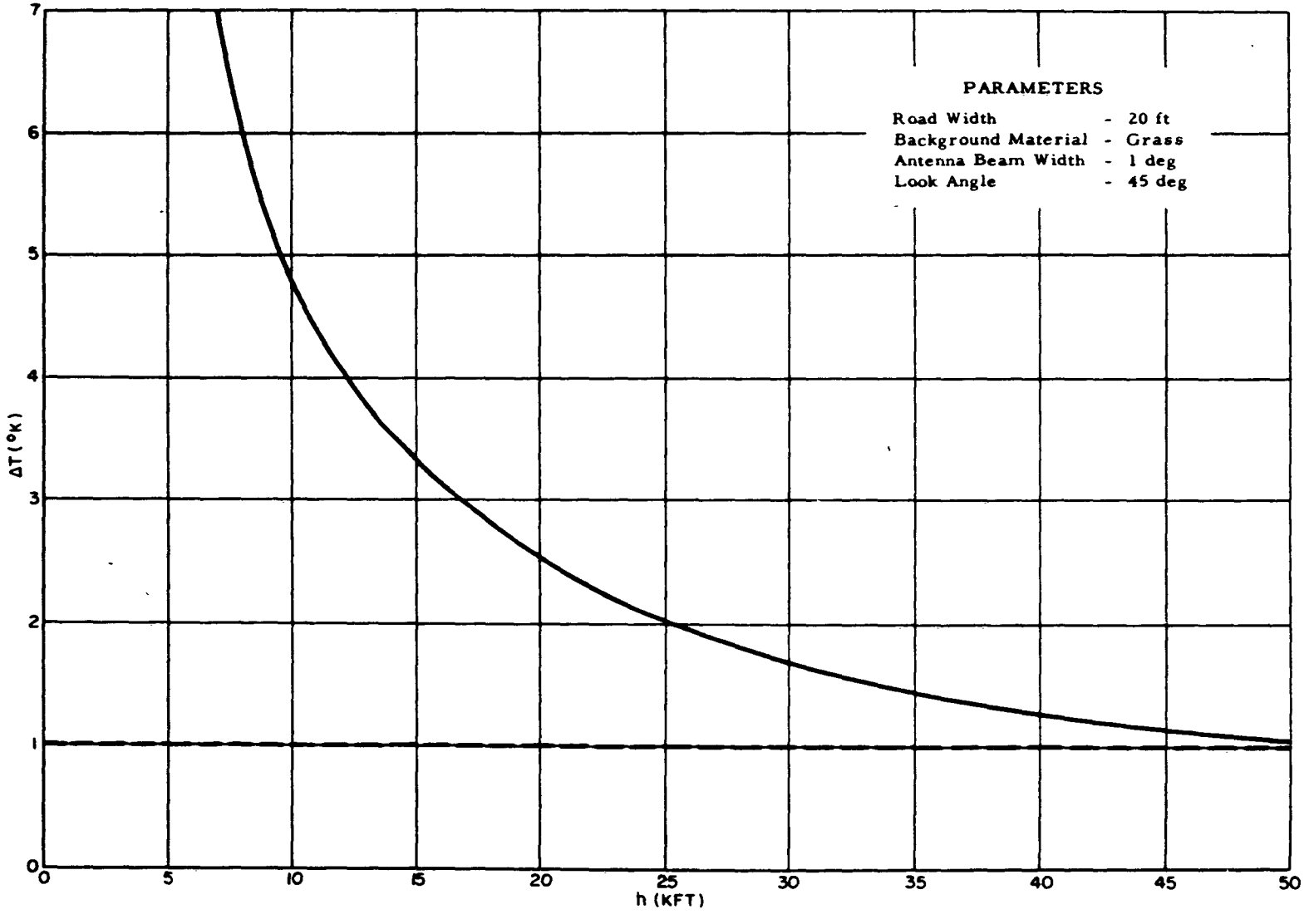

FIGURE 18. ΔT for a Concrete Road at X-Band in Moderate Clouds

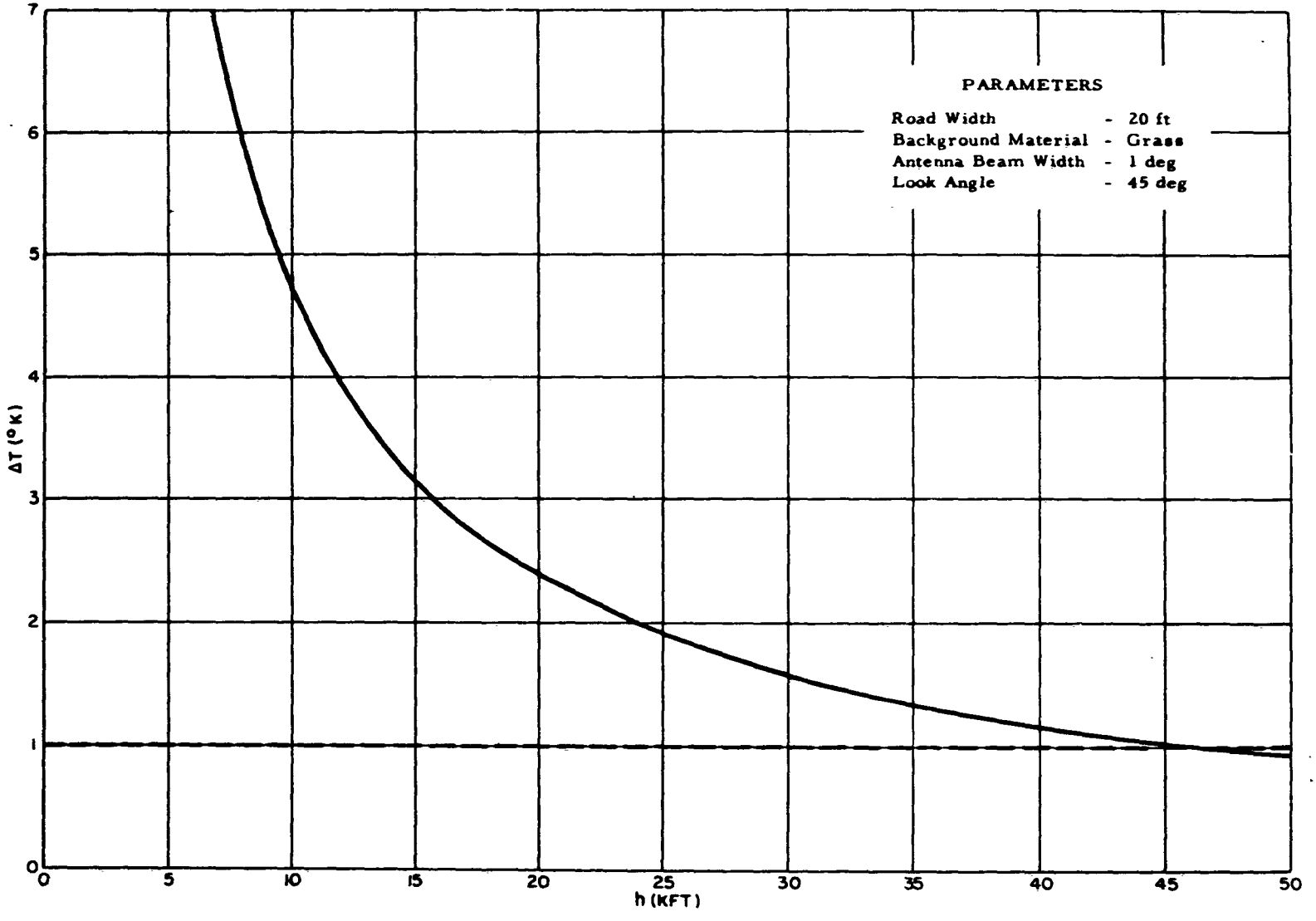

FIGURE 19. ΔT for a Concrete Road at X-Band in Moderate Rain

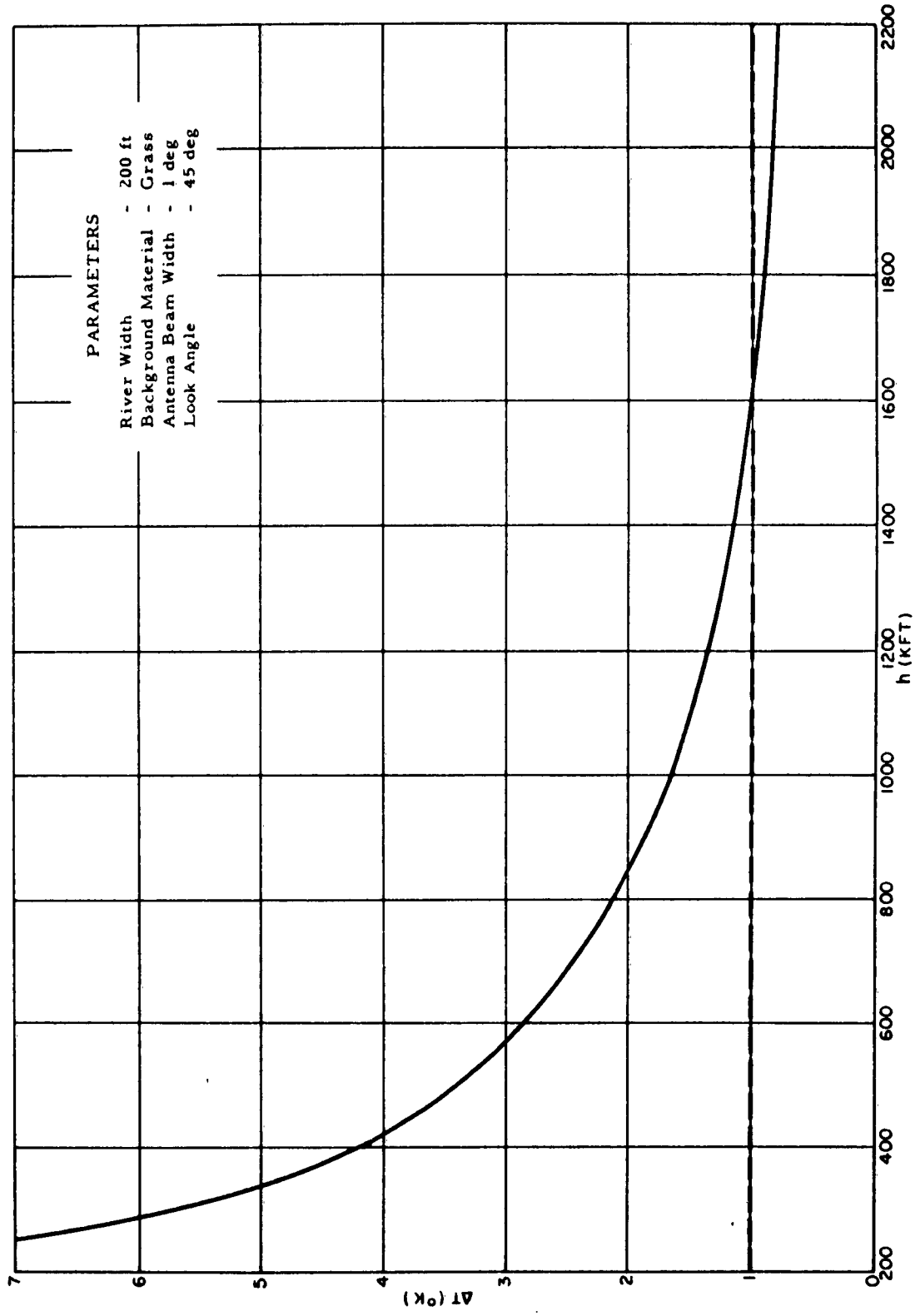

FIGURE 20. ΔT for a River at K_a-Band in Clear Weather

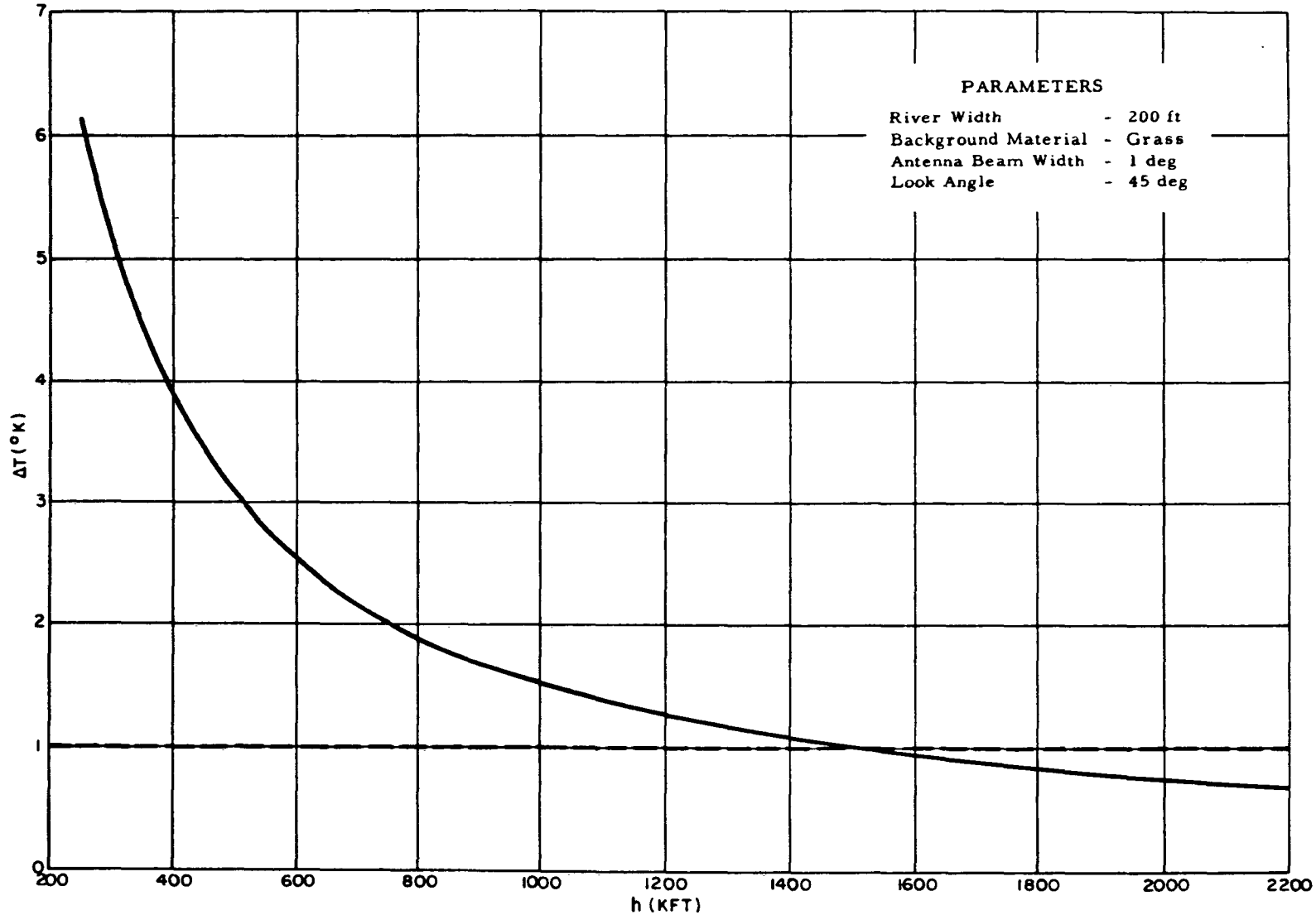

FIGURE 21. ΔT for a River at K_a-Band in Moderate Clouds

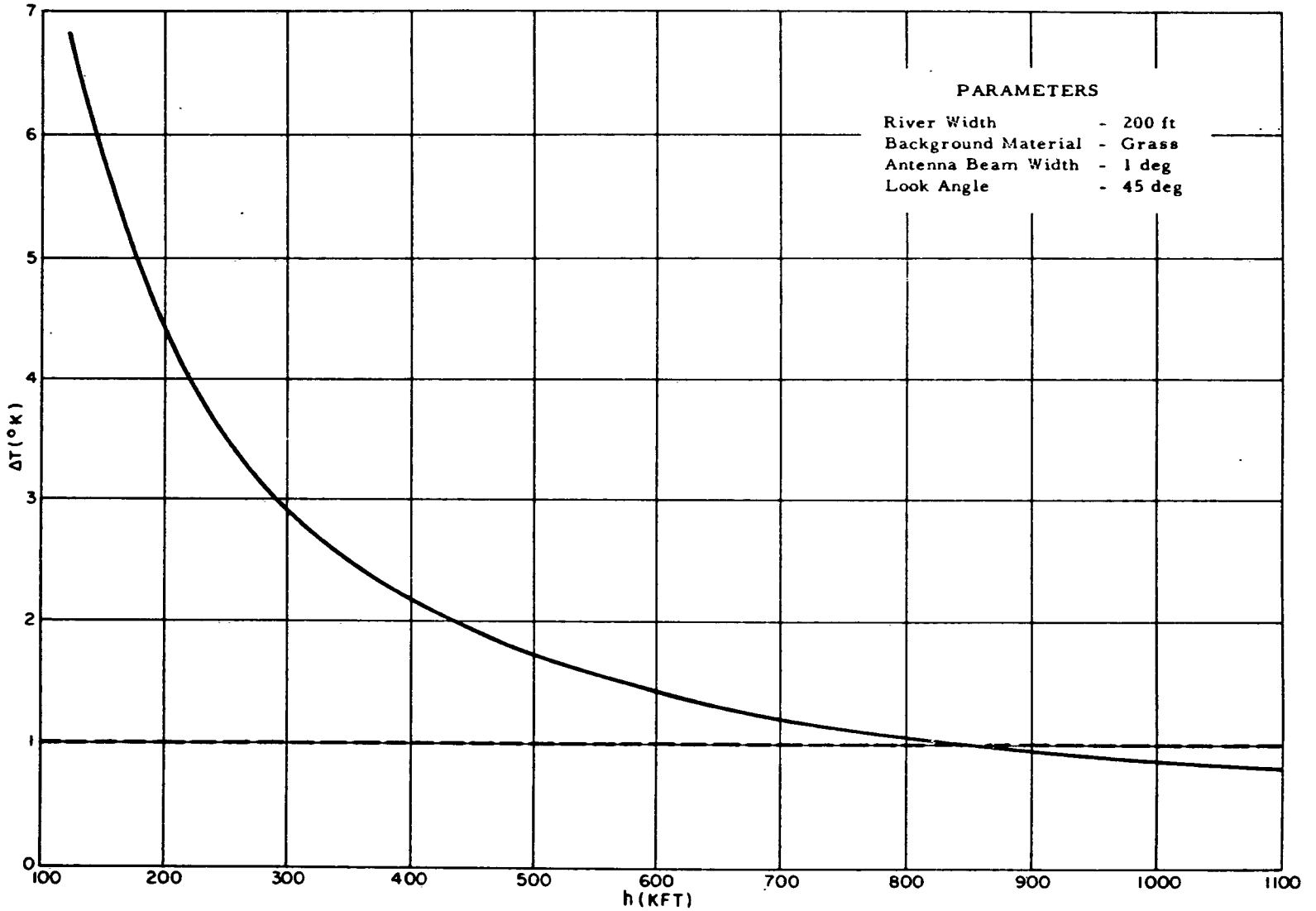

FIGURE 22. ΔT for a River at K_a-Band in Moderate Rain

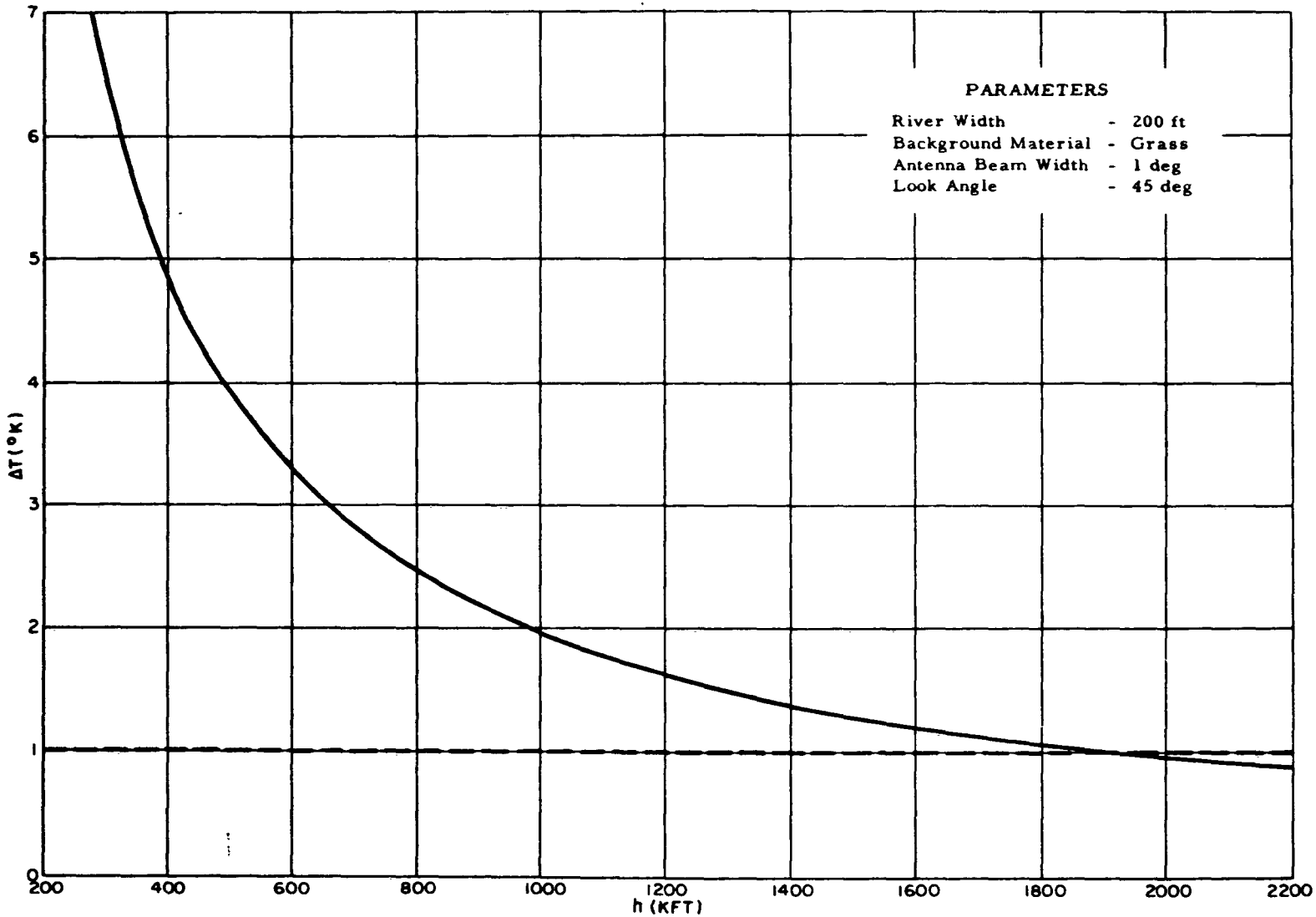

FIGURE 23. ΔT for a River at X-Band in Clear Weather

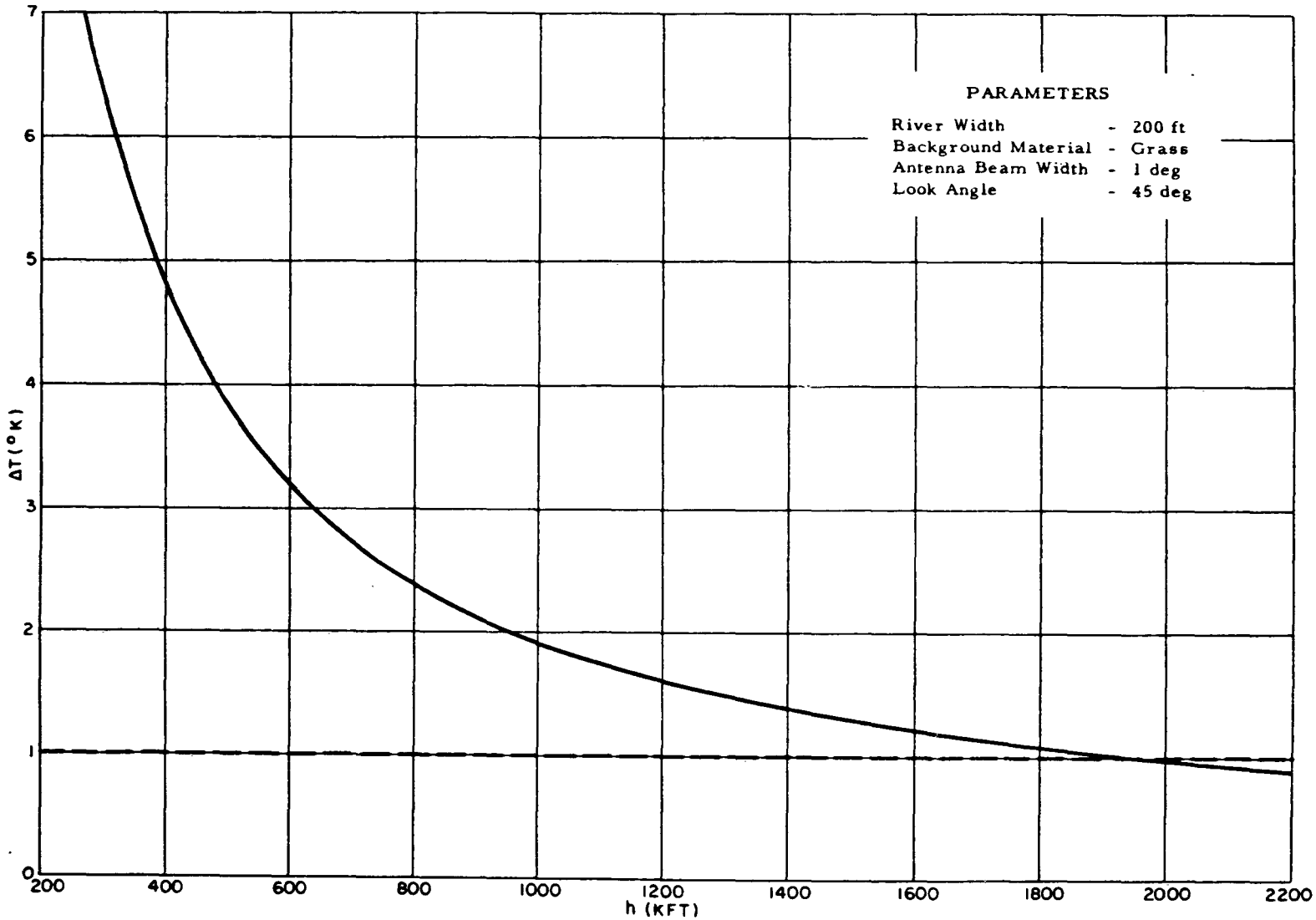

FIGURE 24. ΔT for a River at X-Band in Moderate Clouds

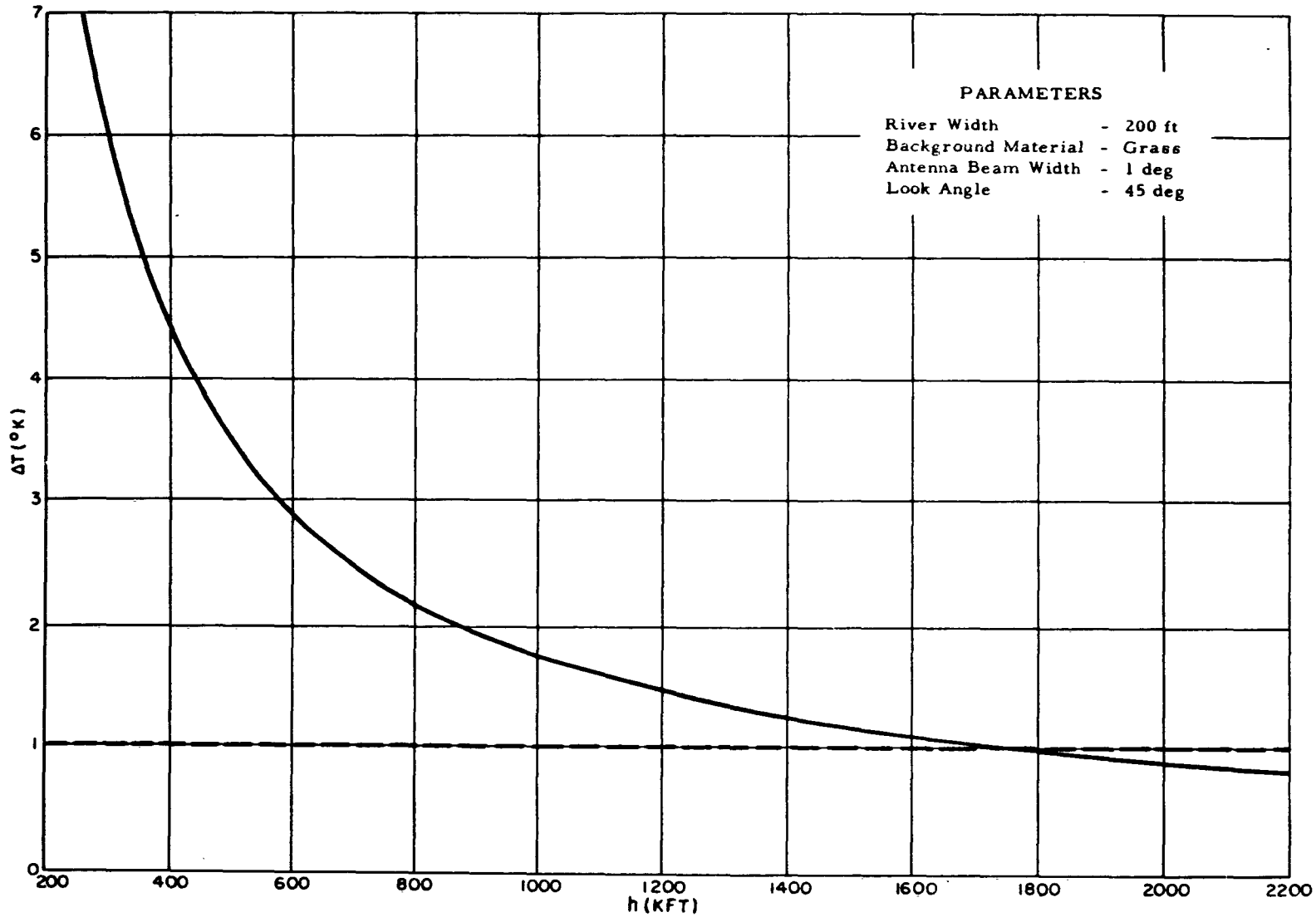

FIGURE 25. ΔT for a River at X-Band in Moderate Rain

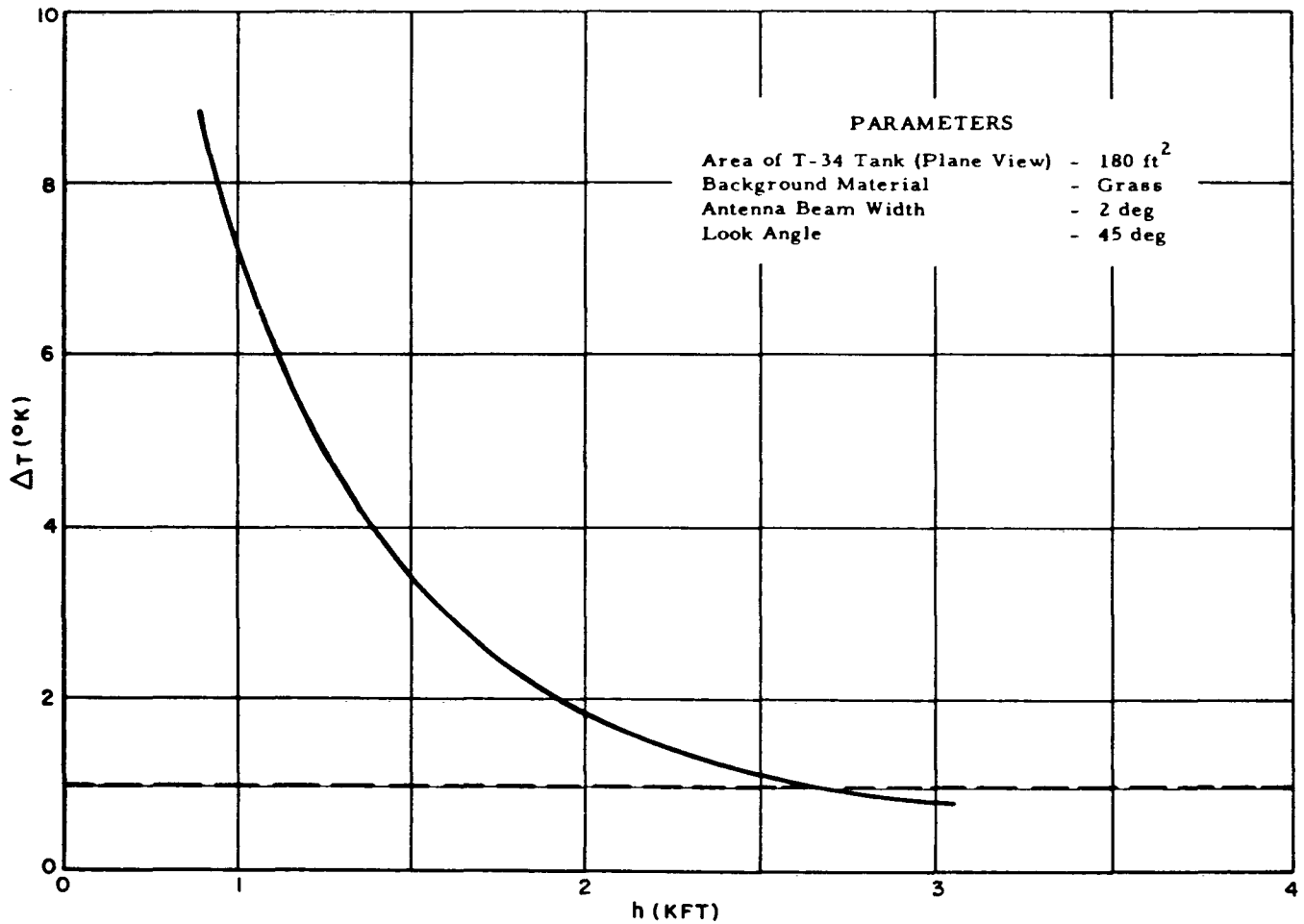

FIGURE 26. ΔT for One T-34 Tank at X-Band in Clear Weather

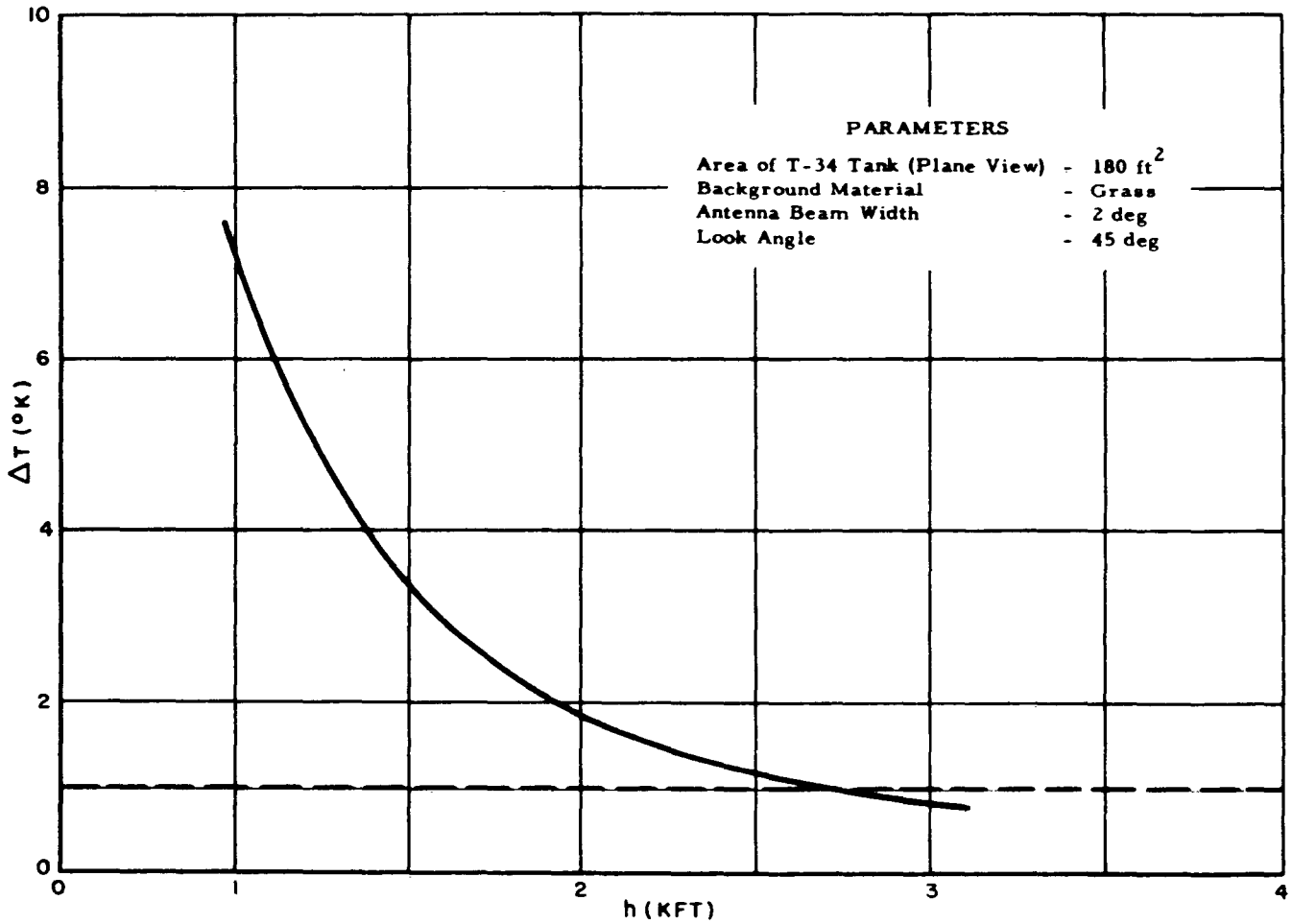

FIGURE 27. ΔT for One T-34 Tank at X-Band in Moderate Clouds

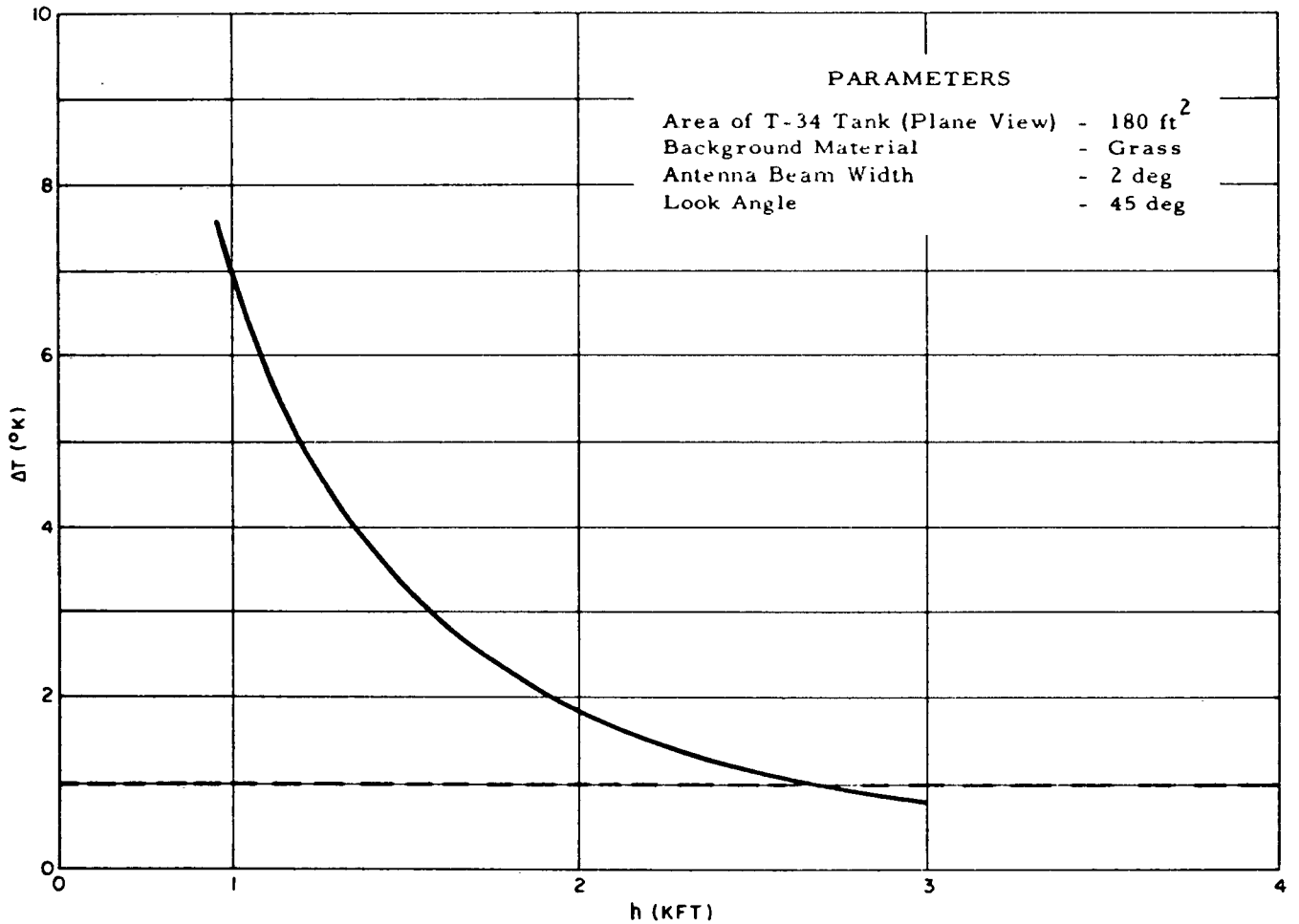

FIGURE 28. ΔT for One T-34 Tank at X-Band in Moderate Rain

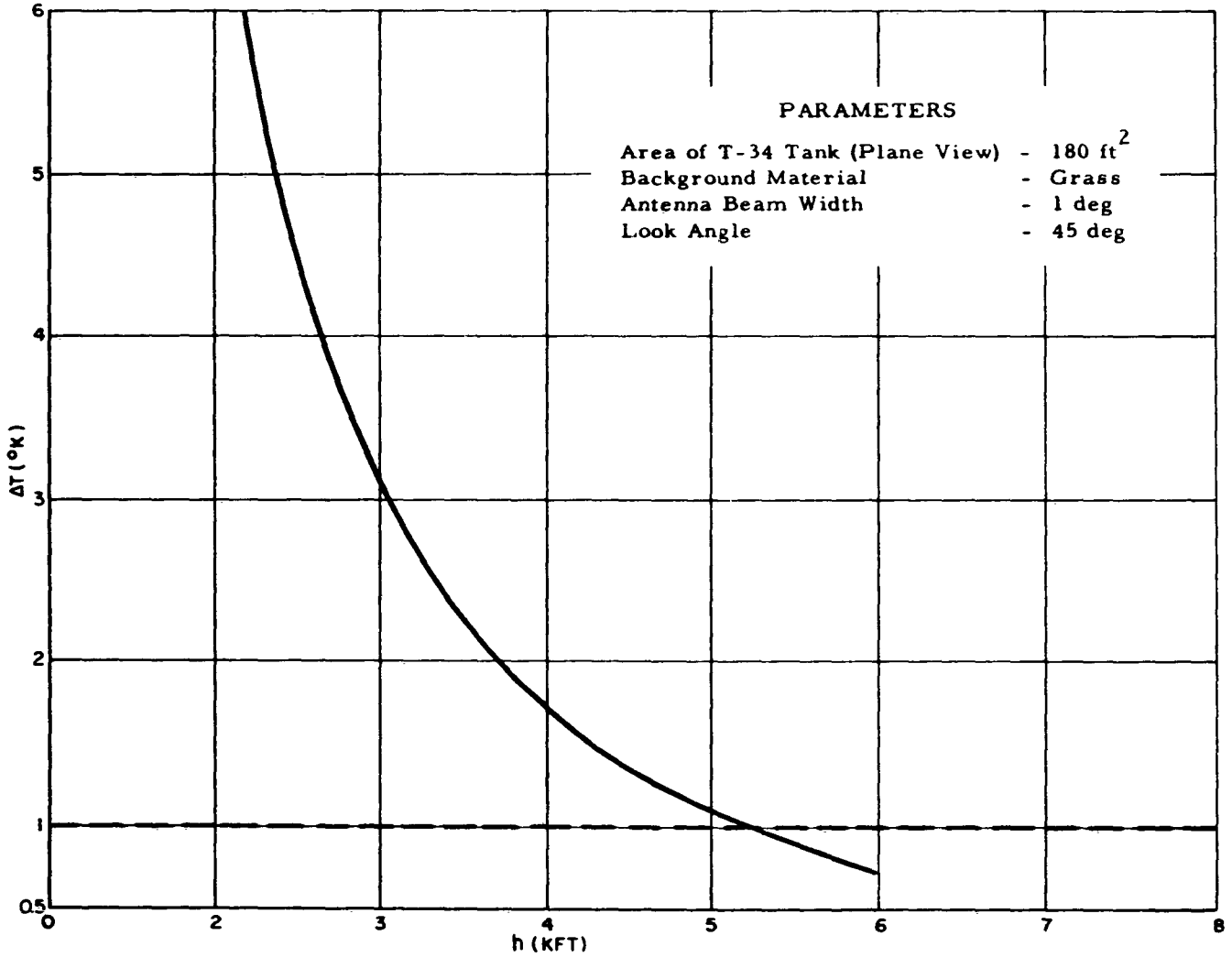

FIGURE 29. ΔT for One T-34 Tank at K_a-Band in Clear Weather

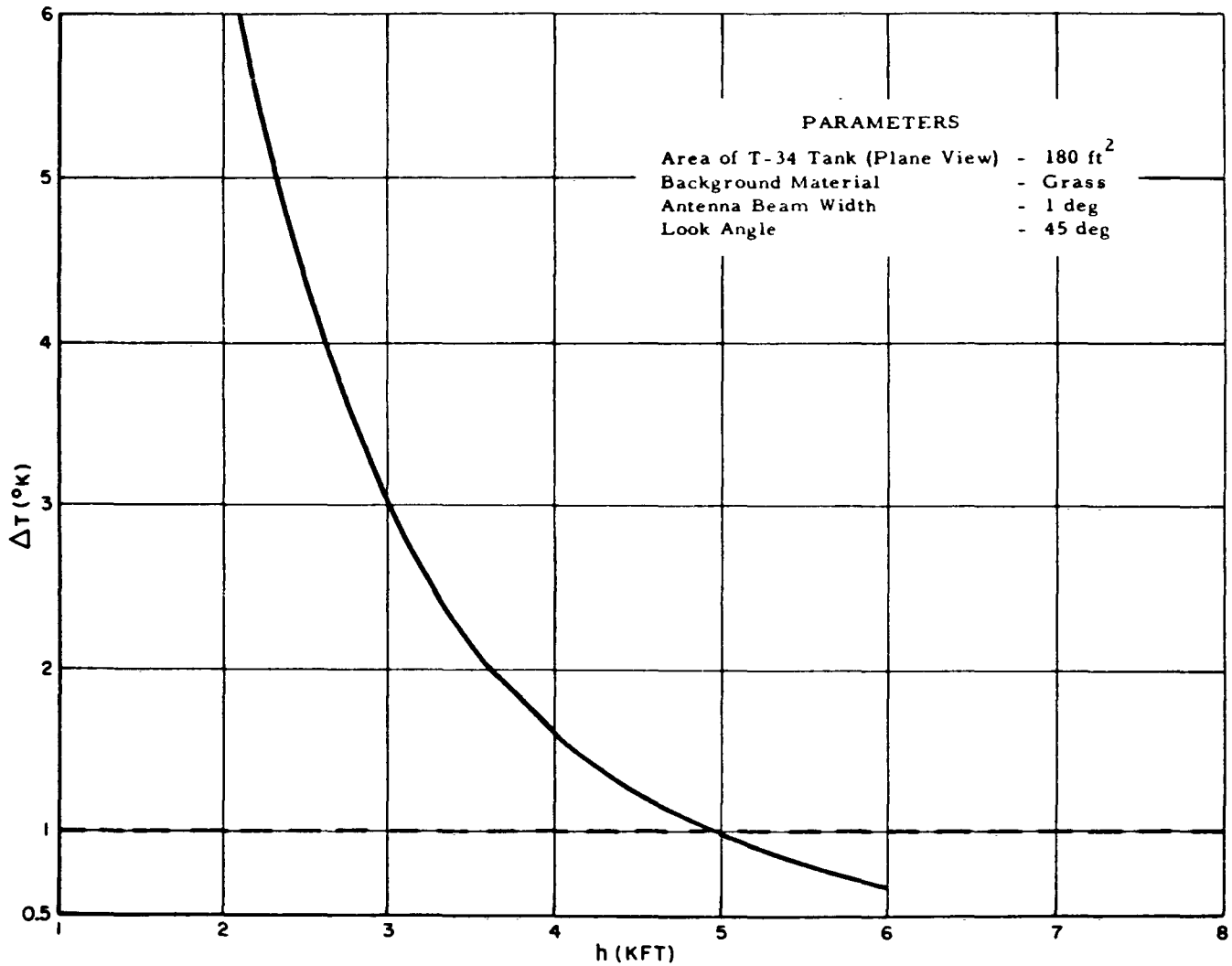

FIGURE 30. ΔT for One T-34 Tank at K_a-Band in Moderate Clouds

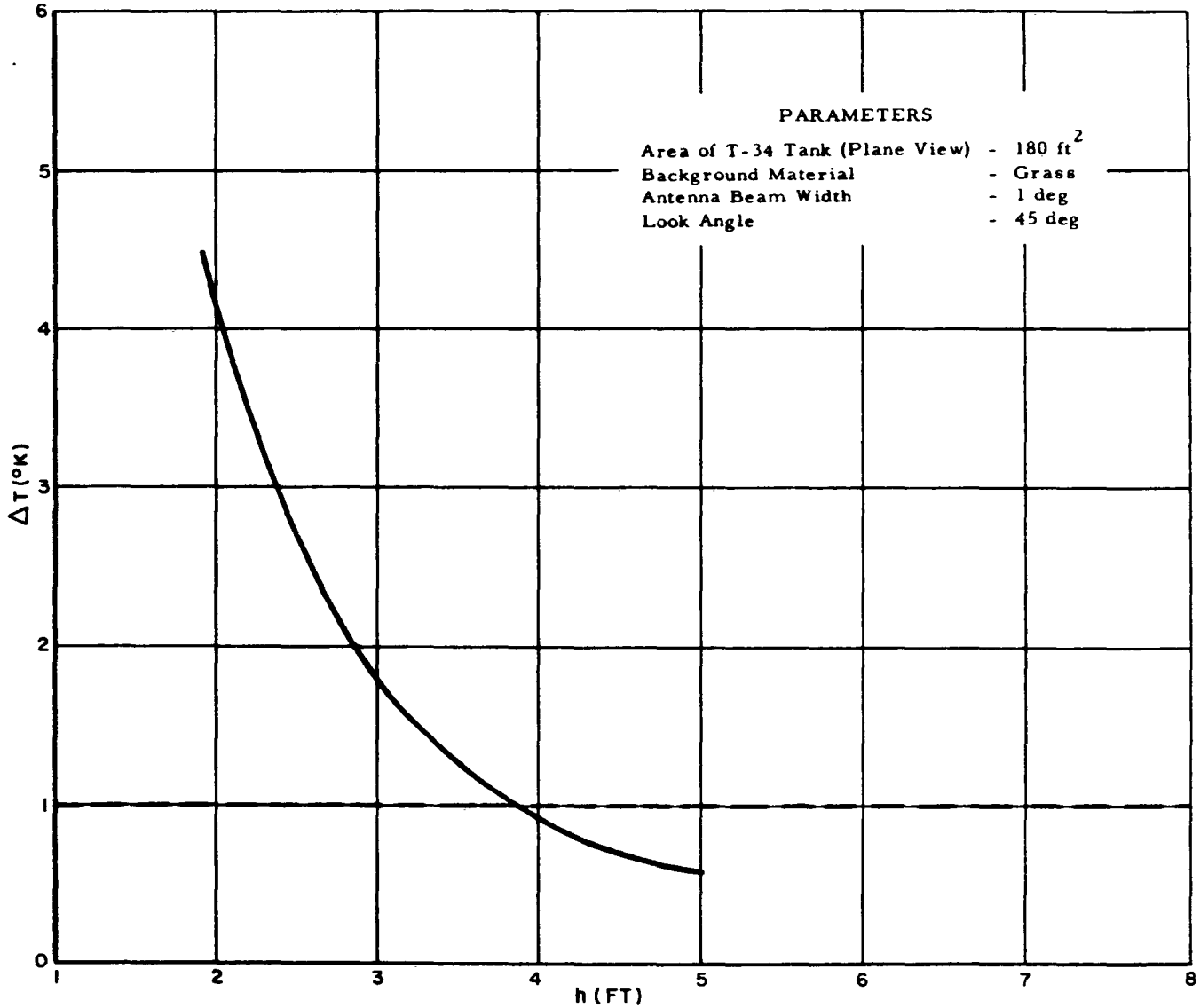

FIGURE 31. ΔT for One T-34 Tank at K_a-Band in Moderate Rain

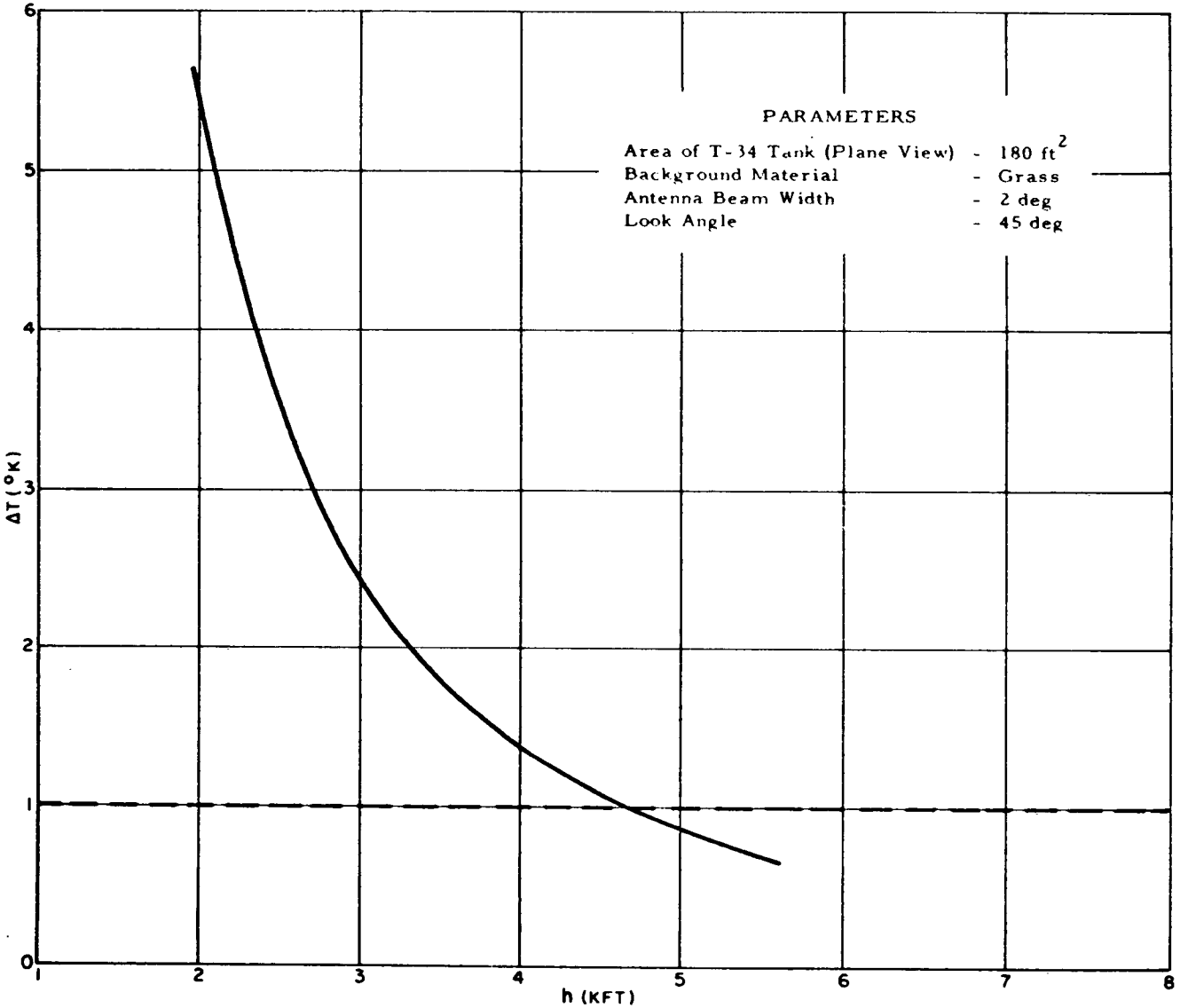

FIGURE 32. ΔT for Three T-34 Tanks at X-Band in Clear Weather

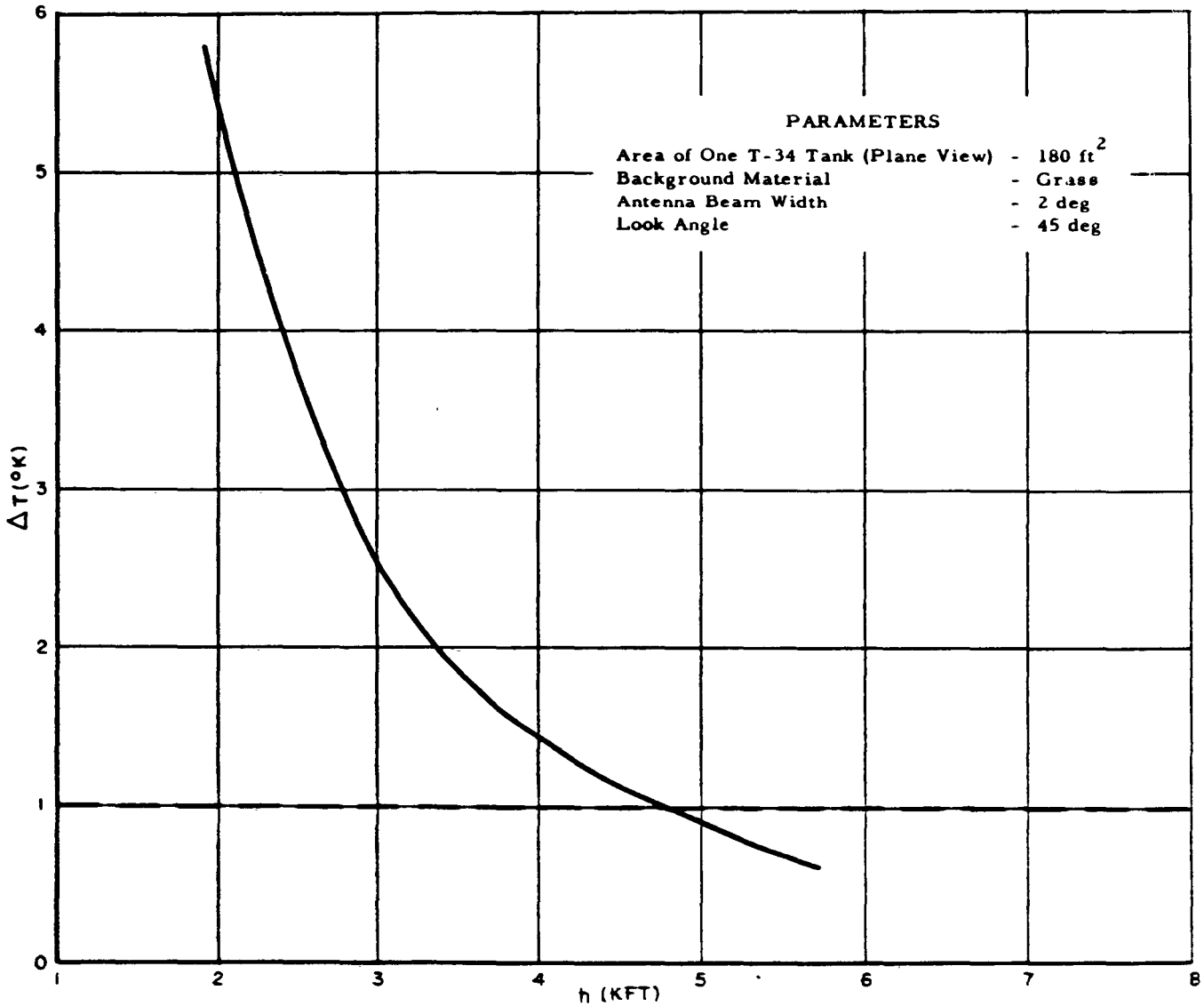

FIGURE 33. ΔT for Three T-34 Tanks at X-Band in Moderate Clouds

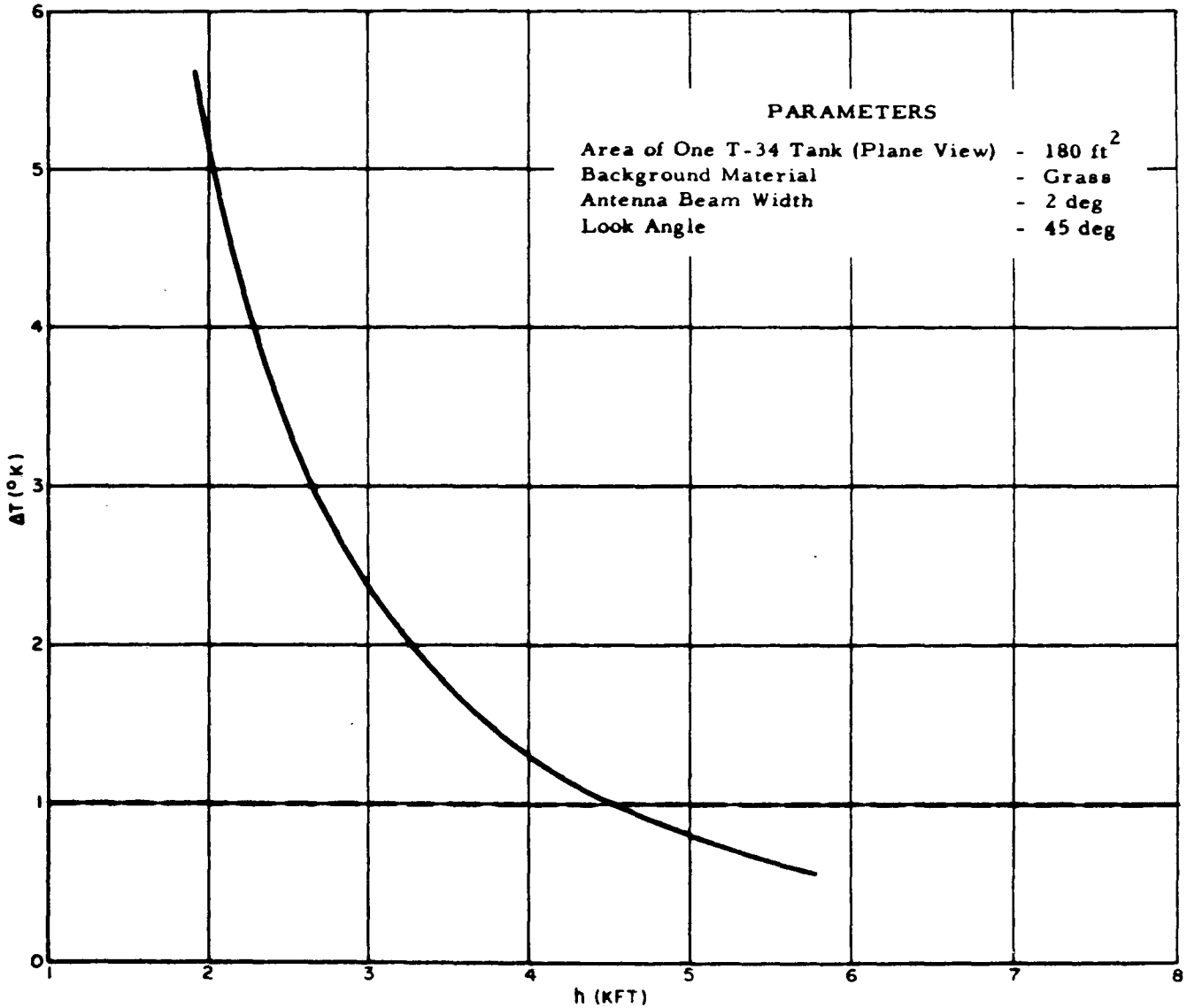

FIGURE 34. ΔT for Three T-34 Tanks at X-Band in Moderate Rain

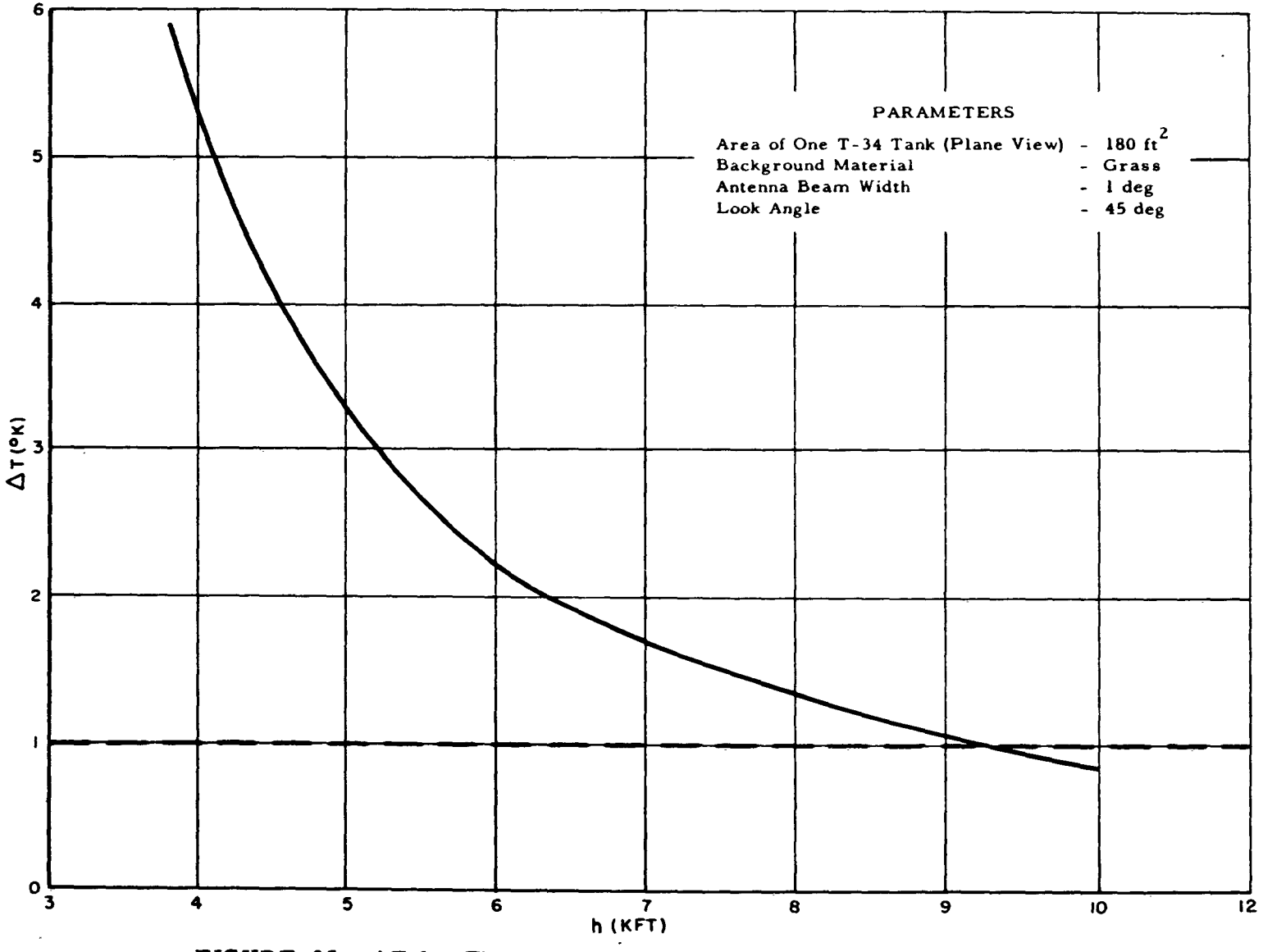

FIGURE 35. ΔT for Three T-34 Tanks at K_a-Band in Clear Weather

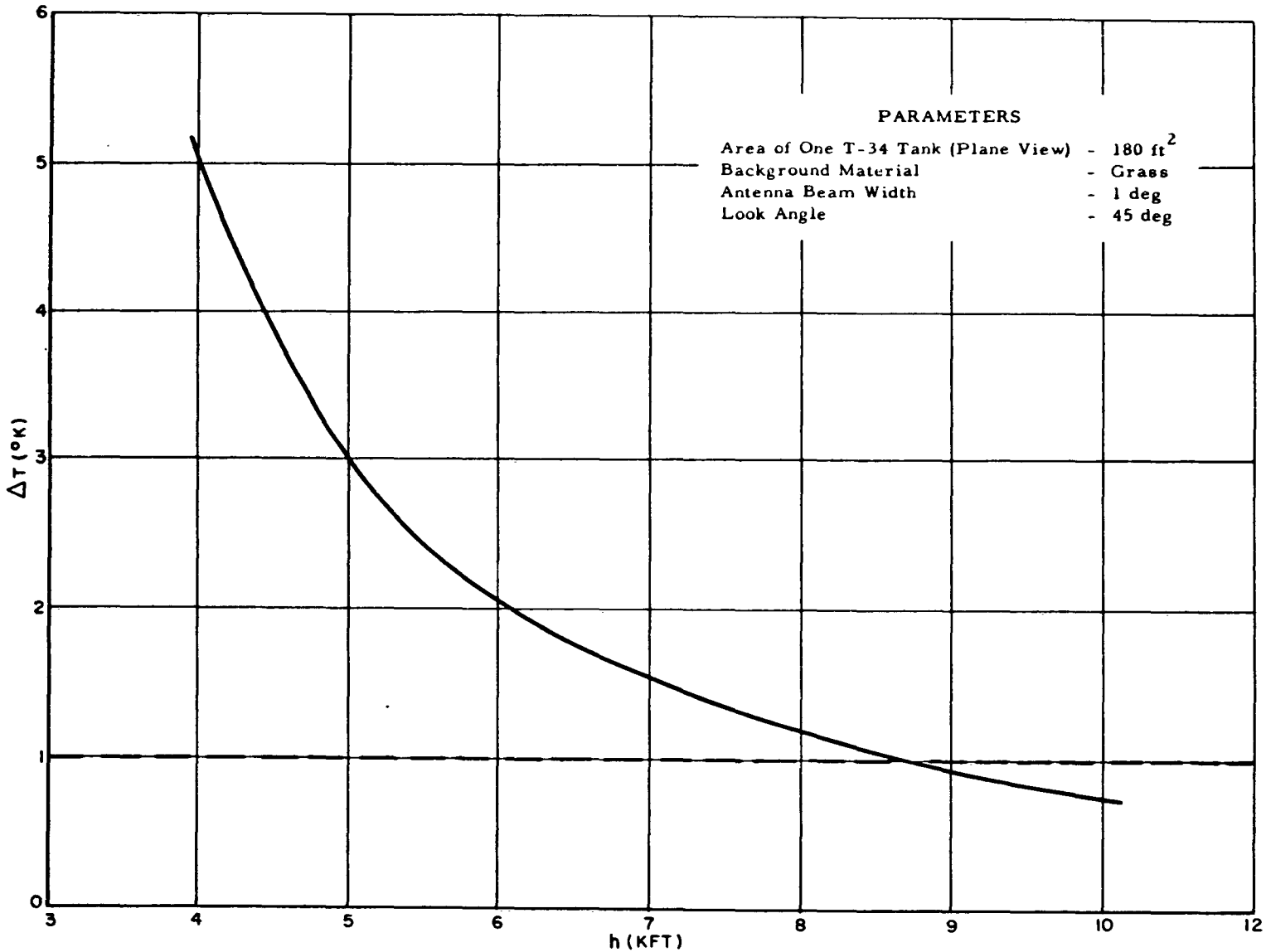

FIGURE 36. ΔT for Three T-34 Tanks at K_a-Band in Moderate Clouds

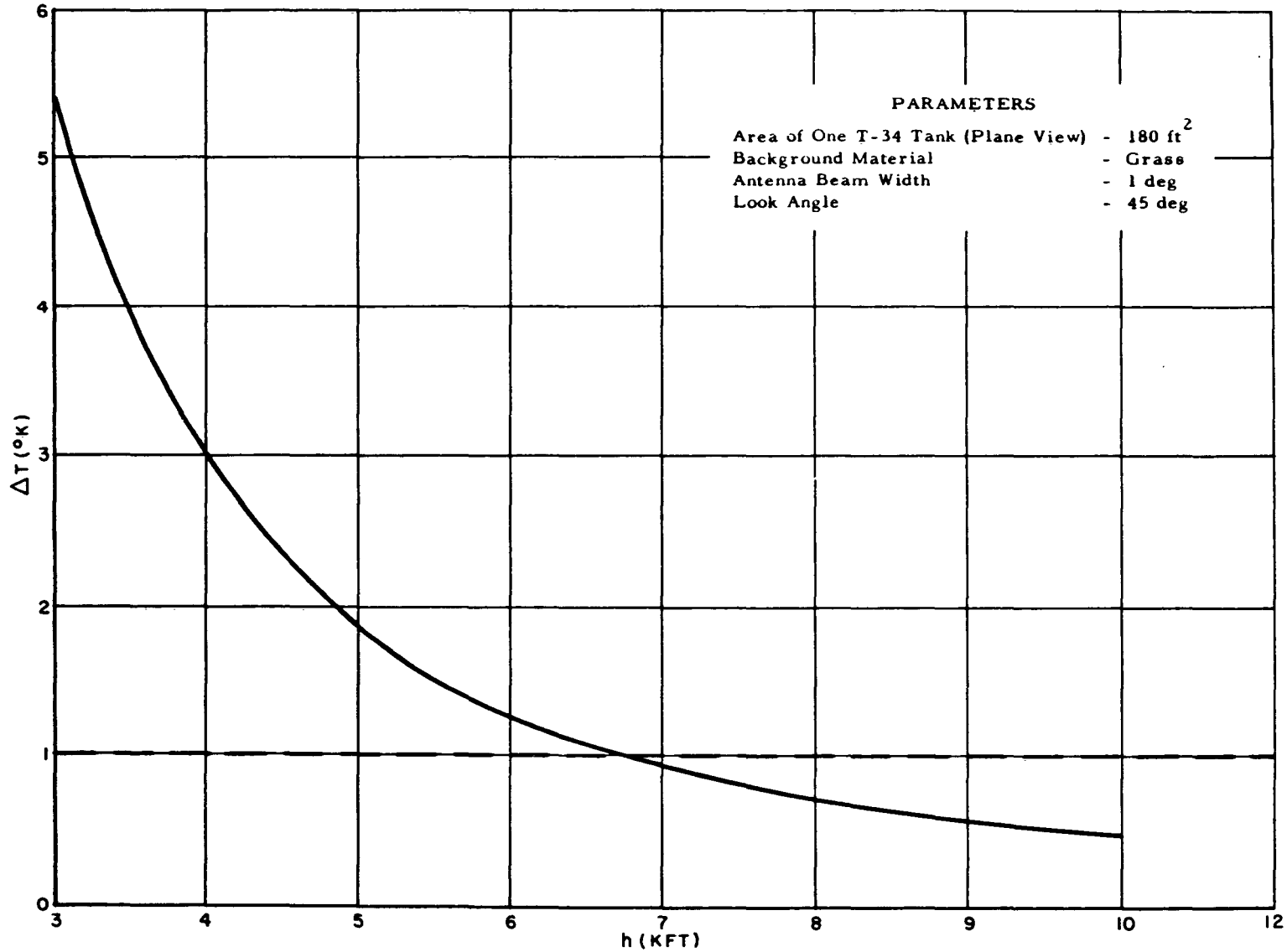

FIGURE 37. ΔT for Three T-34 Tanks at K_a-Band in Moderate Rain

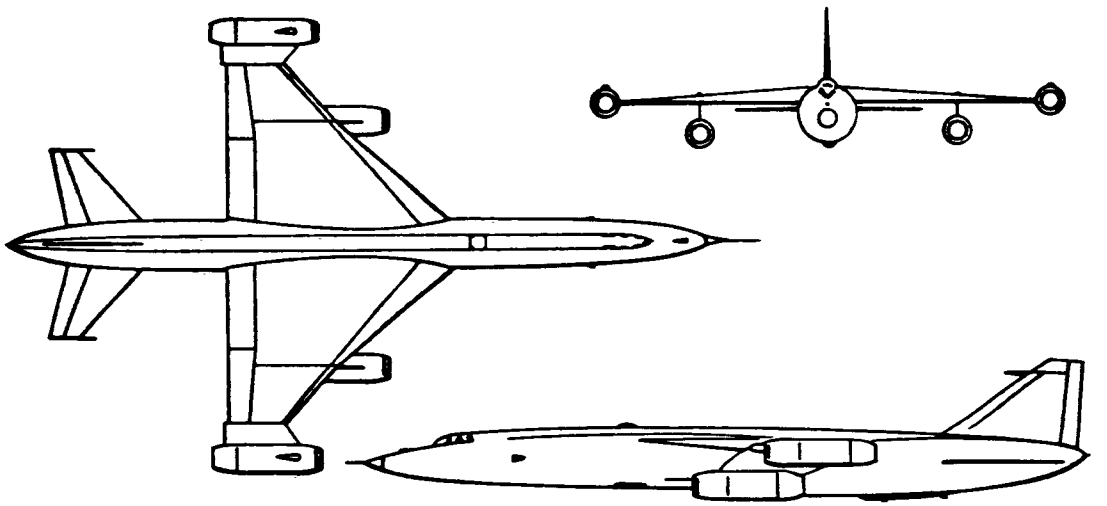

FIGURE 38. Scale Drawing of the Bounder, a Supersonic Bomber

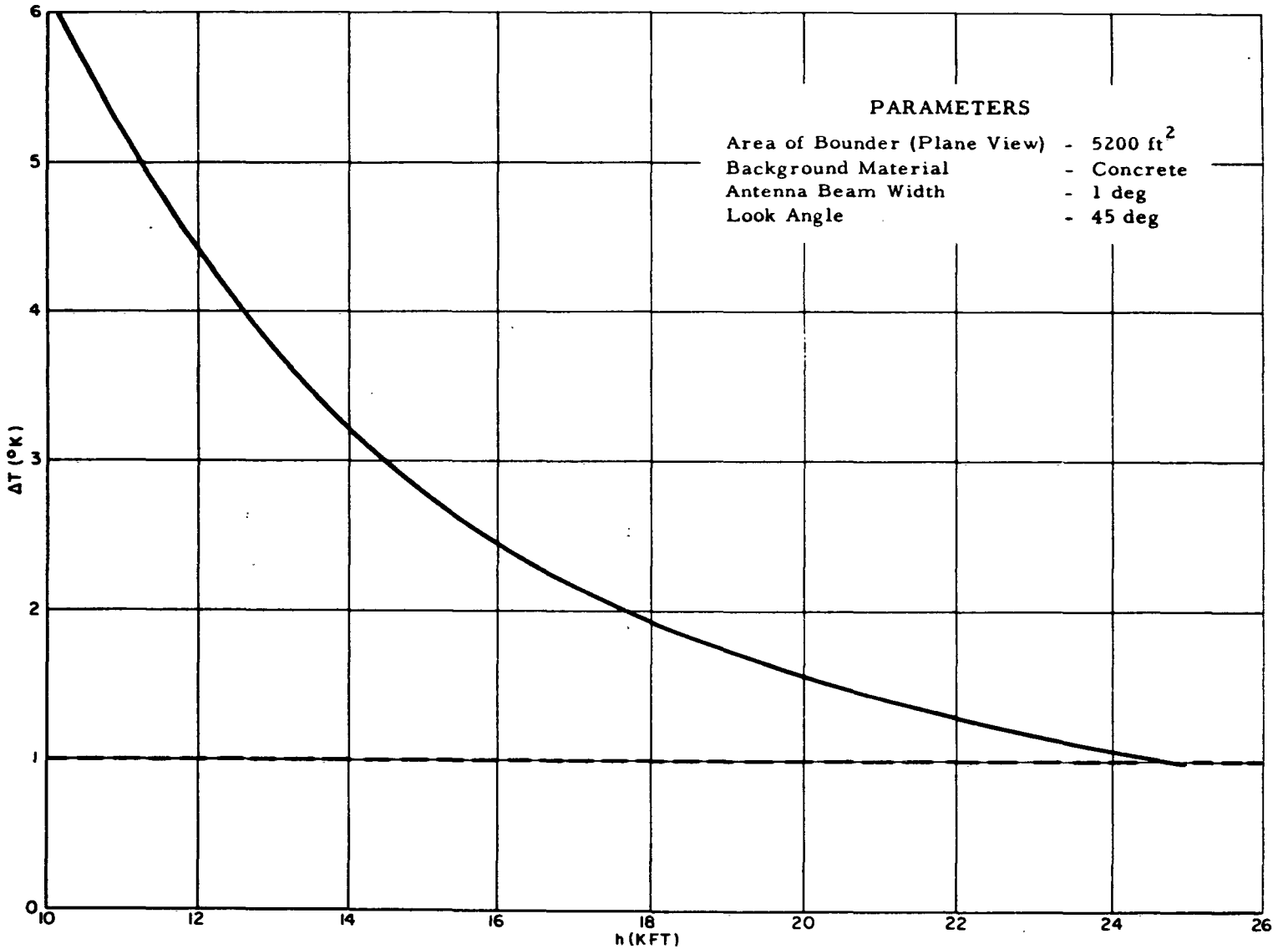

FIGURE 39. ΔT for the Bounder at K_a-Band in Clear Weather for 1-deg Beam Width

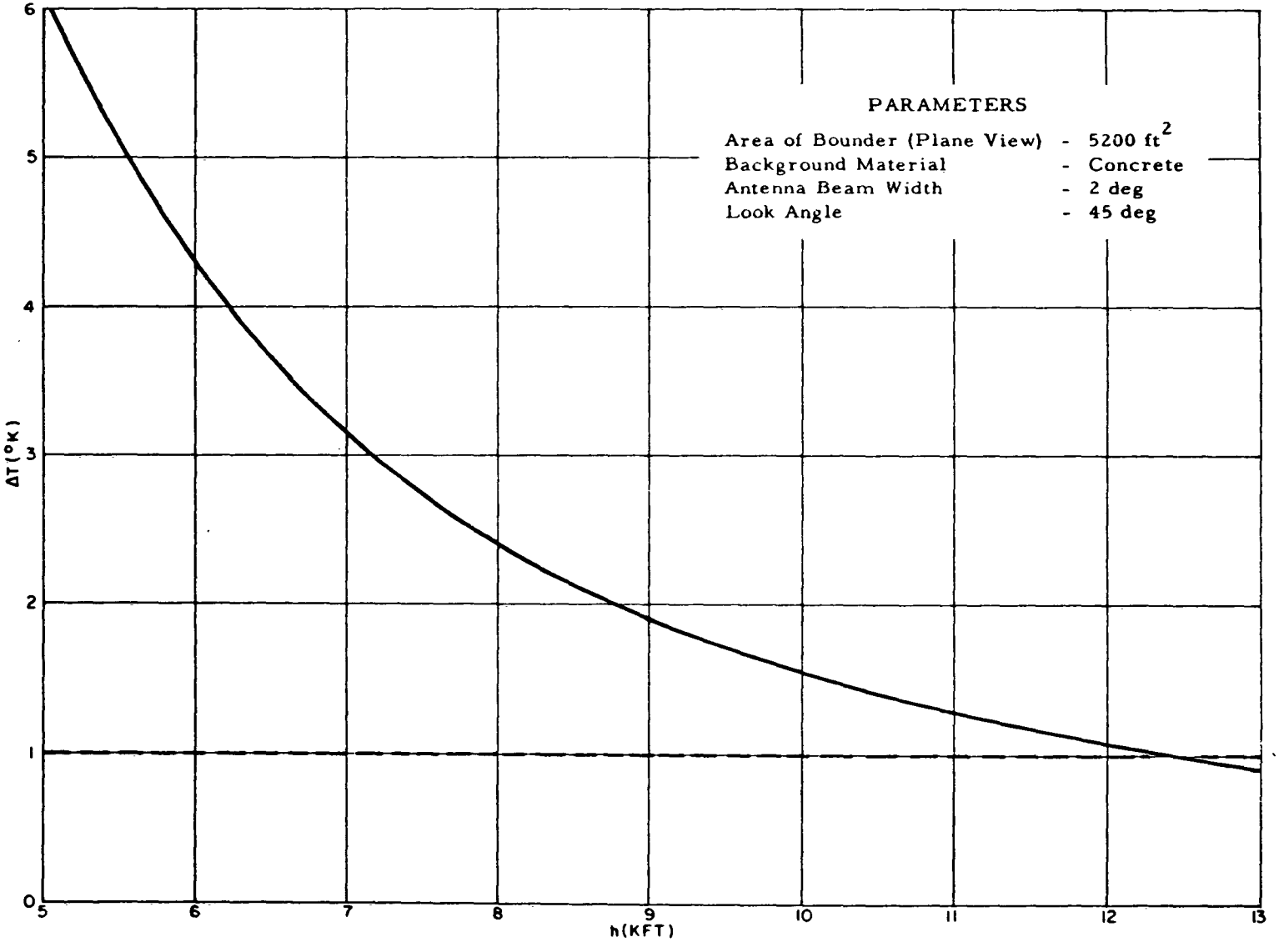

FIGURE 40. ΔT for the Bounder at K_a-Band in Clear Weather for 2-deg Beam Width

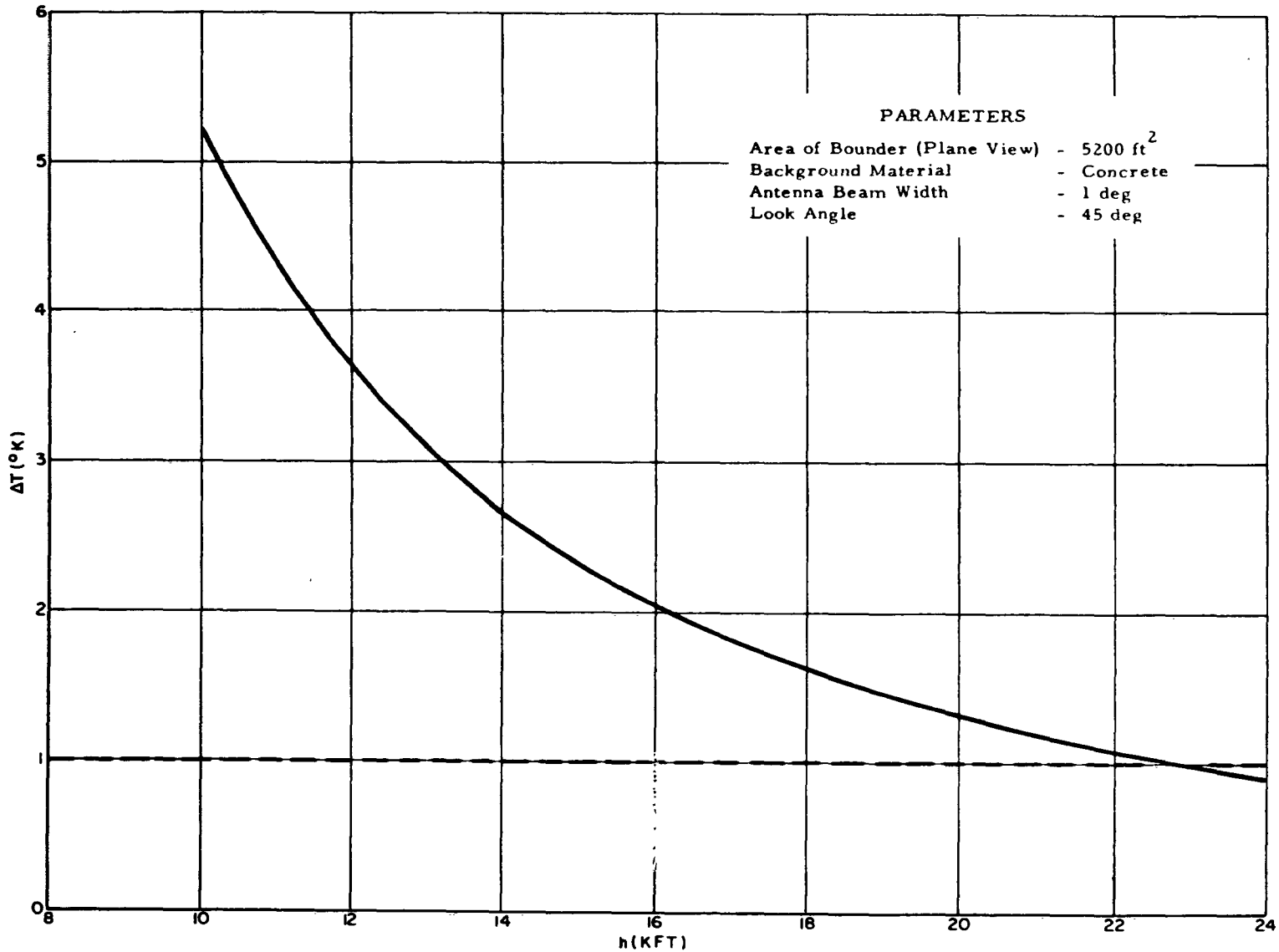

FIGURE 41. ΔT for the Bounder at K_a-Band in Moderate Clouds for 1-deg Beam Width

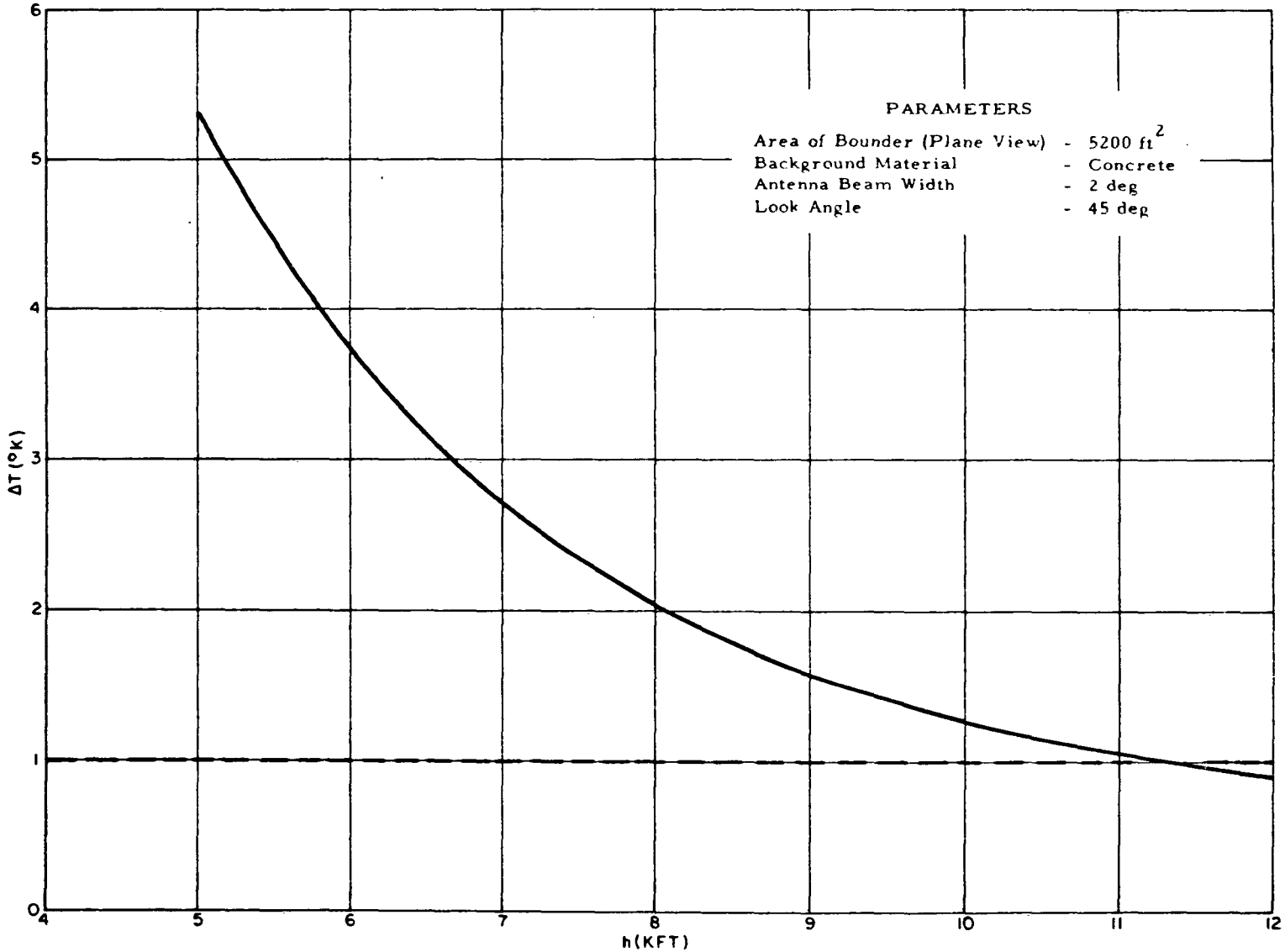

FIGURE 42. ΔT for the Bounder at K_a-Band in Moderate Clouds for 2-deg Beam Width

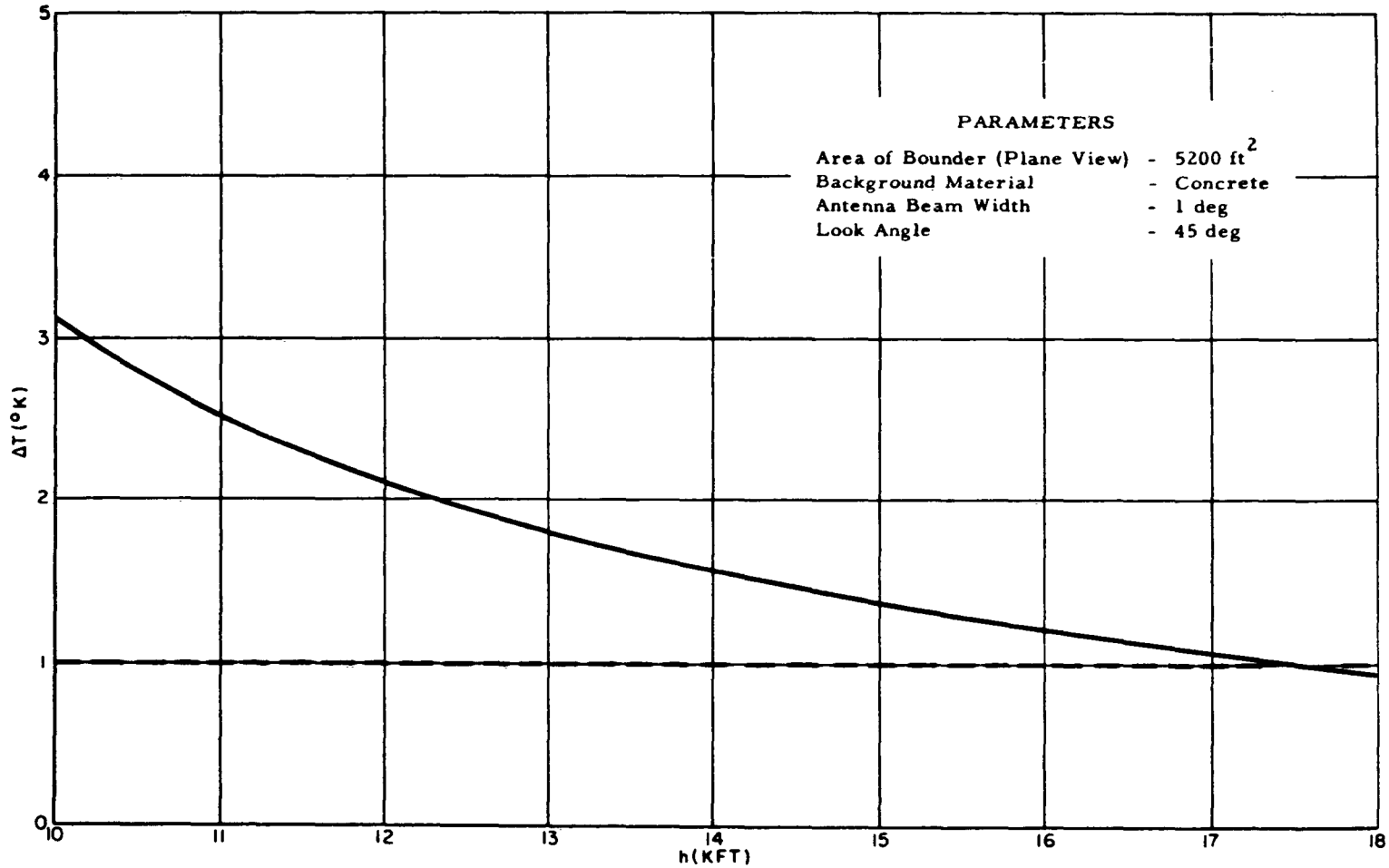

FIGURE 43. ΔT for the Bounder at K_a-Band in Moderate Rain for 1-deg Beam Width

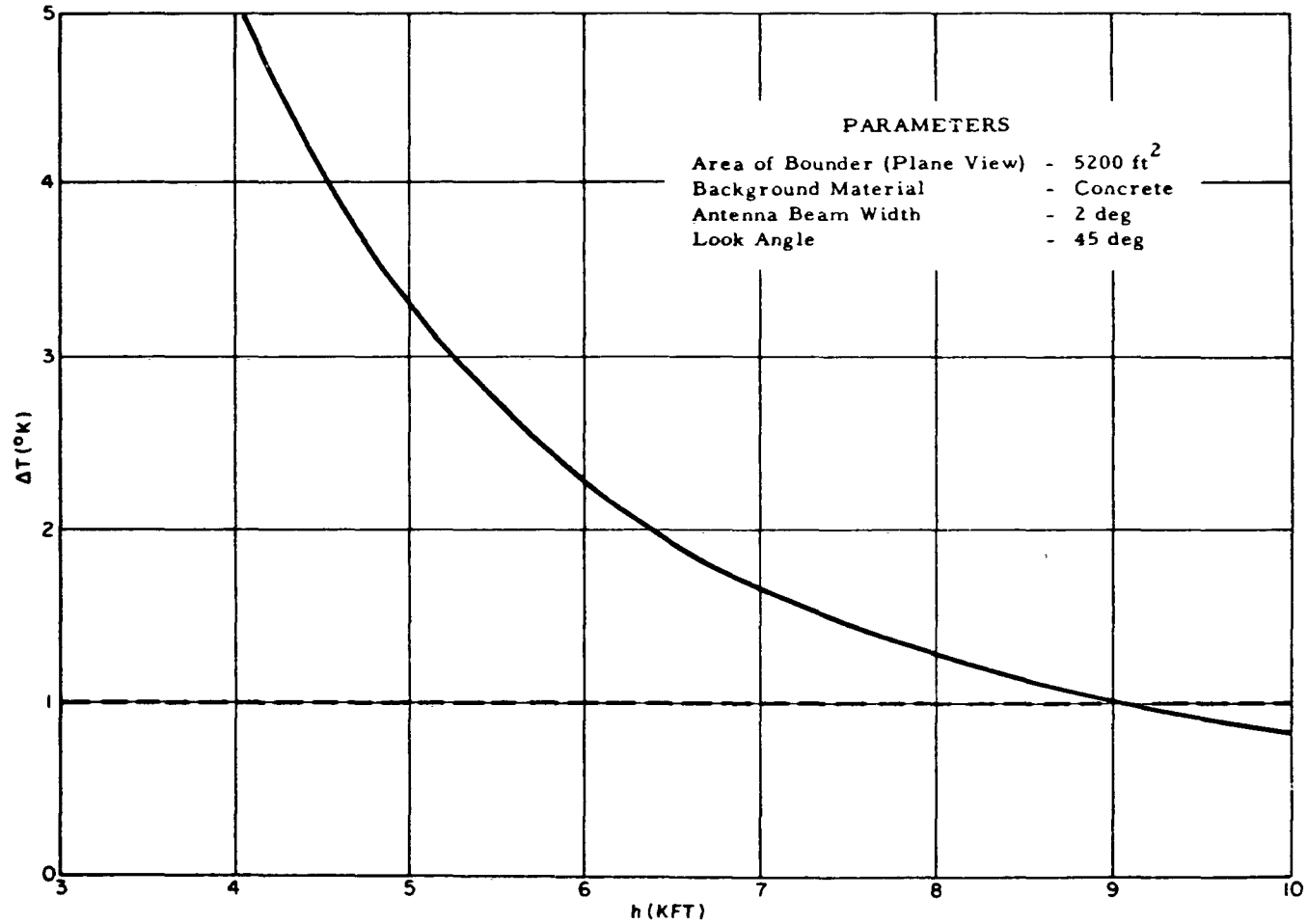

FIGURE 44. ΔT for the Bounder at K_a-Band in Moderate Rain for 2-deg Beam Width

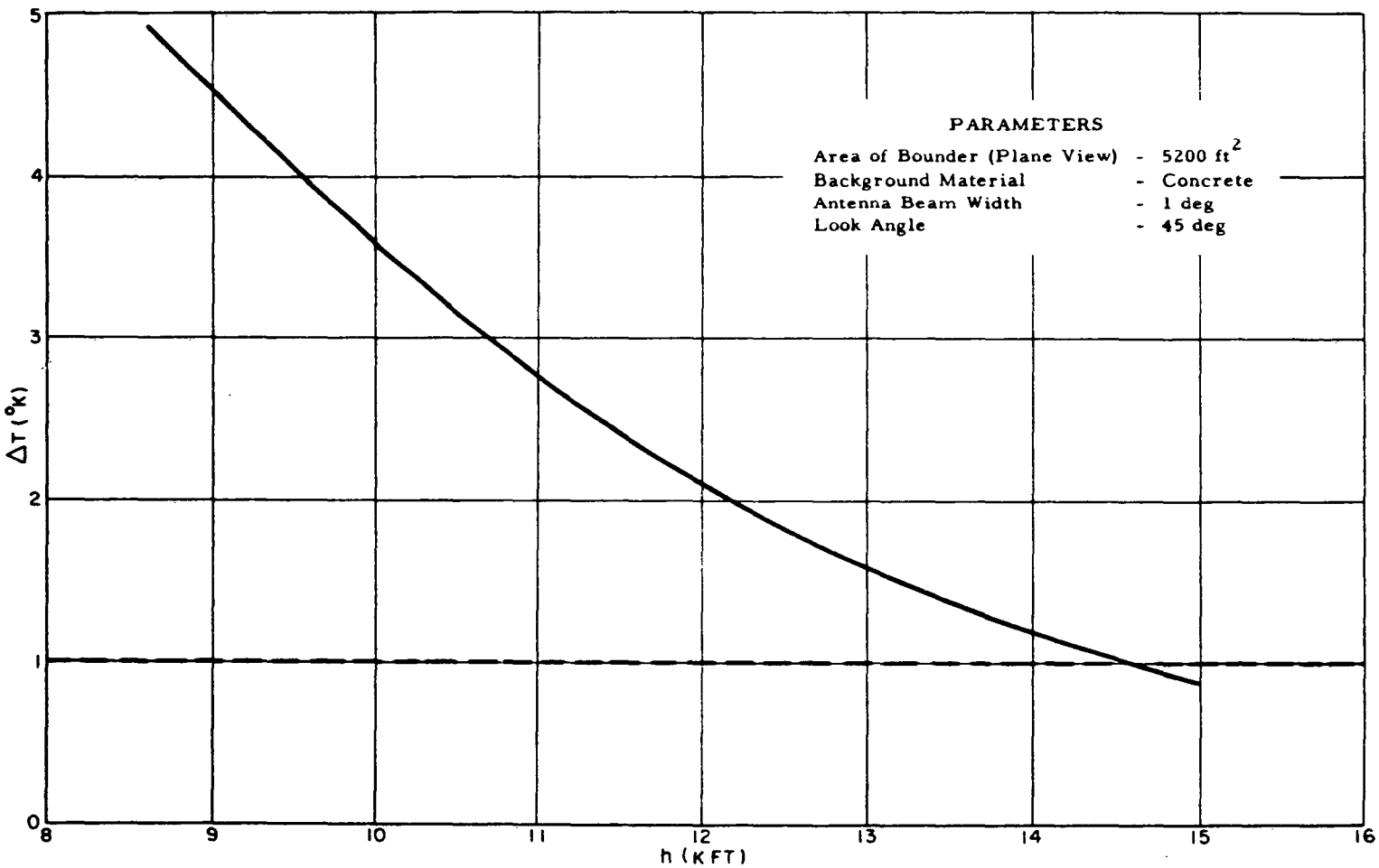

FIGURE 45. ΔT for the Bounder at K_a-Band in Cumulus Clouds for 1-deg Beam Width

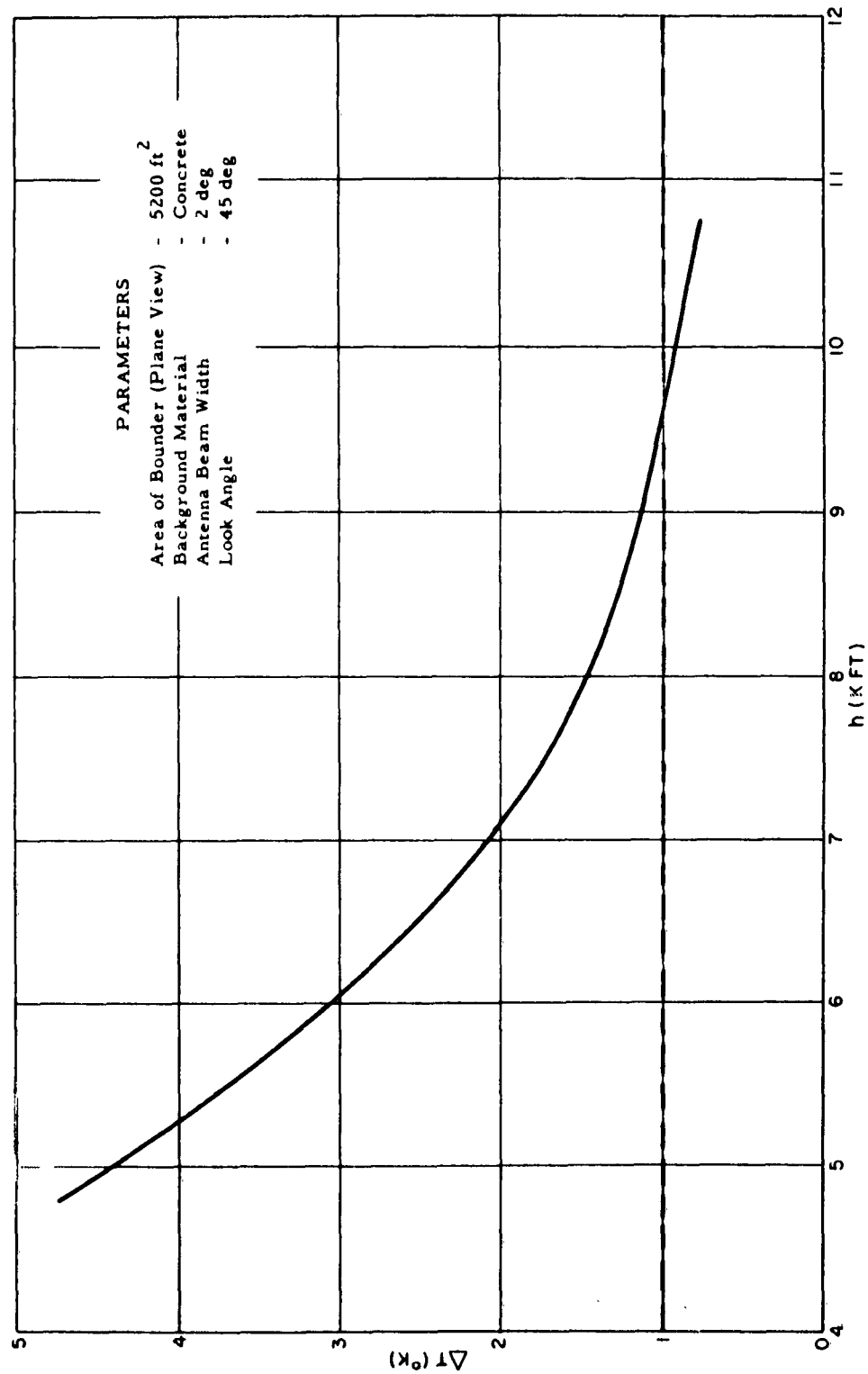

FIGURE 46. ΔT for the Bounder at K_a-Band in Cumulus Clouds for 2-deg Beam Width

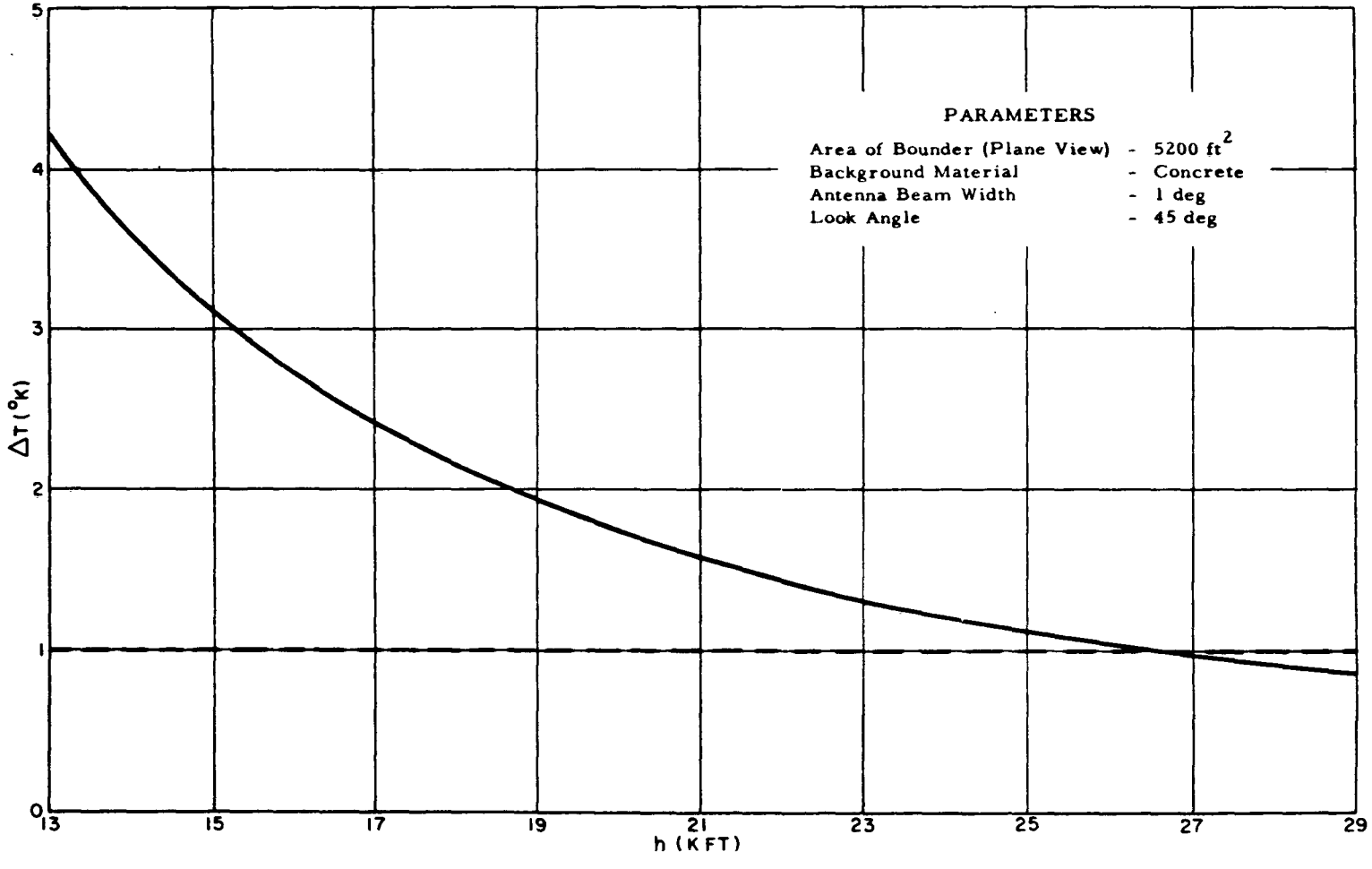

FIGURE 47. ΔT for the Bounder at X-Band in Clear Weather for 1-deg Beam Width

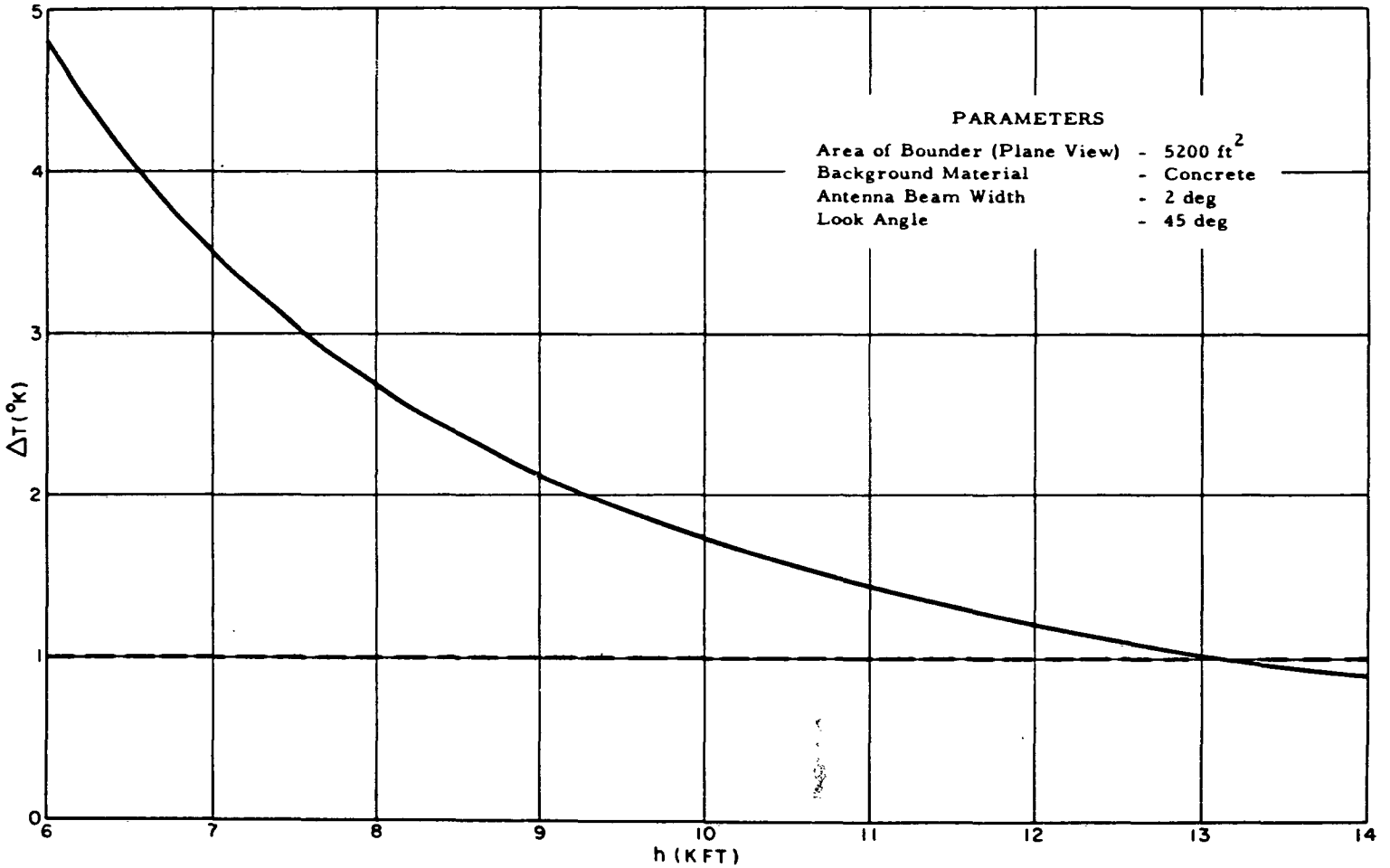

FIGURE 48. ΔT for the Bounder at X-Band in Clear Weather for 2-deg Beam Width

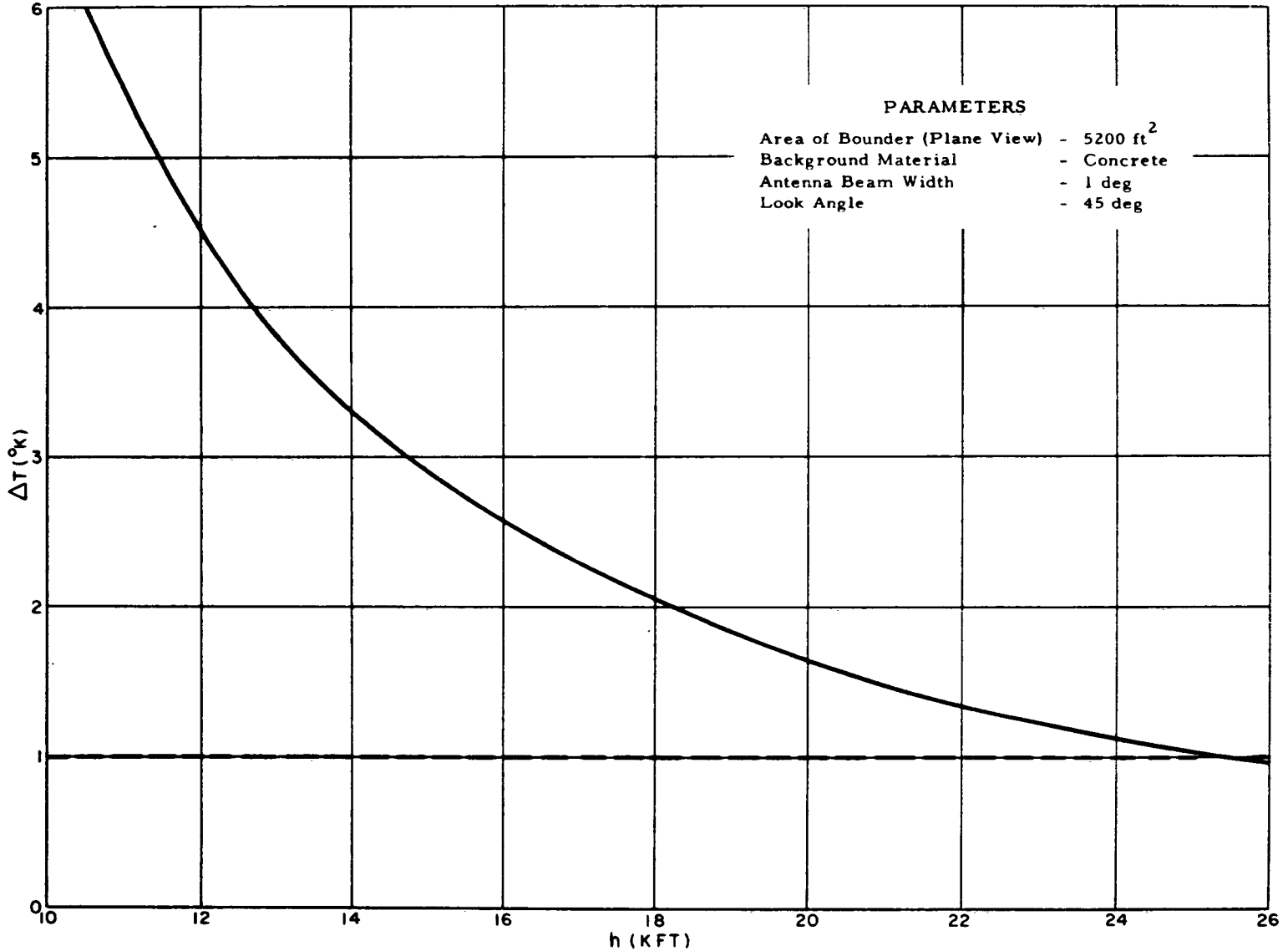

FIGURE 49. ΔT for the Bounder at X-Band in Moderate Clouds for 1-deg Beam Width

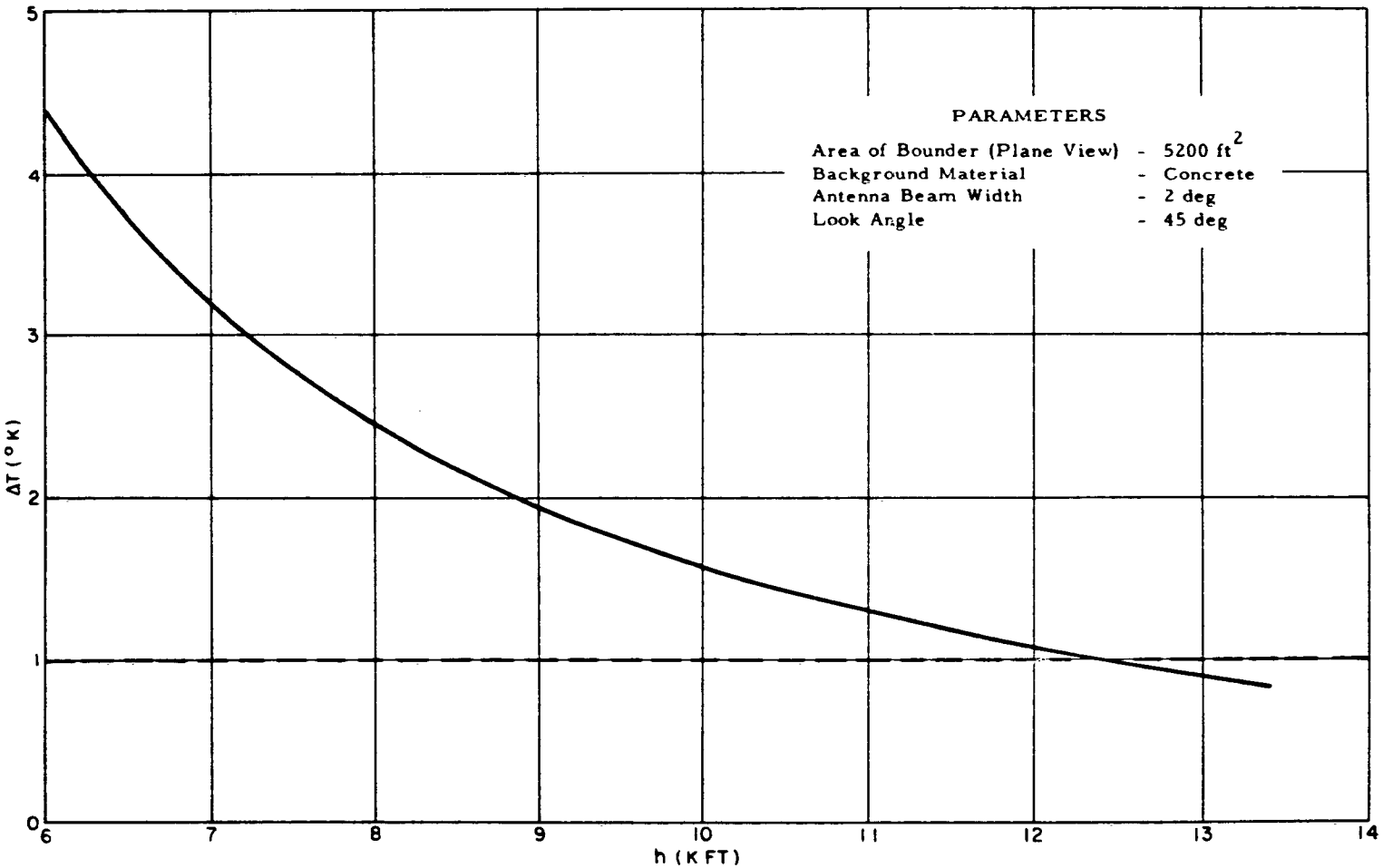

FIGURE 50. ΔT for the Bounder at X-Band in Moderate Clouds for 2-deg Beam Width

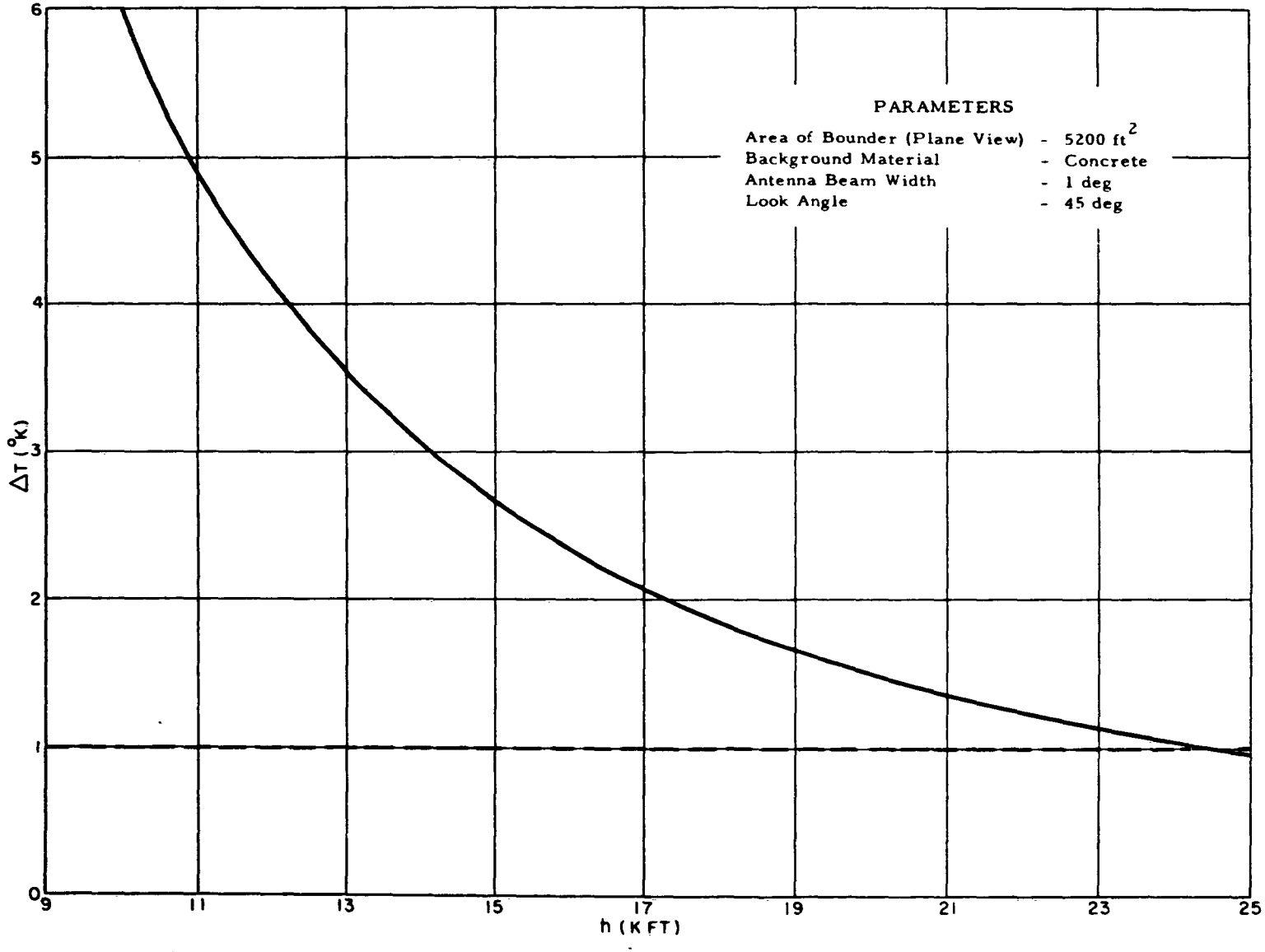

FIGURE 51. ΔT for the Bounder at X-Band in Moderate Rain for 1-deg Beam Width

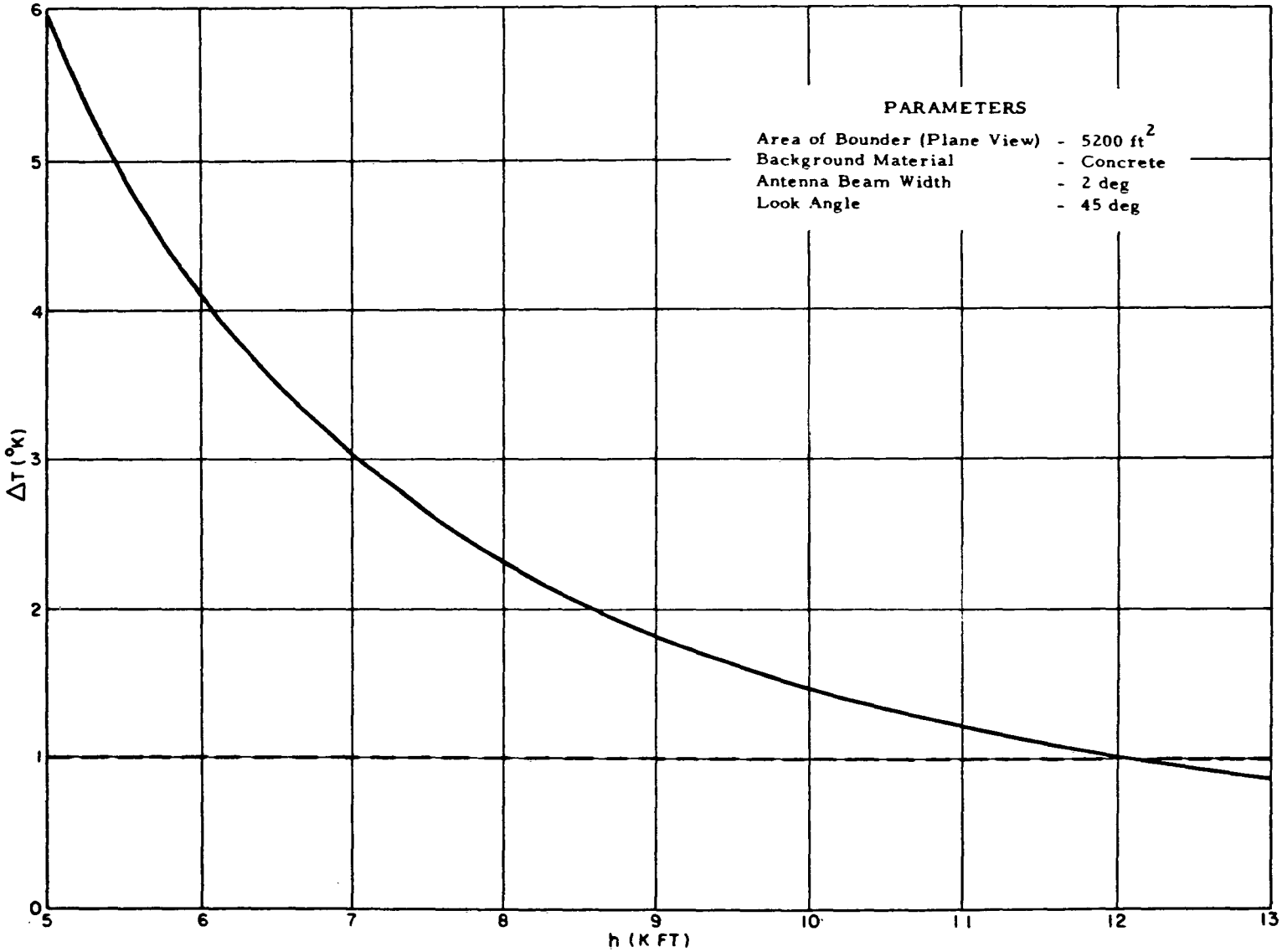

FIGURE 52. ΔT for the Bounder at X-Band in Moderate Rain for 2-deg Beam Width

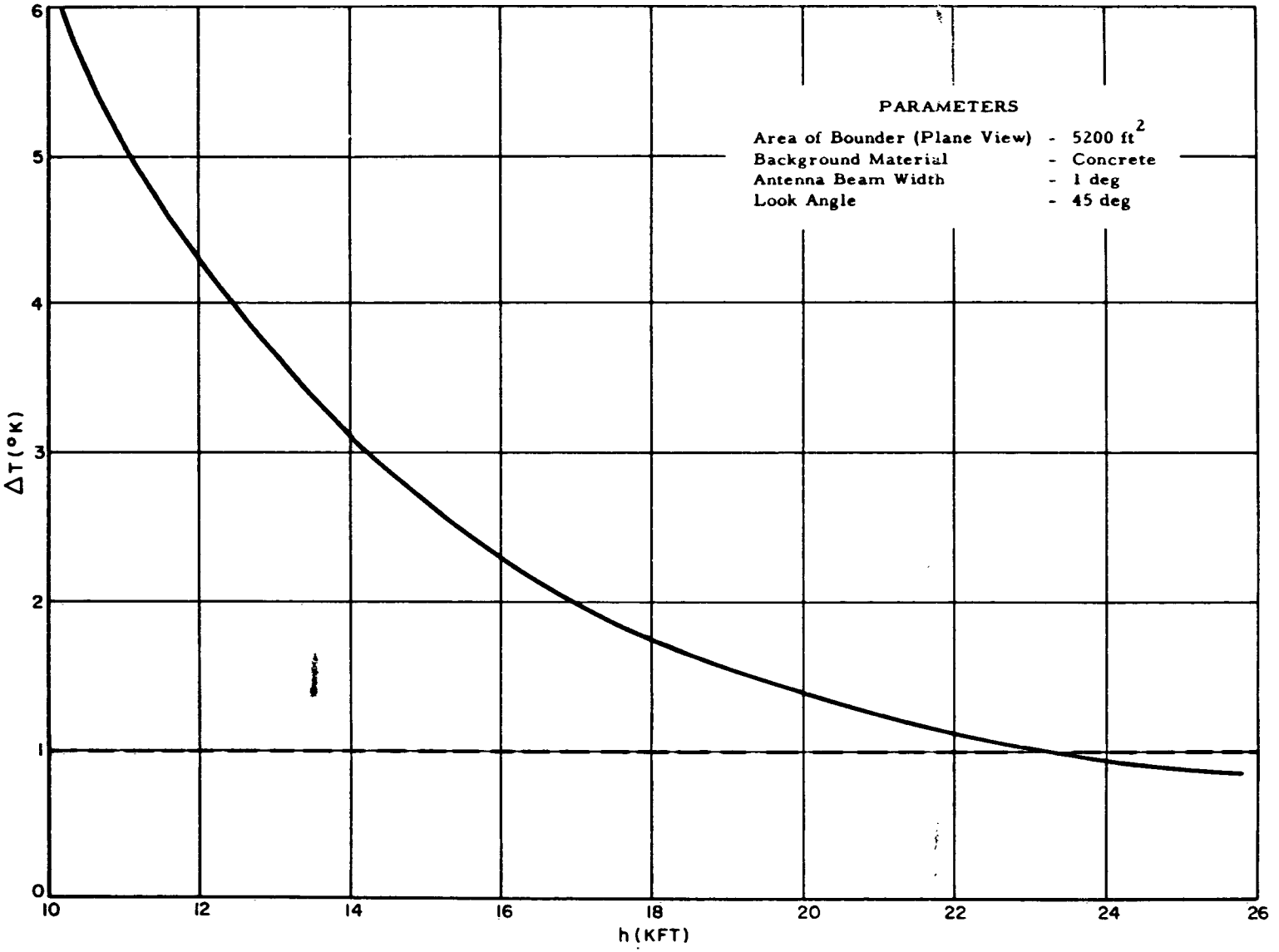

FIGURE 53. ΔT for the Bounder at X-Band in Cumulus Clouds for 1-deg Beam Width

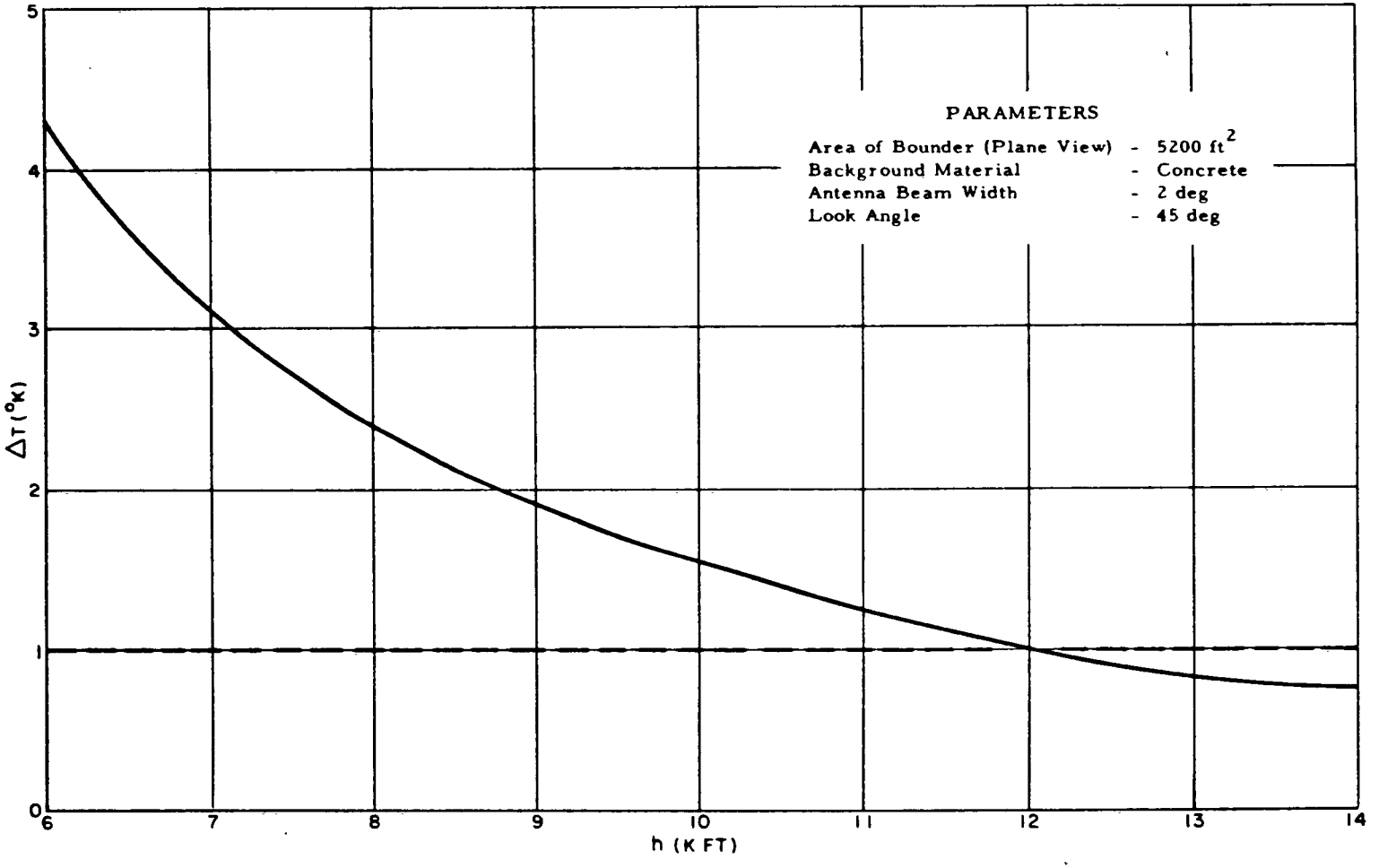

FIGURE 54. ΔT for the Bounder at X-Band in Cumulus Clouds for 2-deg Beam Width

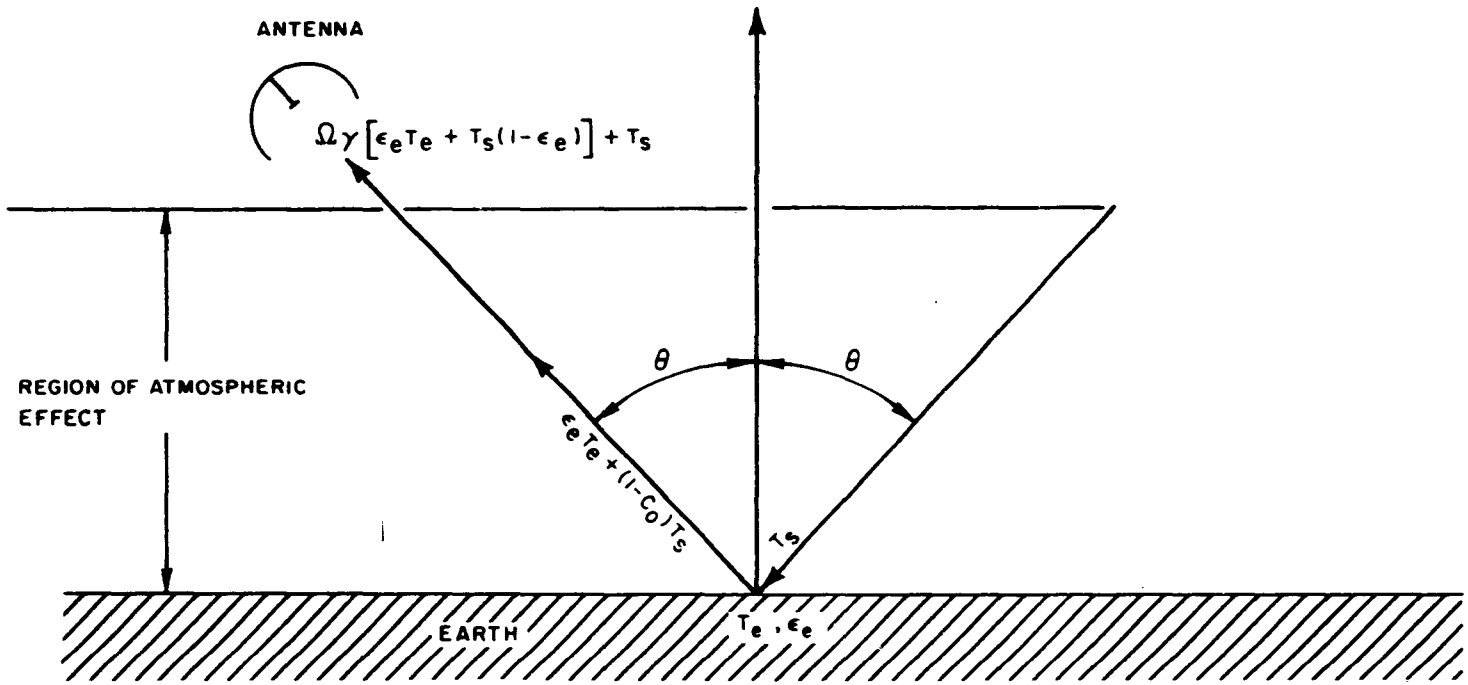

FIGURE 55. Geometry for Determining the Radiometric Temperature of the Earth From Above the Atmosphere

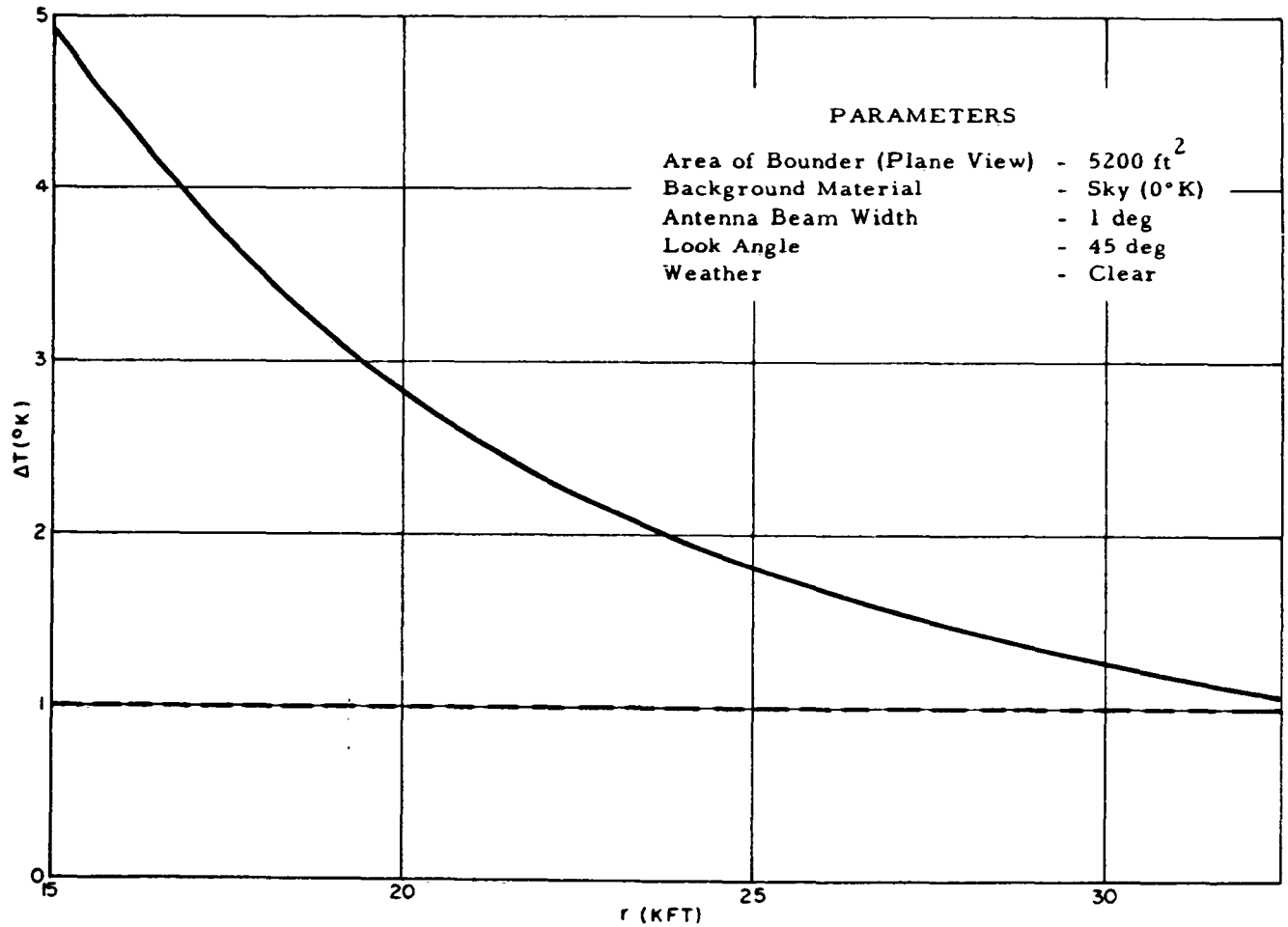

FIGURE 56. ΔT for the Bounder at K_a-Band for β = 1 deg, θ = 45 deg, and a Sky Background

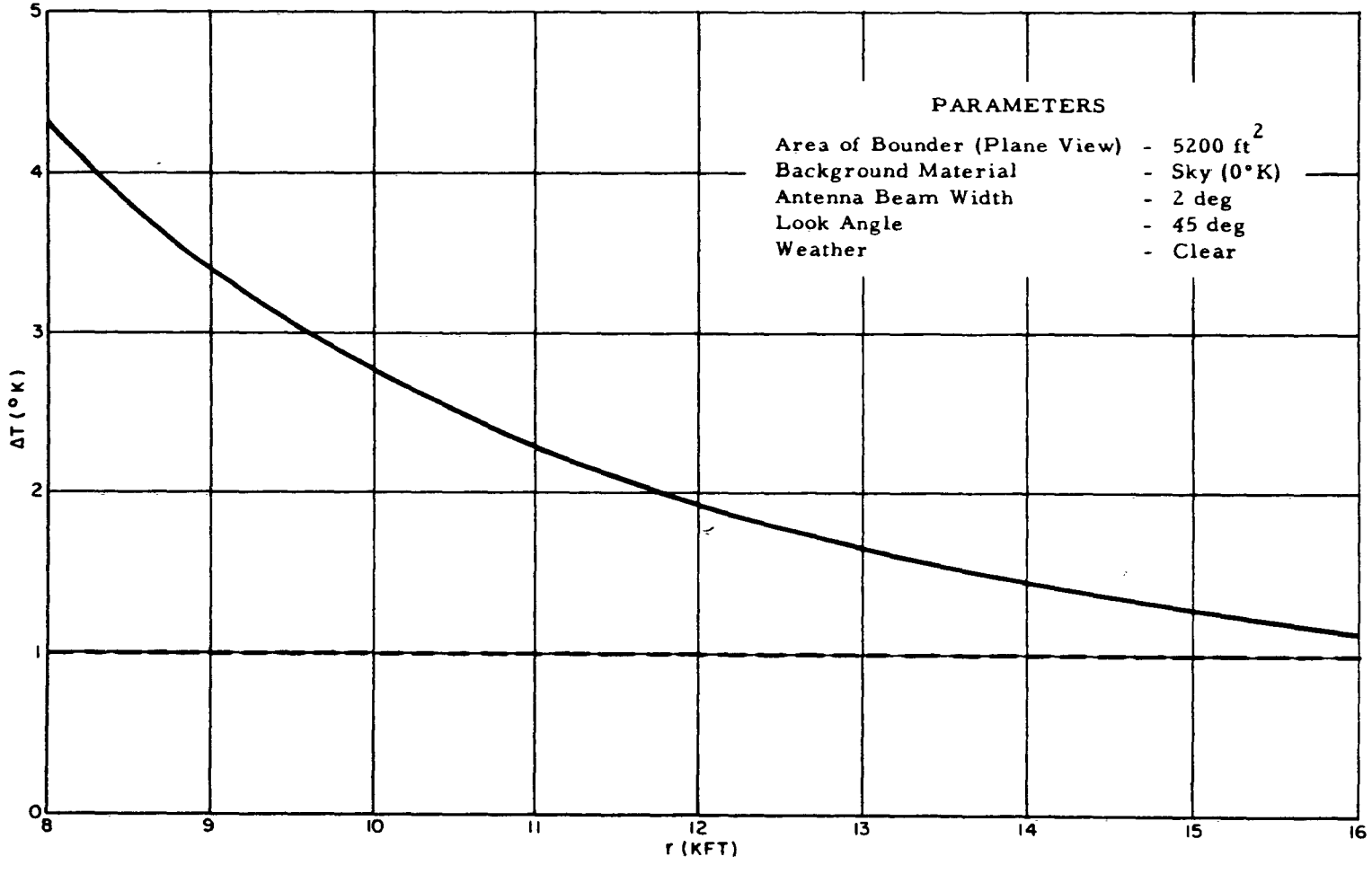

FIGURE 57. ΔT for the Bounder at K_a-Band for β = 2 deg, θ = 45 deg, and a Sky Background

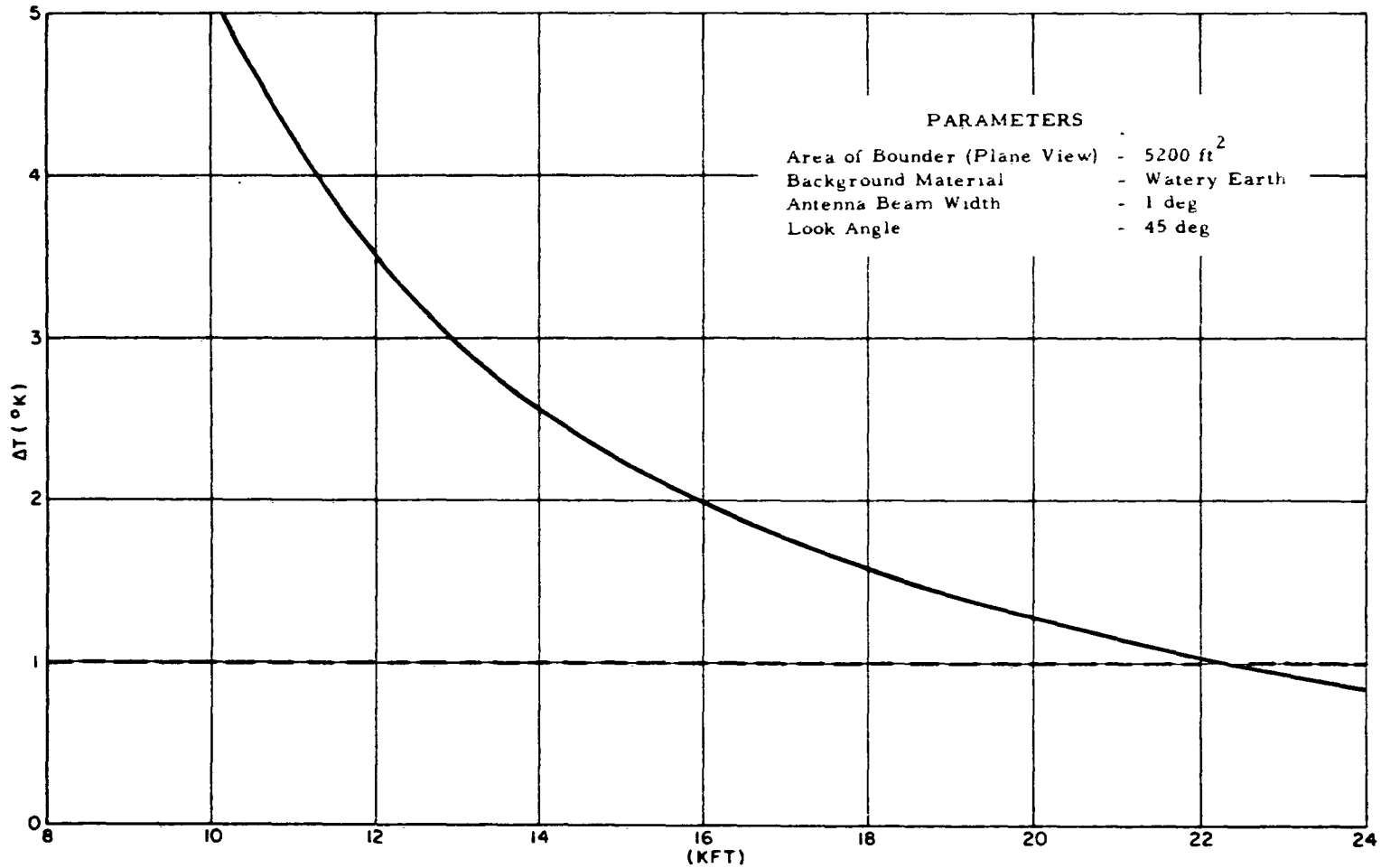

FIGURE 58. ΔT for the Bounder at K_a-Band for β = 1 deg, θ = 45 deg, and an Earth Background

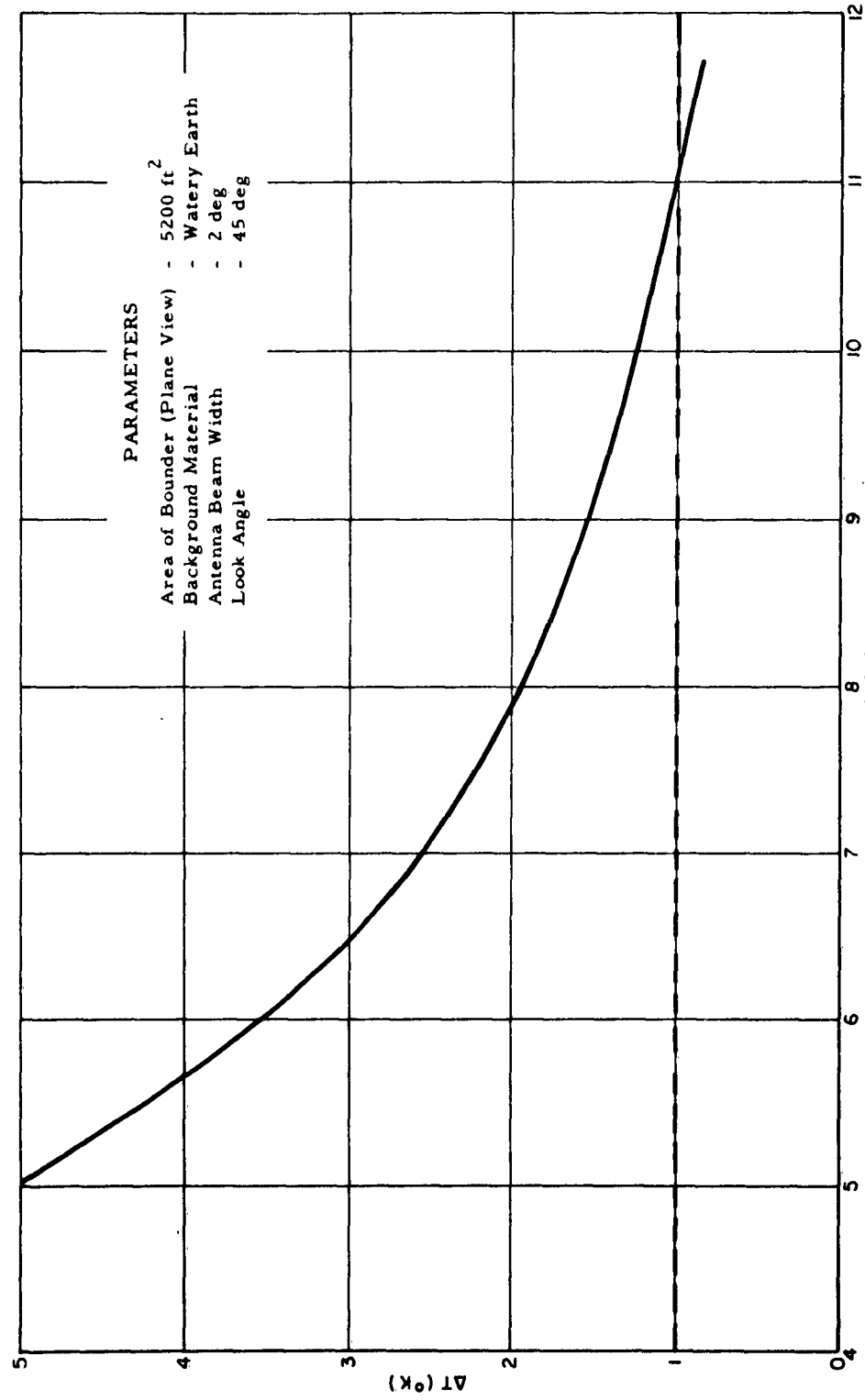

FIGURE 59. ΔT for the Bounder at K_a-Band for β = 2 deg, θ = 45 deg, and an Earth Background

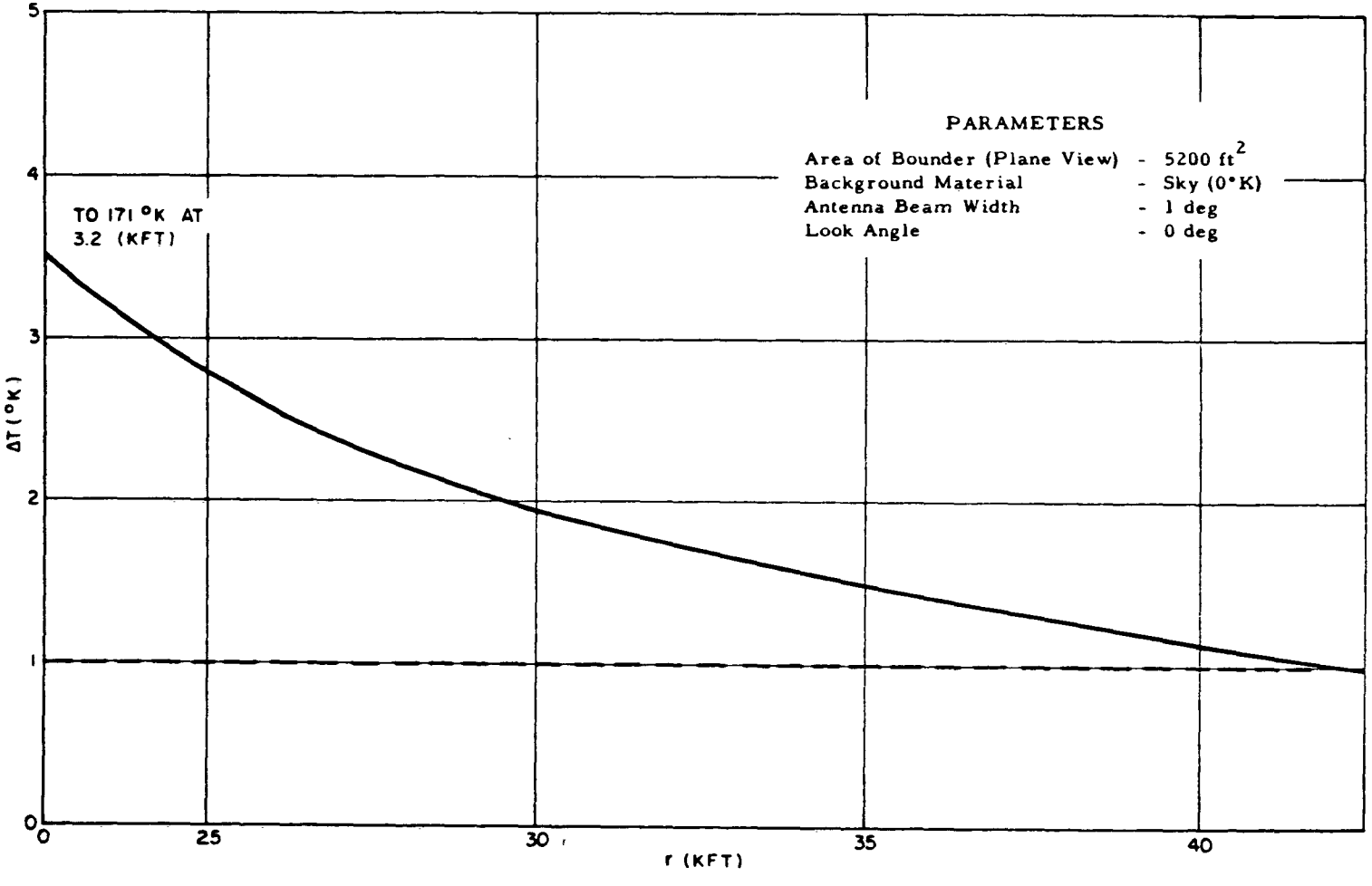

FIGURE 60. ΔT for the Bounder at K_a-Band for β = 1 deg, θ = 0 deg, and a Sky Background

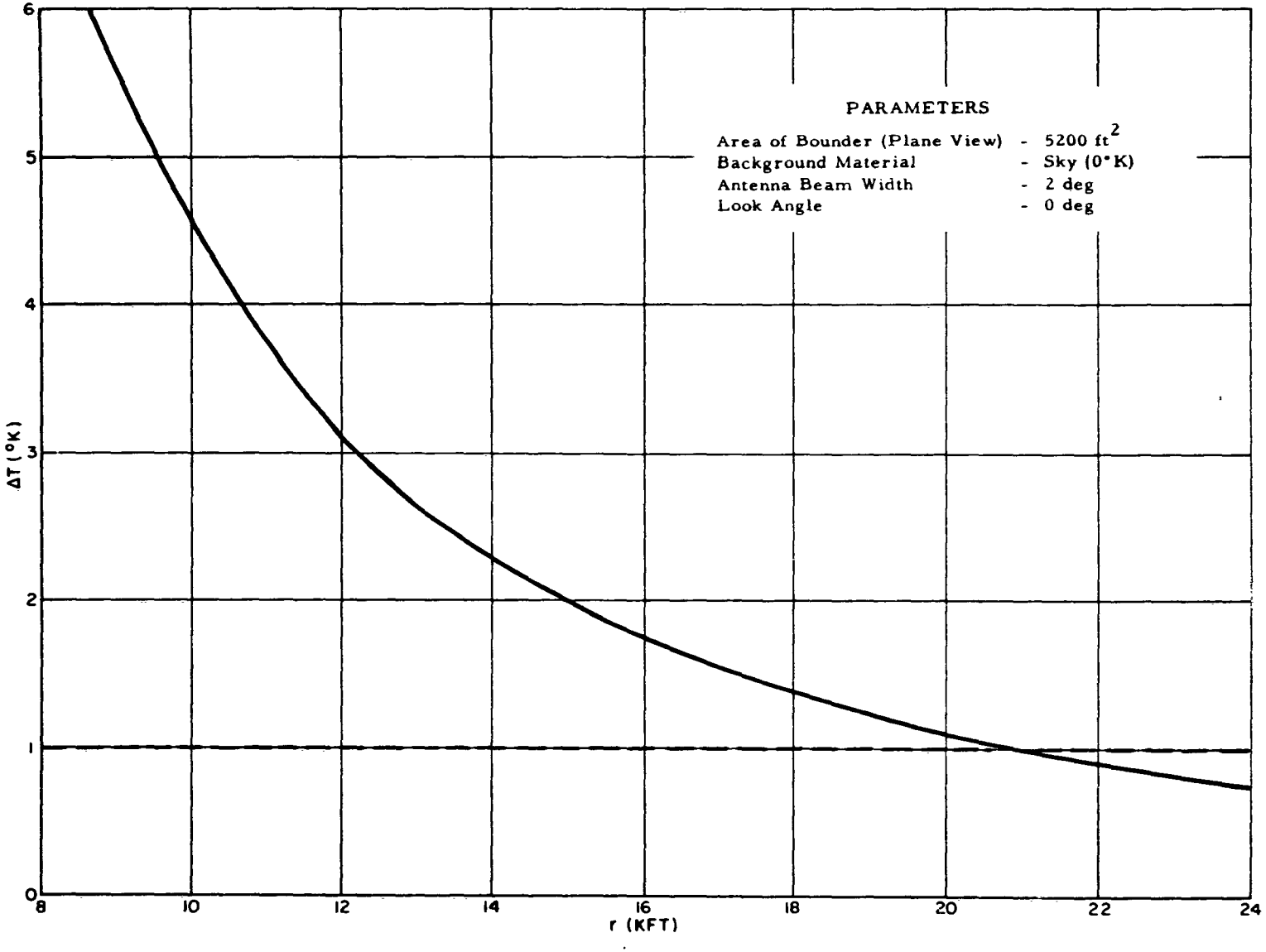

FIGURE 61. ΔT for the Bounder at K_a-Band for β = 2 deg, θ = 0 deg, and a Sky Background

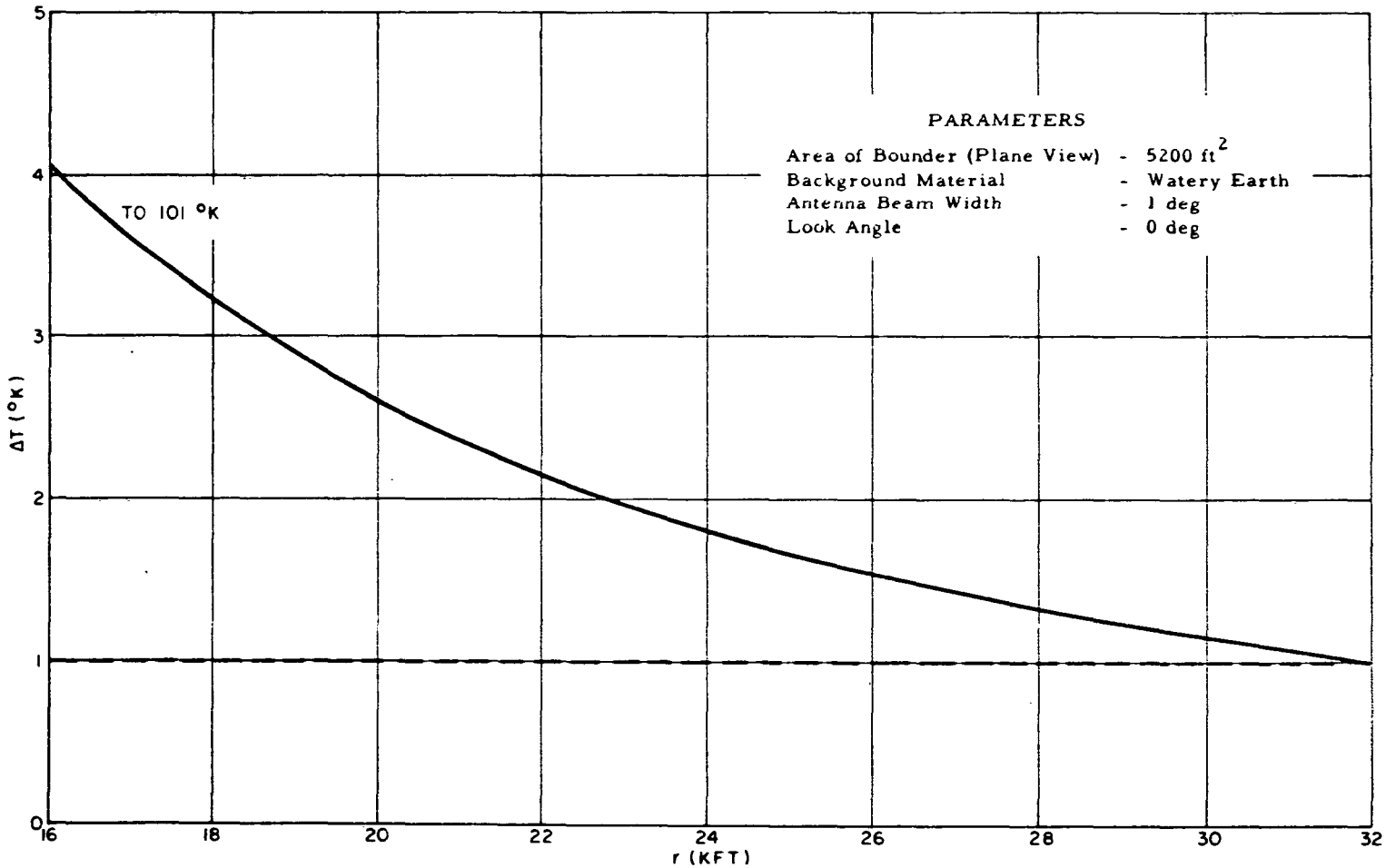

FIGURE 62. ΔT for the Bounder at K_a-Band for β = 1 deg, θ = 0 deg, and an Earth Background

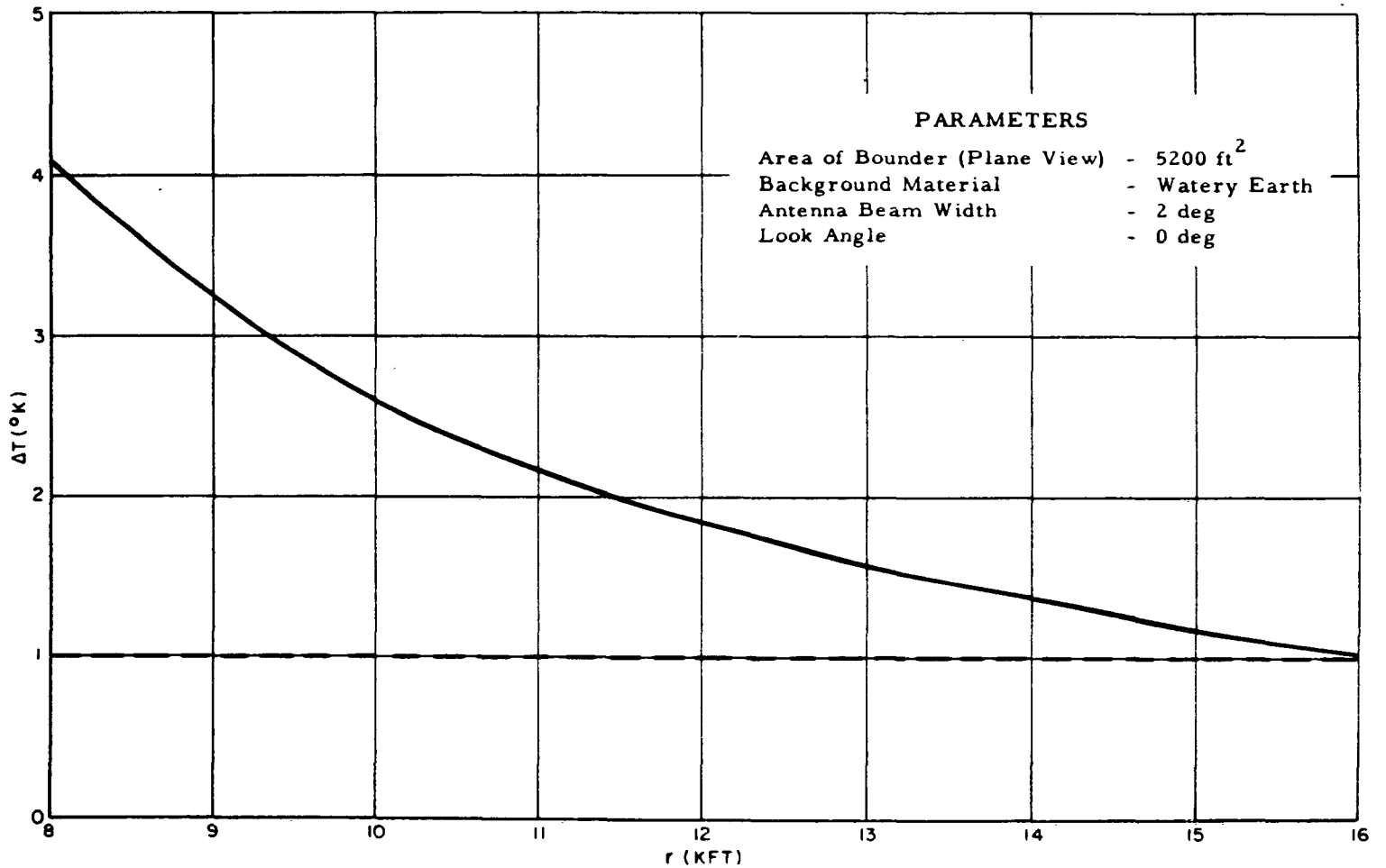

FIGURE 63. ΔT for the Bounder at K_a-Band for β = 2 deg, θ = 0 deg, and an Earth Background

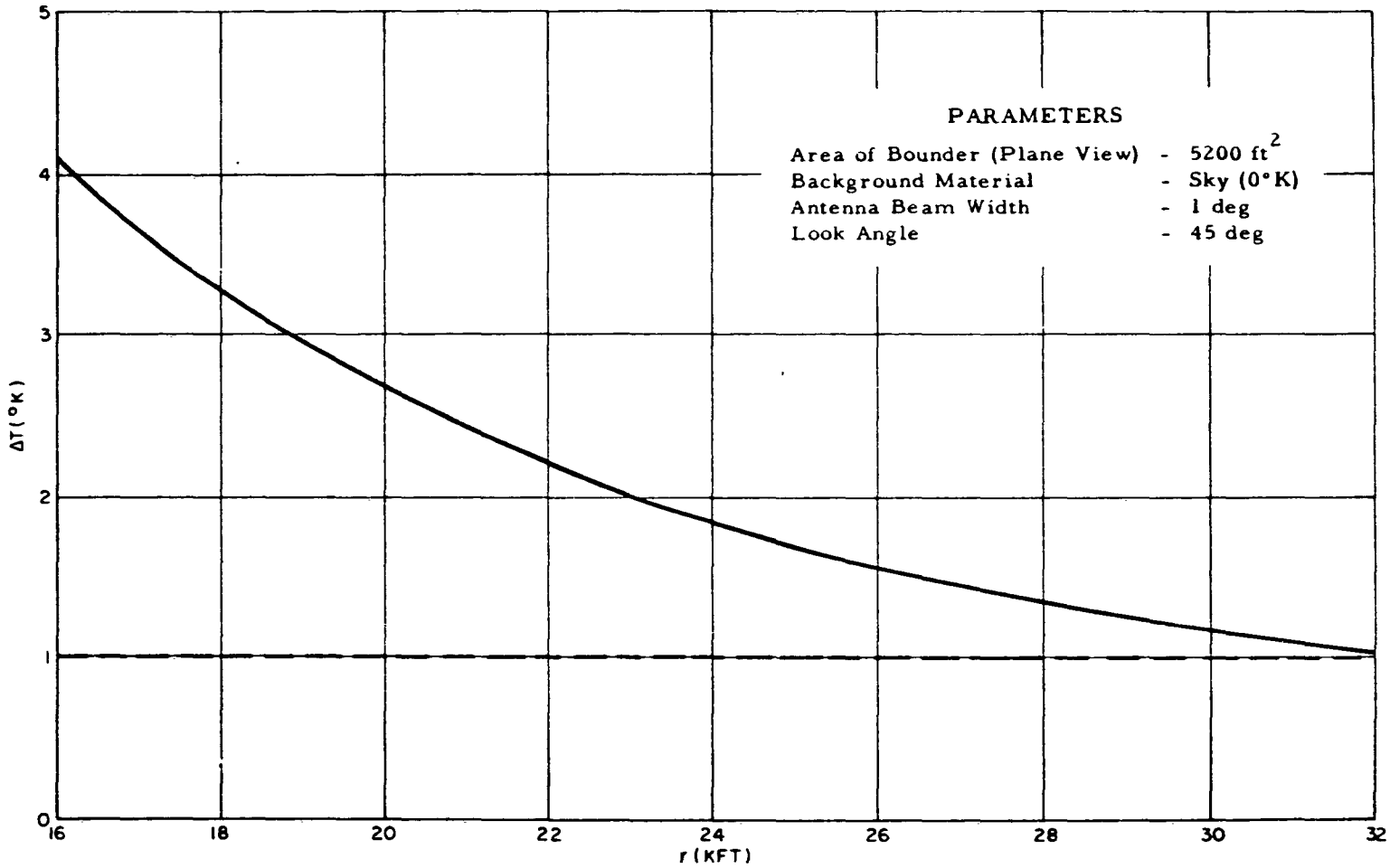

FIGURE 64. ΔT for the Bounder at X-Band for β = 1 deg, θ = 45 deg, and a Sky Background

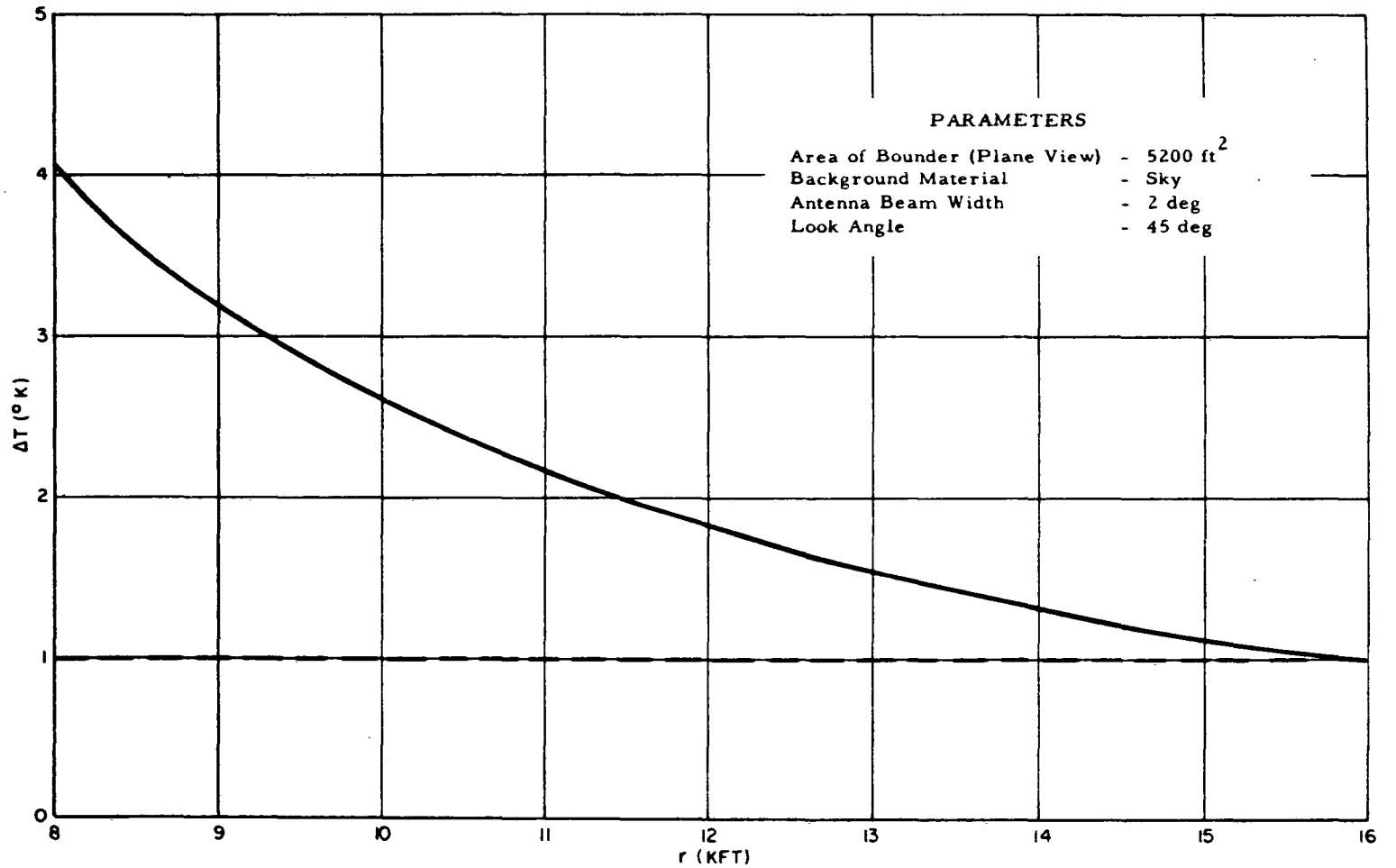

FIGURE 65. ΔT for the Bounder at X-Band for β = 2 deg, θ = 45 deg, and a Sky Background

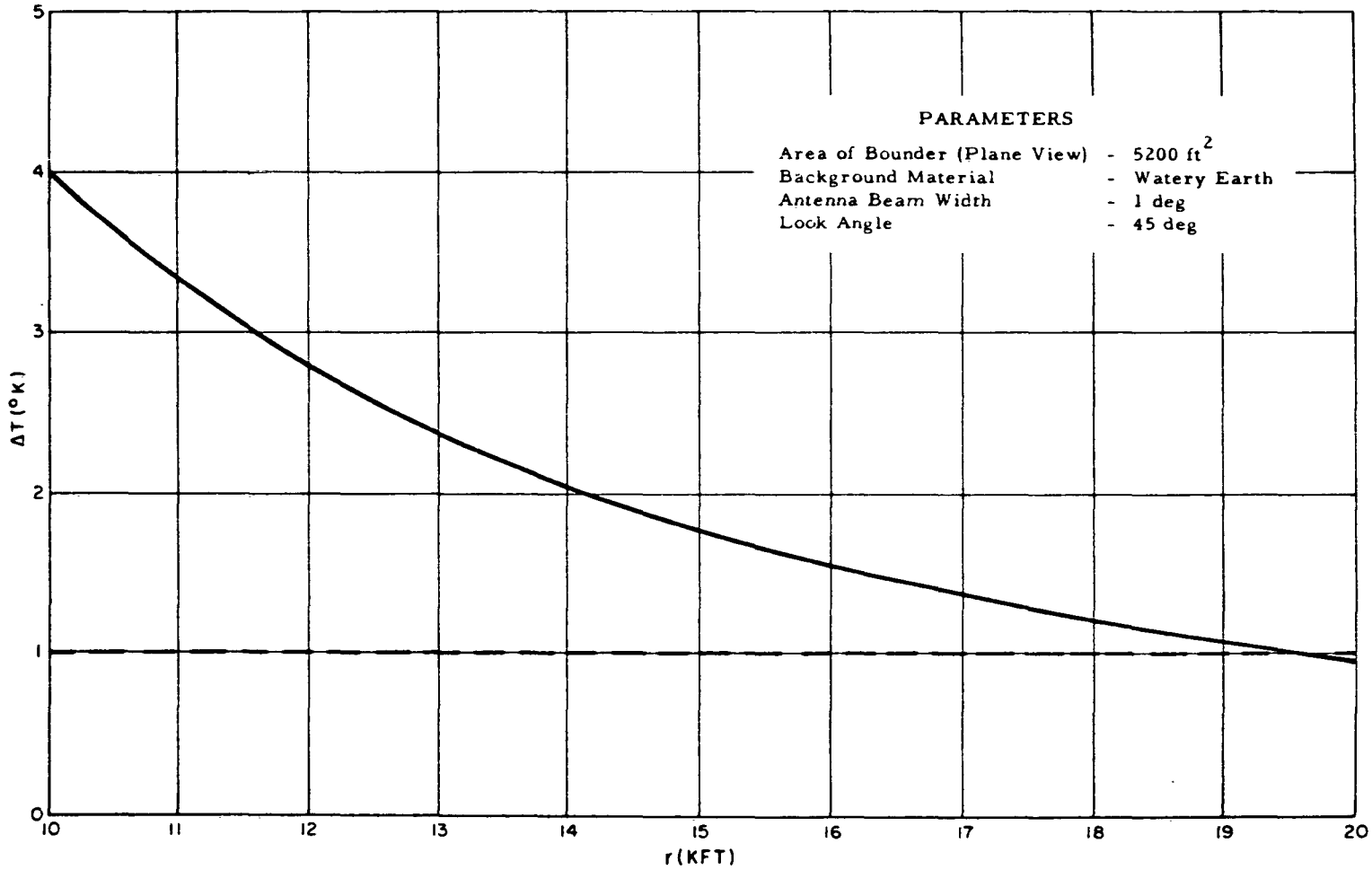

FIGURE 66. ΔT for the Bounder at X-Band for β = 1 deg, θ = 45 deg, and an Earth Background

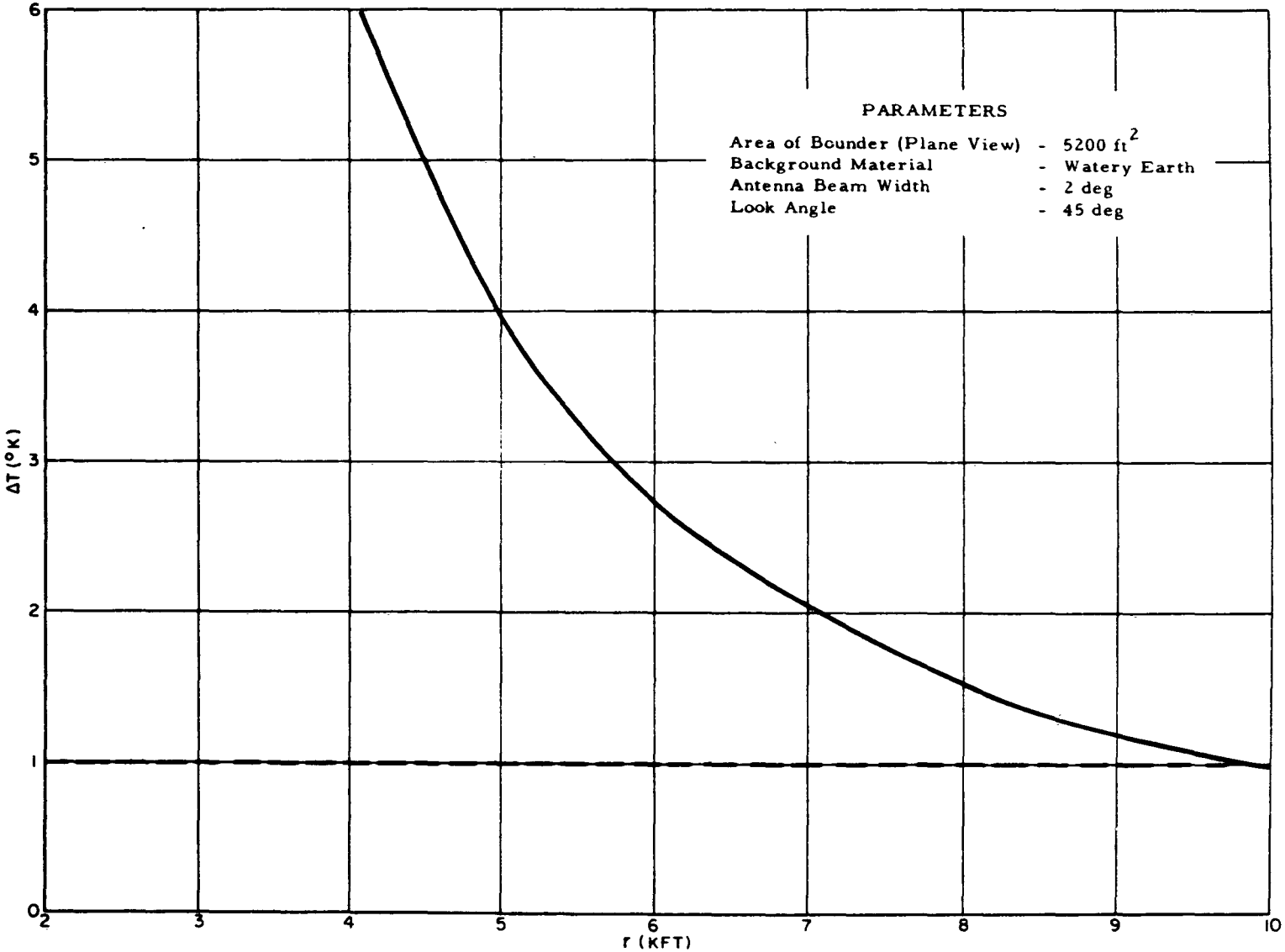

FIGURE 67. ΔT for the Bounder at X-Band for β = 2 deg, θ = 45 deg, and an Earth Background

FIGURE 68. Geometry of Ground-to-Air Observations

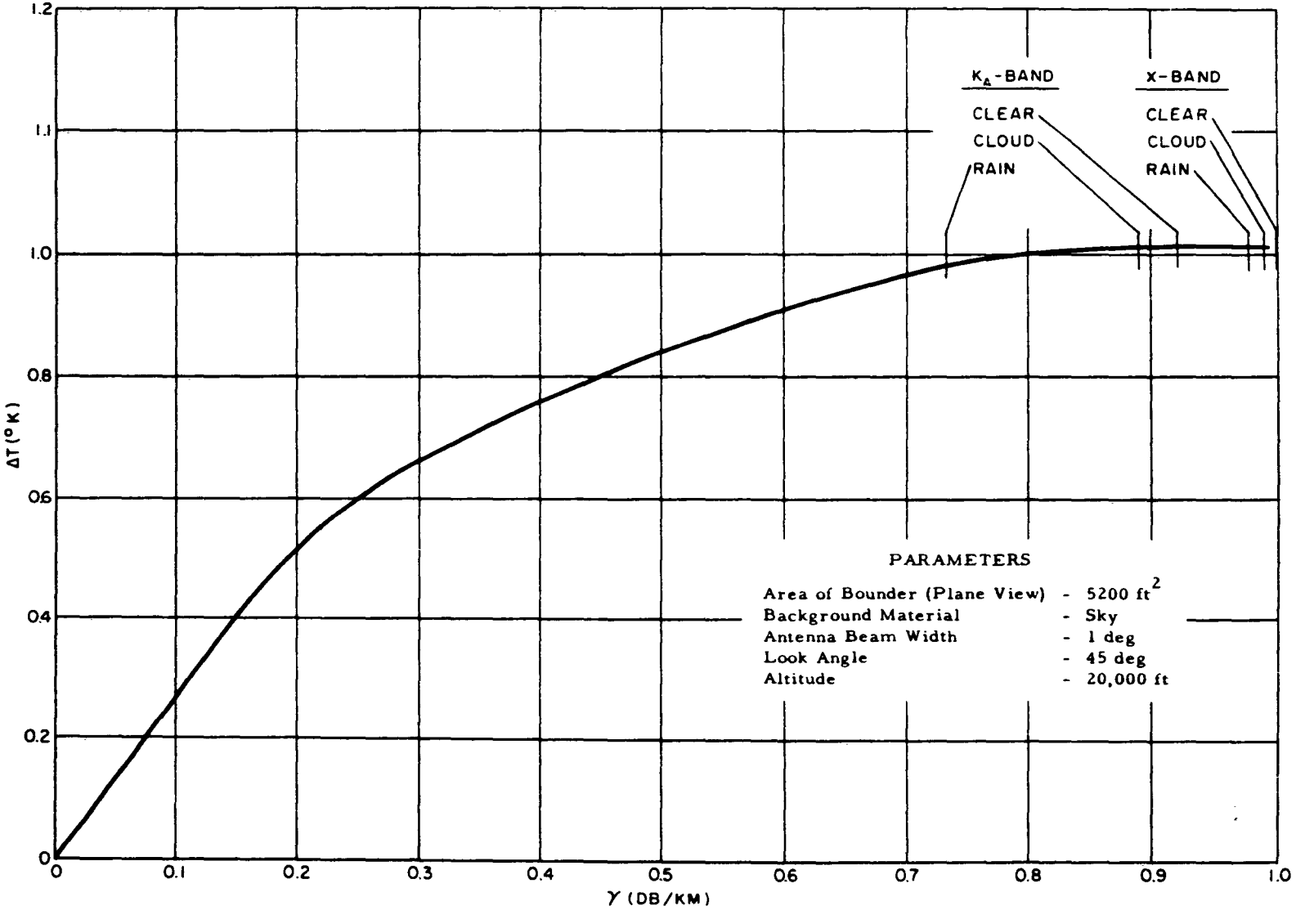

FIGURE 69. ΔT as a Function of Atmospheric Transmissivity

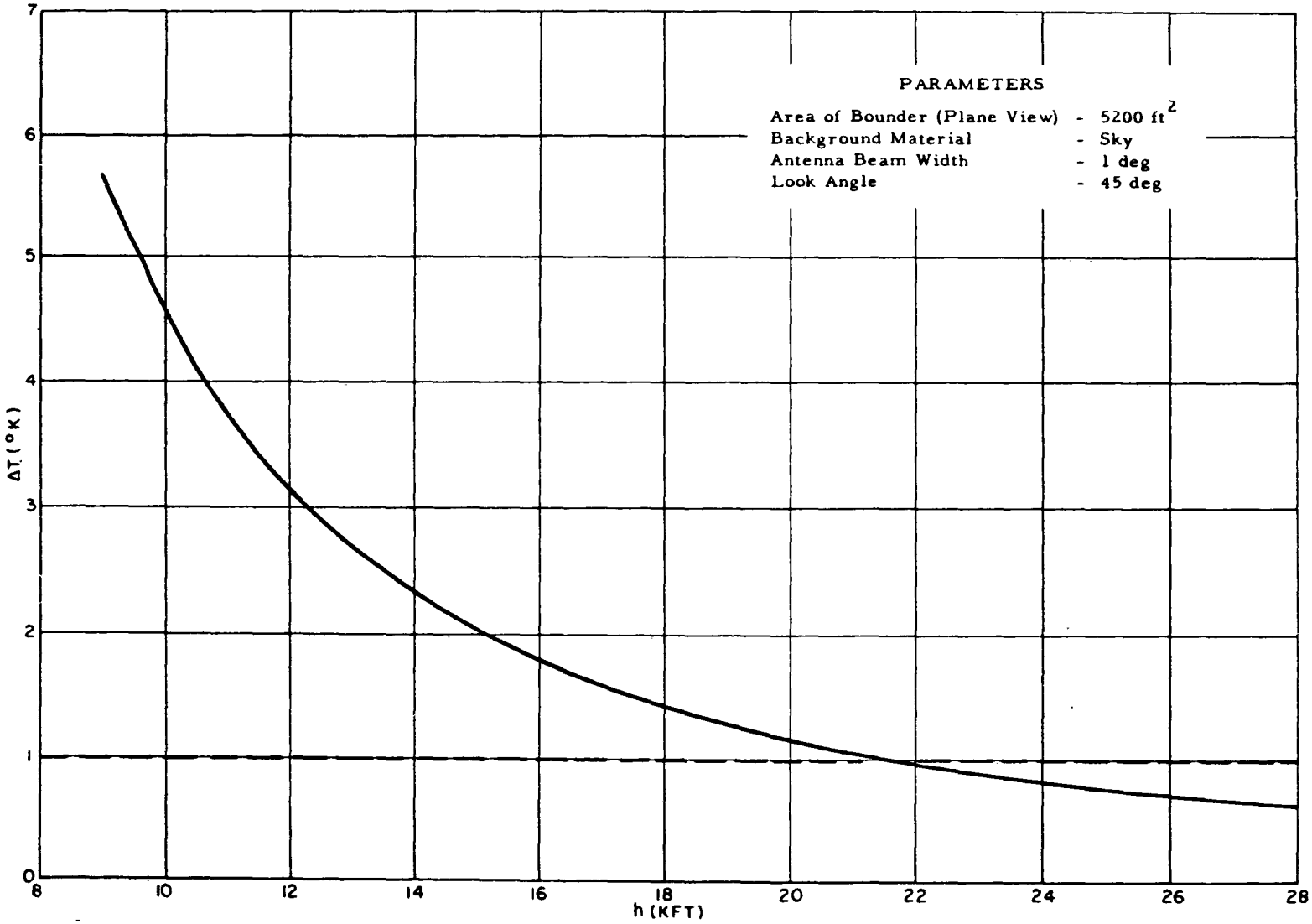

FIGURE 70. ΔT for the Bounder at K_a-Band in Clear Weather

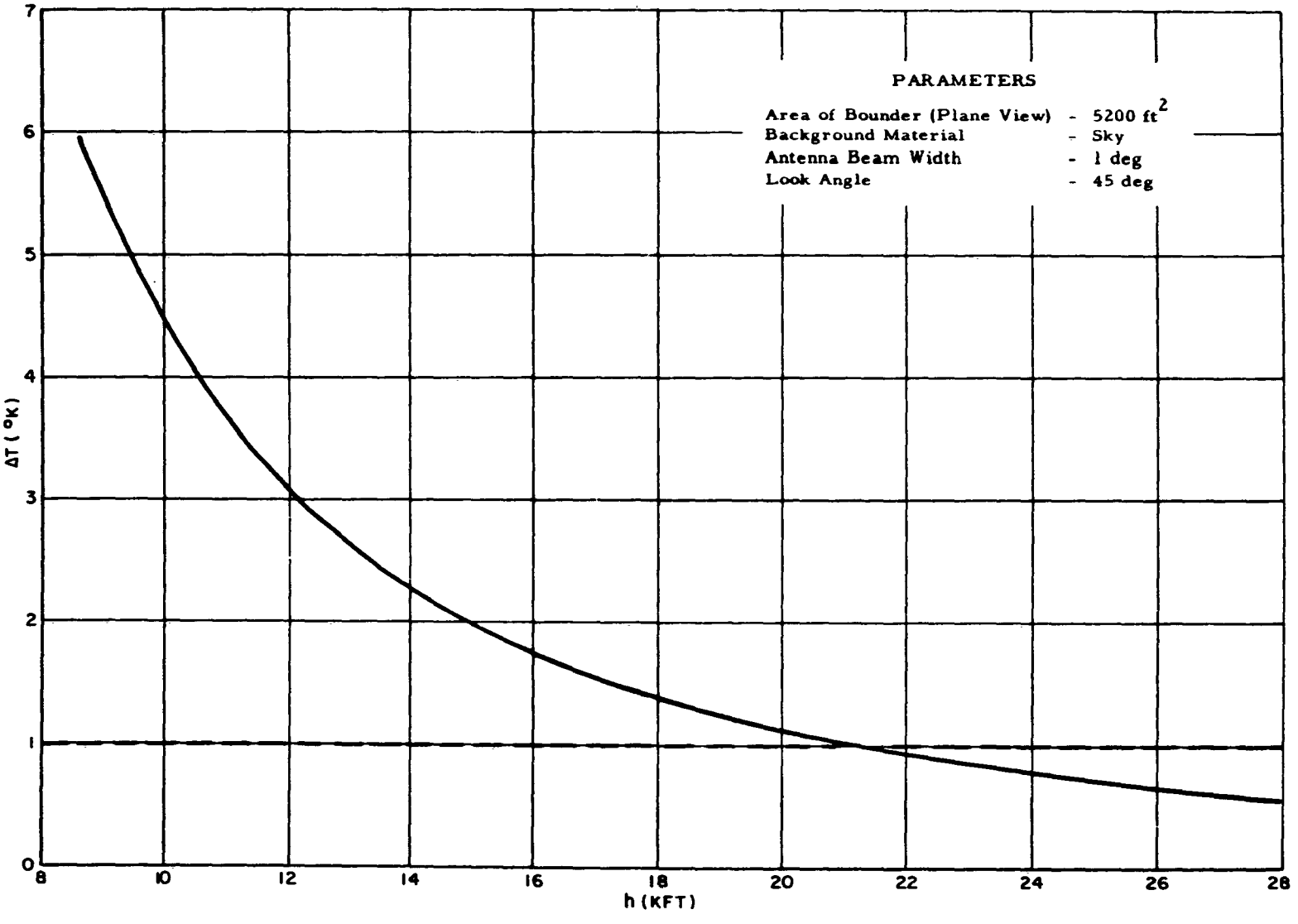

FIGURE 71. ΔT for the Bounder at K_a-Band in Moderate Clouds

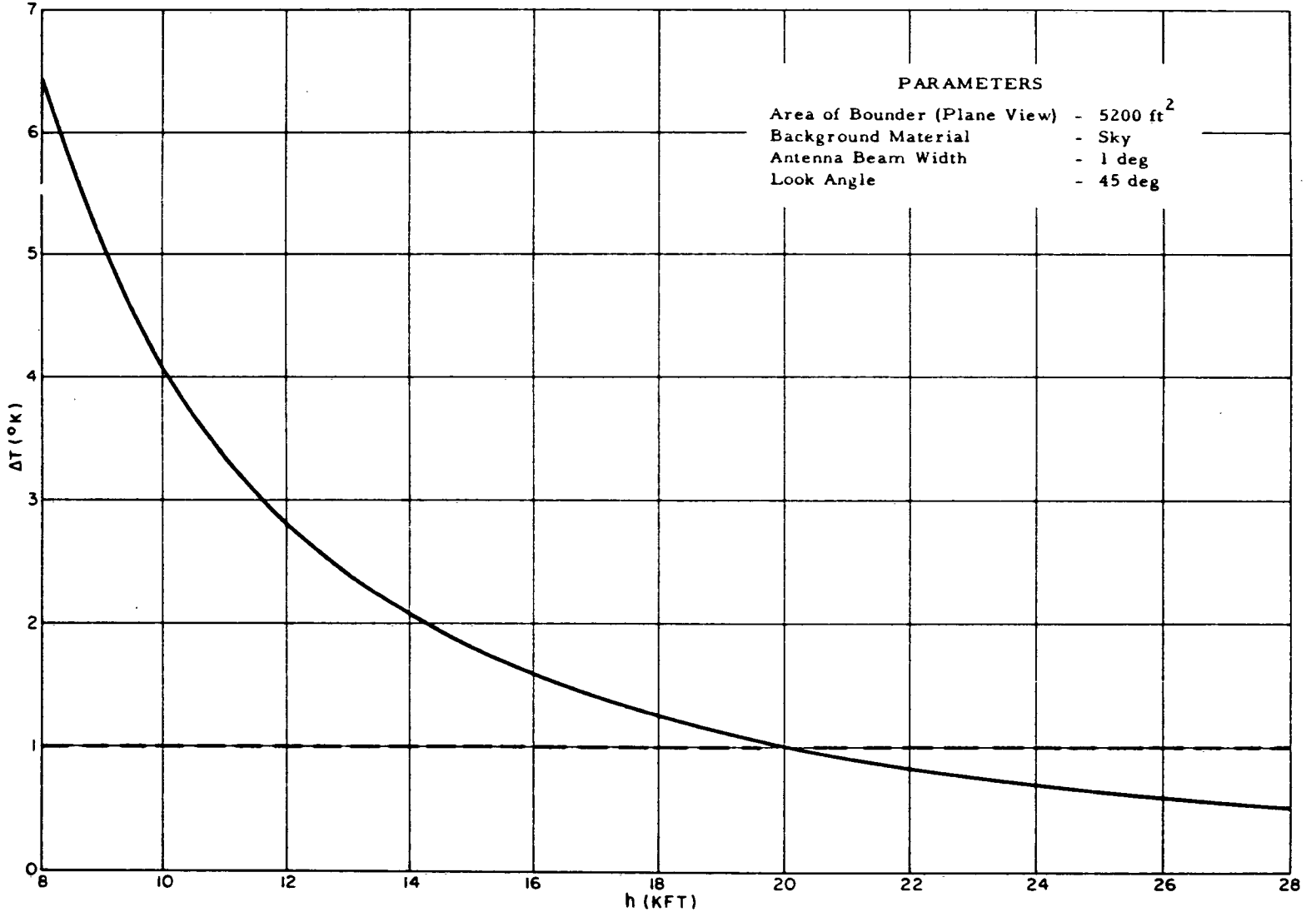

FIGURE 72. ΔT for the Bounder at K_a-Band in Moderate Rain

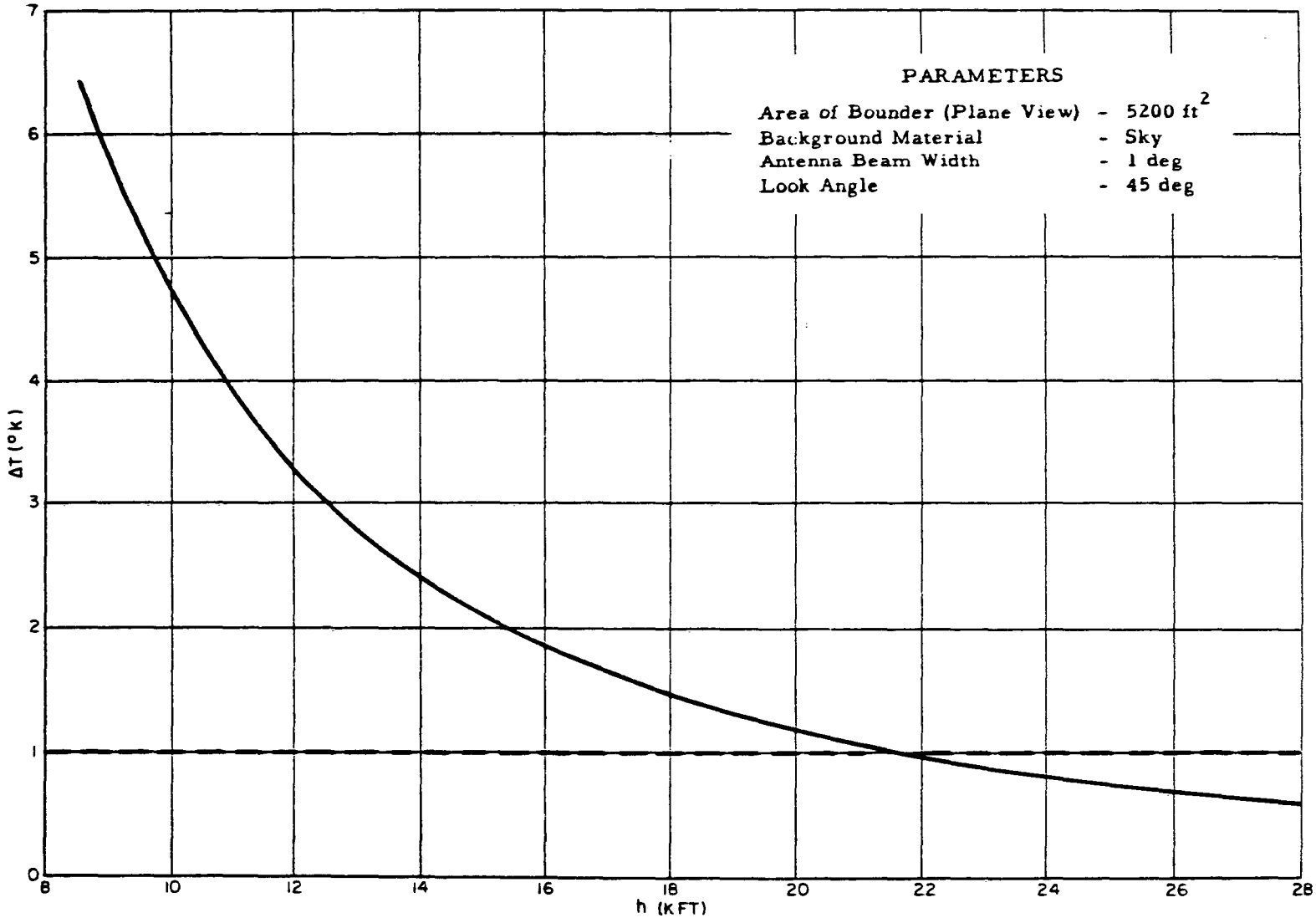

FIGURE 73. ΔT for the Bounder at X-Band in Clear Weather

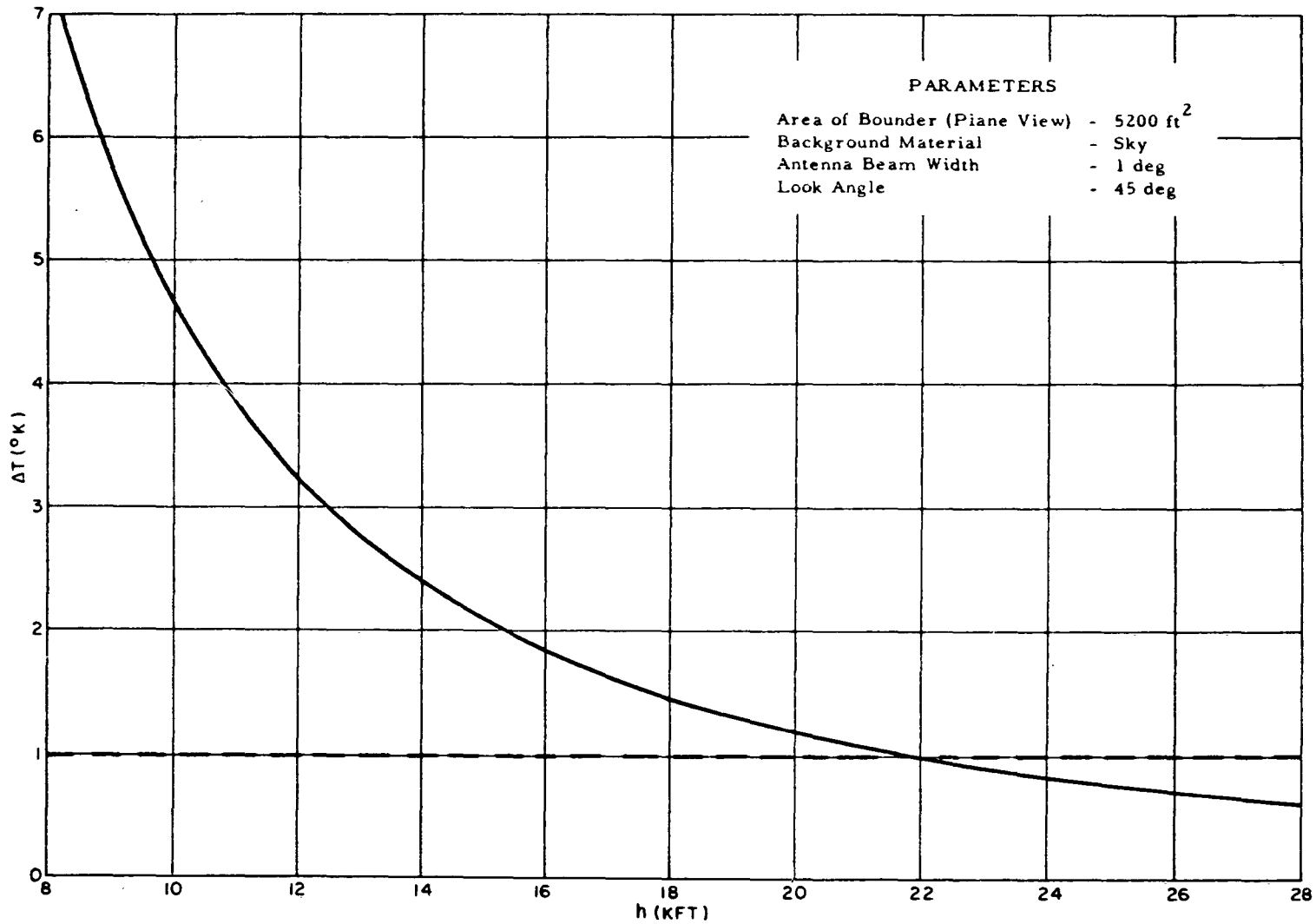

FIGURE 74. ΔT for the Bounder at X-Band in Either Moderate Clouds or Moderate Rain

Naval Ordnance Laboratory Corona. (NAVWEPS Report 8140)
SOME CALCULATIONS OF TARGET TEMPERATURES IN MICROWAVE RADIOMETRY, by John O. Hooper and James W. Battles, Research Department. 15 March 1963. 110 pp. UNCLASSIFIED

Calculations of the radiometric temperature differences between various targets and backgrounds have been performed, and the results are presented in graphical form. In addition, an analysis is made of the effects of the varying target, radiometer system, and weather parameters on the detectability of targets.

The data indicate that variable-area targets, such as roads and rivers (especially rivers), will be detectable from very high altitudes during all weather conditions considered. Constant-area targets, such as military tanks and aircraft, will be detectable at much lower altitudes or ranges, unless the area of the target is very large.

1. Radiometers—Applications—Mathematical analysis
I. Microwave radiometry
II. Title: Target temperatures in microwave radiometry
III. Hooper, J. O.
IV. Battles, J. W.

WepTask: RMWC-42-016/211-1/F008-22-07

This card is UNCLASSIFIED

Naval Ordnance Laboratory Corona. (NAVWEPS Report 8140)
SOME CALCULATIONS OF TARGET TEMPERATURES IN MICROWAVE RADIOMETRY, by John O. Hooper and James W. Battles, Research Department. 15 March 1963. 110 pp. UNCLASSIFIED

Calculations of the radiometric temperature differences between various targets and backgrounds have been performed, and the results are presented in graphical form. In addition, an analysis is made of the effects of the varying target, radiometer system, and weather parameters on the detectability of targets.

The data indicate that variable-area targets, such as roads and rivers (especially rivers), will be detectable from very high altitudes during all weather conditions considered. Constant-area targets, such as military tanks and aircraft, will be detectable at much lower altitudes or ranges, unless the area of the target is very large.

1. Radiometers—Applications—Mathematical analysis
I. Microwave radiometry
II. Title: Target temperatures in microwave radiometry
III. Hooper, J. O.
IV. Battles, J. W.

WepTask: RMWC-42-016/211-1/F008-22-07

This card is UNCLASSIFIED

Naval Ordnance Laboratory Corona. (NAVWEPS Report 8140)
SOME CALCULATIONS OF TARGET TEMPERATURES IN MICROWAVE RADIOMETRY, by John O. Hooper and James W. Battles, Research Department. 15 March 1963. 110 pp. UNCLASSIFIED

Calculations of the radiometric temperature differences between various targets and backgrounds have been performed, and the results are presented in graphical form. In addition, an analysis is made of the effects of the varying target, radiometer system, and weather parameters on the detectability of targets.

The data indicate that variable-area targets, such as roads and rivers (especially rivers), will be detectable from very high altitudes during all weather conditions considered. Constant-area targets, such as military tanks and aircraft, will be detectable at much lower altitudes or ranges, unless the area of the target is very large.

1. Radiometers—Applications—Mathematical analysis
I. Microwave radiometry
II. Title: Target temperatures in microwave radiometry
III. Hooper, J. O.
IV. Battles, J. W.

*WepTask: RMWC-42-016/*211-1/F008-22-07

This card is UNCLASSIFIED

Naval Ordnance Laboratory Corona. (NAVWEPS Report 8140)
SOME CALCULATIONS OF TARGET TEMPERATURES IN MICROWAVE RADIOMETRY, by John O. Hooper and James W. Battles, Research Department. 15 March 1963. 110 pp. UNCLASSIFIED

Calculations of the radiometric temperature differences between various targets and backgrounds have been performed, and the results are presented in graphical form. In addition, an analysis is made of the effects of the varying target, radiometer system, and weather parameters on the detectability of targets.

The data indicate that variable-area targets, such as roads and rivers (especially rivers), will be detectable from very high altitudes during all weather conditions considered. Constant-area targets, such as military tanks and aircraft, will be detectable at much lower altitudes or ranges, unless the area of the target is very large.

1. Radiometers—Applications—Mathematical analysis
I. Microwave radiometry
II. Title: Target temperatures in microwave radiometry
III. Hooper, J. O.
IV. Battles, J. W.

*WepTask: RMWC-42-016/*211-1/F008-22-07

This card is UNCLASSIFIED

NAVWEPS Report 8140; WepTask RMWC-42-016/211-1/F008-22-07.

INITIAL DISTRIBUTION

	Copies
Chief, Bureau of Naval Weapons Navy Department Washington 25, D. C.	
Attn: Code R-12	1
RM-12	1
RMGA-41	1
RMWC-421	1
RMWC-422	1
SP-001	1
DLI-31	4
Commander Naval Ordnance Test Station China Lake, Calif.	
Attn: Code 4503	1
Commander Naval Ordnance Laboratory White Oak Silver Spring 19, Md.	
Attn: R. J. Miller	1
Officer in Charge U. S. Naval Weapons Services Office U. S. Naval Station (Washington Navy Yard Annex) Washington 25, D. C.	2
Armed Services Technical Information Agency Arlington Hall Station Arlington 12, Va.	10

NOLC:	Copies
C. J. Humphreys, Code 40	1
F. C. Essig, Code 45	1
V. E. Hildebrand, Code 453	1
J. W. Battles, Code 454	1
M. C. Hoover, Code 454	1
H. A. Johnson, Code 454	1
R. P. Moore, Code 454	1
F. C. Alpers, Code 71	1
W. F. Meggers, Jr., Code 72	1
Technical Library, Code 234	2